THE UNIVERSITY OF MICHIGAN

7577-1-F

Technical Report ECOM-01499-4 September 1966

Azimuth and Elevation Direction Finder Study

Final Report

1 September 1965 - 1 September 1966

Report No. 4

Contract DA 28-043 AMC-01499(E)
DA Project 5A6 79191 D902 01 04

Prepared by

D. L. Sengupta, J. E. Ferris, R. W. Larson,
G. Hok and T. M. Smith

The University of Michigan Radiation Laboratory
Department of Electrical Engineering
Ann Arbor, Michigan

For

United States Army Electronics Command, Fort Monmouth, N.J.

ABSTRACT

Radiation characteristics of a spherical antenna array of circularly polarized elements are studied both theoretically and experimentally. It is found that such an array is capable of providing broadband and complete hemispherical coverage suitable for direction finding purposes. The theory developed should be adequate for the design of such arrays.

On the basis of the above study, an exploratory model of a UHF spherical array azimuth and elevation direction finder is proposed. The array uses flat spirals as individual elements. The necessary phasing of the antenna elements and the scanning of the beam for direction finding are accomplished by using delay lines and diode switches in conjunction with a general purpose computer.

An alternative method where a correlation processing technique is applied to the output data from the antenna elements for direction finding purposes is also discussed.

FOREWORD

This report was prepared by The University of Michigan Radiation Laboratory of the Department of Electrical Engineering under United States Army Electronics Command Contract No. DA 28-043 AMC-01499(E). This contract was initiated under United States Army Project No. 5A6 79191 D902 01 04 "Azimuth and Elevation Direction Finder Study". The work is administered under the direction of the Electronics Warfare Division, Advanced Techniques Branch at Fort Monmouth, New Jersey. Mr. S. Stiber is the Project Manager and Mr. E. Ivone is the Contract Monitor.

The material reported herein represents the results of the preliminary investigation into the study of the feasibility of designing a broadband circularly polarized direction finder antenna with hemispherical coverage.

TABLE OF CONTENTS

LIST OF ILLUSTRATIONS

I

INTRODUCTION

This is the final report on a study to determine the feasibility of developing a broadband VHF azimuth and elevation direction finder. The system is to operate over 5:1 frequency band (0.6-3 GHz) and is to employ circularly polarized antenna elements. Direction finding is to be done over a complete hemisphere.

It is well known that in the case of planar arrays with electronic scanning, the spatial coverage is restricted due to the fact that the directive gain of the antenna array decreases with beam steering. The requirement of complete hemispherical coverage with appropriate gain and electronic scanning rules out the use of planar arrays for our purpose. The polarization requirement of the radiated field and the physical symmetry of a spherical surface suggest the possibility of using an antenna array where the individual elements are placed on the surface of a sphere. At any instant of time, a predetermined number of elements (or a sector of the spherical surface) will be activated so that the beam is directed in a particular direction in space. Direction finding over the entire hemispherical region is to be done by scanning the beam. The scanning may be accomplished either by activating different sectors of the spherical surface or by introducing variable time delay to the elements in one particular sector or by a combination of both.

The major effort during this phase of the investigation has been to study the radiation characteristics of a spherical antenna array sufficiently to determine whether or not it may be used for azimuth and elevation direction finding.

Our theoretical studies on the spherical array have shown that it is feasible to develop a spherical array of circularly polarized antenna elements with some distinct advantages. An experimental investigation has been conducted to verify some of the theoretical conclusions. During the experimental study, only the feasibility of arraying circularly polarized antenna elements over a hemispherical surface was considered. We have also considered theorectically the problem of scanning and the implementation of a possible complete system for an azimuth and elevation direction finding.

The plan of the present report is as follows. Chapter II discusses the results obtained from a theorectial investigation of the radiation characteristics of a spherical antenna array. It is mainly based on the work reported in our three previous quarterly reports. Chapter III gives results obtained from experimental investigation. Both individual elements and the spherical antenna array characteristics have been studied. Wherever possible experimental results are compared with the theory. Chapter IV discusses the implementation of a proposed exploratory model of a spherical array direction finder system. Chapter V discusses the data processing aspects of the direction finding system. The correlation processing of the output data from the antenna elements and its application to direction finding are discussed. Although the preliminary model proposed in Chapter IV uses the conventional approach to the antenna array, the correlation approach seems to have some advantages. Chapter VI gives our conclusions and recommendations for future studies.

II

SPHERICAL ARRAY CHARACTERISTICS: THEORETICAL DISCUSSION

This chapter discusses briefly the results obtained from a theoretical study on spherical antenna array which have been reported in our previous three quarterly reports (Sengupta, et al, 1965; March 1966; June 1966). The details of the analysis have been left out since they may be found in these references.

No spherical array theory seems to have been previously published although Harris and Shanks (1962) and Du and Tai (1964) have discussed somewhat similar problems. Our initial effort was therefore devoted to the development of the theory and design of such type of antenna arrays. Our first quarterly report (Sengupta, et al, 1965) discussed this. Theoretical expressions were given there for the radiation patterns produced by a spherical antenna array. Each antenna element was assumed to produce elliptically polarized radiation having a maximum along its axial direction. The theory was kept as general as possible so that the results can be used when different parameters of the array are varied. The case of circular polarization was derived as a special case. The individual antenna element distribution on the spherical surface was kept arbitrary.

2.1 Element Distribution

There are many arrangements one could use in placing antenna elements on the surface of a sphere. The ideal case would be to place elements such that the distribution may appear to be the same from all observation angles so that the antenna maintains a constant pattern during scanning. The maximum number of elements that can be spaced uniformly on a spherical surface is only twenty, which is too low a number to produce the desired gain from the antenna. However,

elements can be arranged on the sphere as if they were being placed on the twenty faces of an icosahedron. This provides an approximately uniform distribution. From a study of the icosahedron geometry a special element distribution was developed. The details of the element distribution may be found in our earlier reports (Sengupta et al, 1965; March 1966). Two types of distribution were studied. Both of the distributions give approximately seven rings of elements roughly fifteen degrees apart. In the first distribution the number of elements in the seven rows is 1, 5, 10, 15, 20, 25, 25 (total number=101) counting from the vertex to the equator. In the second distribution the number of elements in the seven rings is 1, 5, 10, 15, 20, 20 and 20 respectively. Consequently, active areas or caps may be defined by the half-cone angles, $\alpha_o = 15^o$, 30^o, 45^o, ... 75^o, or 90^o in such a way that there are (for example in second type of distirbution) approximately 6, 16, 31, 51, 71 or 91 elements in these caps. This number varies somewhat with bean pointing position. Since the second distribution resembles more to the icosahedron geometry we have chosen this as our final distribution. The average element spacing for this distribution is approximately given by $s \approx 0.3a$, where s is the element spacing, and a is the radius of the sphere.

2.2 Theoretical Expressions for the Radiation Patterns

By neglecting mutual coupling and assuming a radially directed, circularly polarized, half-cosine element pattern for all frequencies, it can be shown (Sengupta et al, 1965) that the electric field for the hemispherical array at a far field point $P(R, \theta, \phi)$ is

$$\vec{E}(R, \theta, \phi) = -(\hat{e}_\theta - i\,\hat{e}_\phi)\, A(\theta, \phi)\, \frac{e^{i(\omega t - kR)}}{R}, \qquad (2.1)$$

where

$$A(\theta,\phi)=\sum_{n=0}^{6}\sum_{m=0}^{M(n)}\delta_{nm}\psi_{nm}\exp\left\{i\left[ka(\psi_{nm}-\Delta_{nm})-(\xi_{nm}-\eta_{nm})\right]\right\} . \tag{2.2}$$

In the above M(n) is the appropriate number of elements in the ring for a particular value of M. In Eqs. (2.1) and (2.3) $\hat{e}_\theta$ and $\hat{e}_\phi$ are unit vectors and ka is the electrical radius of the sphere. The term ψ_{nm} used for both electrical path length and element pattern, is the cosine of the angle between an element position (α_n, β_{nm}) and the far field point $P(R, \theta, \phi)$ and is given by

$$\psi_{nm}(\theta,\phi)=\cos\theta\cos\alpha_n+\sin\theta\sin\alpha_n\cos(\phi-\beta_{nm}) . \tag{2.3}$$

Phase dependence of the radiation field due to the orientation and polarization of the antenna elements can be combined in the expression for ξ_{nm} where,

$$\tan\xi_{nm}=\frac{(\cos\alpha_n+\cos\theta)\sin(\phi-\beta_{nm})}{\sin\alpha_n\sin\theta+(1+\cos\alpha_n\cos\theta)\cos(\phi-\beta_n)} . \tag{2.4}$$

The phase correction terms $\Delta_{nm}=\psi_{nm}(\theta_o,\phi_o)$ and $\eta_{nm}=\xi_{nm}(\theta_o,\phi_o)$ are used to direct the pattern maximum towards the point θ_o, ϕ_o.

For an active cap centered at θ_o, ϕ_o with half-cone angle α_o, the on-off condition switch δ_{nm} is,

$$\delta_{nm} = \begin{cases} 1 & \text{if } \Delta_{nm} \geq \cos \alpha_o, \ \psi_{nm} \geq 0 \\ 0 & \text{otherwise} \end{cases} . \qquad (2.5)$$

This condition means physically that only those elements which are both visible from the observation point (θ, ϕ) and which lie within α_o degrees of the point (θ_o, ϕ_o) contribute to the pattern. It is a reasonable assumption when the elements are assumed to lie on a spherical ground plane.

2.3 Numerical Investigations

Using the above model for the antenna array, radiation patterns have been numerically computed with help of Eqs. (2.1)-(2.5) under various operating conditions. The results were reported and discussed in detail in our earlier reports. Based on those results we make the following observations regarding the radiation characteristics of a spherical array:

(1) For a complete hemispherical illumination the main beam of the pattern stays the same in two orthogonal planes. There appears to be 3db difference in the first sidelobe amplitudes. This discrepancy is attributed to the difference in the element distribution along the meridian and equatorial planes.

(2) The pattern stays approximately the same when the beam is steered over $0-90^o$ in elevation.

(3) With increase of a/λ the main beam narrows as it should and the level of the first sidelobe stays practically the same. After studying the computed patterns of the hemispherical array, we conclude that typically the first sidelobe level is -18 db and the second sidelobe level -24 db. For $a/\lambda > 3$ pseudo-grating lobes appear in the pattern.

(4) As the activated region is varied (say from $\alpha_o = 75^o$ to $\alpha_o = 30^o$) the main beam broadens with corresponding reduction of the first sidelobe amplitude.

(5) It is found that for $\alpha_o = 75^o$, the directivity is 19.3 db (compared to an isotropic source) for $a/\lambda = 1.5$, and as a/λ is increased to 8 the directivity at first increases and then fluctuates about the value 21 db. For $\alpha_o = 45^o$, the directivity is 15.5 db at $a/\lambda = 1.5$ and then fluctuates around the mean value 21.5 db as a/λ is increased.

(6) The half-power beamwidth of the pattern produced by an activated spherical cap of half-angle α_o is approximately given by:

$$\Theta_{1/2} \approx 2\sin^{-1}\left[\frac{0.258}{ka\sin\alpha_o}\right] . \qquad (2.6)$$

2.4 Pseudo-grating Lobes in the Pattern

As mentioned earlier for large element spacing (i.e. a/λ large) there appear strong lobes in the patterns. These are referred to as subsidiary or pseudo-grating lobes. In general, with the increase of a/λ, these lobes increase both in amplitude and number. In our previous reports (Sengupta et al, March 1966; June 1966) we discussed in detail the pseudo-grating lobes in the patterns produced by circular arrays of isotropic elements. It was found that for the element spacing $s > \lambda/2$ pseudo-grating lobes appear in the pattern. The amplitude and location of these lobes depend on the number of elements used and the spacing between them. However, in no case do the pseudo-grating lobe amplitudes achieve values equal to the maximum value of the main beam. In the spherical array case, the behavior of the pseudo-grating lobes should be similar although in general, the amplitudes of these lobes will be much reduced due to the spherical distribution of elements.

2.5 Concluding Remarks

The above discussion shows that a spherical array with circularly polarized elements can provide extensive spatial coverage over a wide band of frequencies. The special arrangement of the elements suppresses the grating lobes and thereby makes the array broadband. The directivity of the array is found to be almost invariant with beam steering. The next chapter discusses the experimental results which confirm some of the above conclusions.

III

EXPERIMENTAL INVESTIGATION AND COMPARISON WITH THEORY

This chapter discusses the results obtained from an experimental investigation of the various aspects of the spherical antenna array. The basic purpose of all the experiments carried out was to evaluate the validity of the theory developed earlier and to obtain other relevant information which was not considered theoretically. The reasons for choosing flat spiral (or the Archimedean) antenna as the individual element of the spherical array are discussed. The results of experimental investigation of the different properties of spiral antennas are given. A two-element (on planar surface) and a five-element circular array of spiral antennas (on a hemisphere) have been studied experimentally in order to obtain some design information. The measured radiation patterns produced by a sixteen-element array of spirals placed on a hemispherical ground plane are given. These results are compared with theoretical patterns. Finally, preliminary results obtained from a study of the mutual coupling between two spiral antennas are given.

3.1 Choice of the Primary Antenna Element

The system requirements for the direction finder antenna are such that one should use circularly polarized broadband antennas as the individual elements of the spherical array. The possible choices for the primary antenna element are: crossed dipoles, helical antennas, log conical helix and flat spiral antennas.

For limited performance crossed dipoles fed in quadrature may be used as circularly polarized elements but their bandwidth is very restricted. The polarization and broadband characteristics of helical antennas are not as good as

those of log conical and flat spiral antennas. Initially we studied (Sengupta et al, 1965) log conical helix antenna as a possible primary element. Radiation patterns and impedance characteristics of the log conical antennas were studied experimentally over the frequency range of interest. It appeared from this study that they are not ideally suited for use on the azimuth and elevation direction finder for the following reasons: (1) the VSWR characteristics over the desired 5: 1 band of frequency are poor; (2) the physical size of the antenna is large; and, (3) with change of frequency the phase center of the antenna may change.

The two wire Archimedean or flat spiral when properly excited have been shown (Kaiser, 1960) to produce circularly polarized radiation which is broadband not only with respect to input impedance but also to the radiation pattern. For the reasons mentioned above we decided to use the cavity backed flat spiral antenna as the primary element of the spherical array. The following sections give a general discussion of flat spiral antennas and also discuss some of the results obtained from our experimental investigation of such antennas.

3.2 Flat Spiral Antennas

3.2.1 Theoretical Considerations

The Archimedean spiral is defined by

$$r = a\theta \tag{3.1}$$

where

r = radius from the spiral center

θ = angular measure in radians

a = a constant which controls the spiral pitch.

A typical bifilar flat spiral is shown in Fig. 3-1. At the present time, there is no rigorous theory to explain the performance of a spiral antenna. However, one may consider qualitatively that the bifilar spiral antenna behaves as though it were

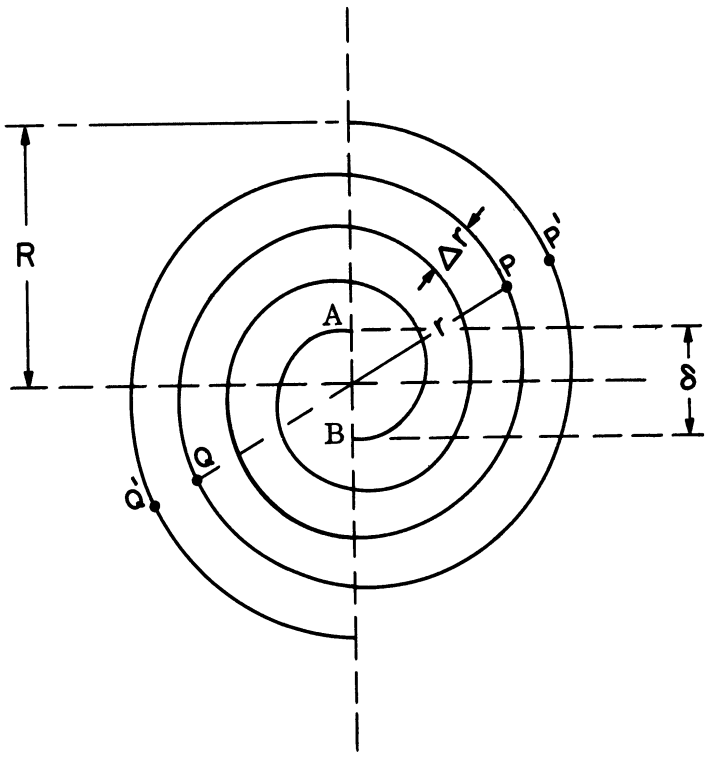

FIG. 3-1: DIMENSIONAL DRAWING OF A TWO WIRE SPIRAL

a two-wire transmission line with input terminals at A-B (Fig. 3-1), which is gradually transformed into a radiating structure or antenna because of the spiral geometry. This can be seen as follows. The two diametrically opposite points P and Q (distant r from the center of the spiral) situated on the two lines are at the same electrical distance from the two input terminals B and A respectively (Fig. 3-1). Thus, the difference in line lengths between the points P and P' is arc QP'. If $\Delta r \ll r$, then this line length difference $\approx \pi r$. Assuming that each wire supports a traveling wave of current and that these current waves are out of phase at the input terminals A and B, it is clear that if $r = \lambda/2\pi$ then the currents at P and P' will be in phase. Similarly, under this situation Q, Q' also will be in phase. Thus, the radiation from the spiral may be assumed to be from the currents confined to an annular ring of turns of one wavelength mean circumference. This property makes the spiral antenna an inherently broadband and constant beamwidth device. The above is the first or the axial mode of operation. The mean diameter d of the annular ring of currents for radiation in different modes may be expressed as:

$$d \approx \frac{n\lambda}{\pi} , \qquad n = 1, 2, 3, 4, \ldots \tag{3.2}$$

Antiphase excitation at the input terminals will produce only the odd modes of radiation while the inphase excitation will produce only the even order modes of radiation. The lowest and the highest frequencies of operation are usually determined by the parameters R and δ respectively (Fig. 3-1).

A planar spiral when excited in the lowest mode produces a broad circularly polarized beam on each side of the spiral (Kaiser, 1960). Each beam is normal to the plane of the spiral and the sense of circularity of polarization of the beam on one side corresponds to the winding sense of the spiral as viewed from

the other side. For producing a beam in one direction only the spiral is usually backed by a cavity.

The circular symmetry of the spiral about its axis allows rotation about the axis to produce a change in phase of the radiated field everywhere in space without variation in the far field amplitude. Thus, in the axial or the lowest mode of operation, one degree of mechanical rotation produces a corresponding change in phase of one electrical degree in the radiated field. In our theoretical model we have assumed that the pattern produced by a flat spiral operating in the axial mode is given by,

$$f(\theta) \simeq \cos\theta \, e^{+j\phi} \quad , \quad -\frac{\pi}{2} \leqslant \theta \leqslant \frac{\pi}{2} \quad , \tag{3.3}$$

where θ, ϕ are the usual spherical coordinates with the polar axis z oriented along the axis of the spiral. As will be seen later, the experimental pattern does not exactly correspond to that given by Eq. (3.3) but, for simplicity of computation in the theoretical analysis, it seemed best to use this equation.

3.2.2 Model of the Primary Element

The particular spiral chosen for our primary antenna element is a 15 turn bifilar configuration similar to that shown in Fig. 3-1. The maximum diameter of the spiral is 8" and it is backed by a flat cavity 1" deep. The spiral is fed by a linear-tapered balun (Duncan and Minerva, 1960) at the center such that it operates in the axial mode. The length of the balun is approximately 15" long, i.e. it was slightly longer than $\lambda/2$ at the lowest frequency of interest (600 MHz). A photograph of a typical spiral is shown in Fig. 3-2.

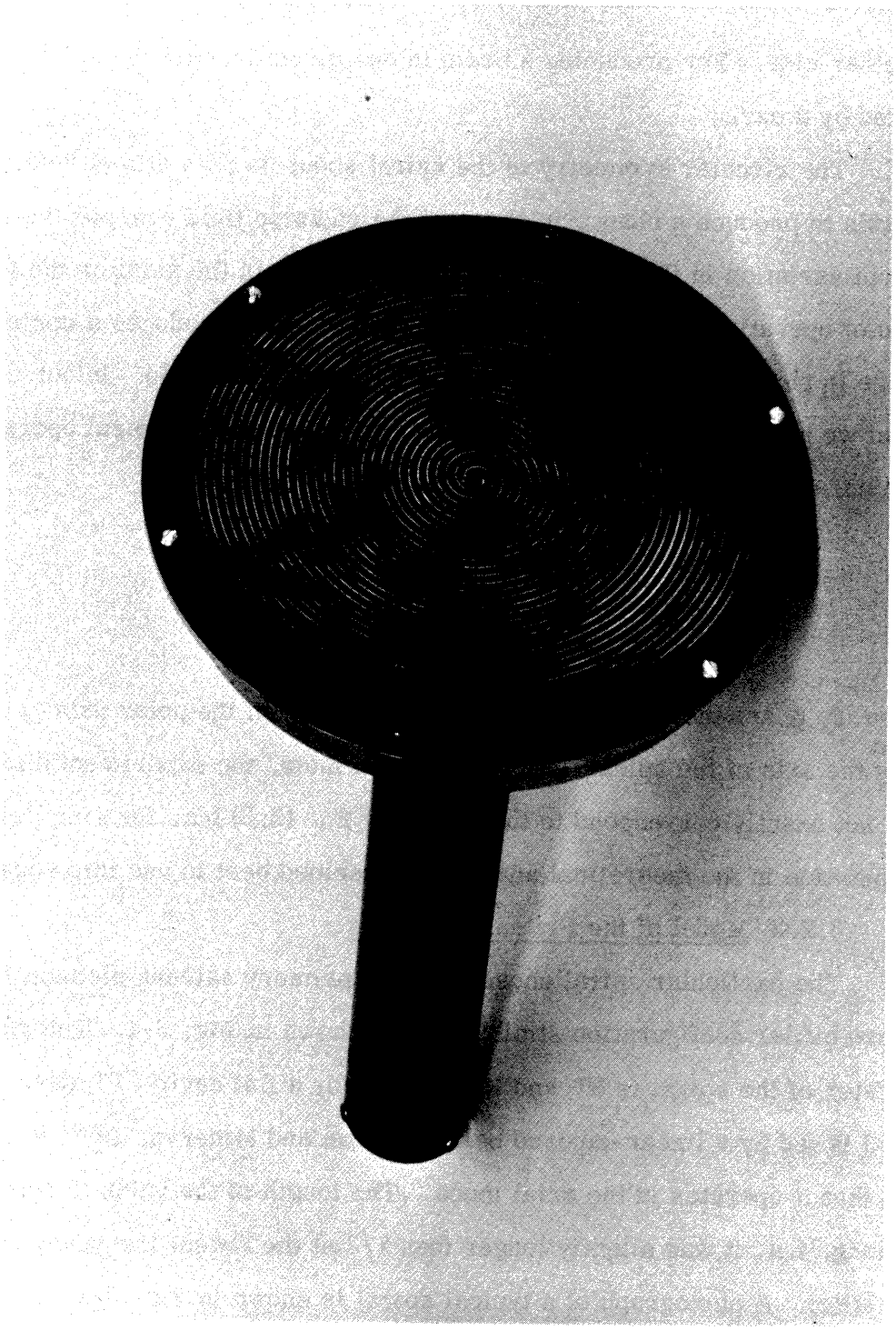

FIG. 3-2: PHOTOGRAPH OF A SPIRAL ELEMENT

Impedance and radiation pattern data were collected for several of the spirals with and without a ground plane at several frequencies within the operating band. Initially, two flat spirals were constructed and tested. Since these performed quite satisfactorily, they were chosen as the primary elements for the hemispherical array and 16 elements were fabricated.

3.2.3 Experimental Results for Spirals: No Ground Plane

The 16 spirals were initially labelled 16-1, 16-2, ...16-16 so they could later be identified in the array. A reference mark was placed on each element to insure proper orientation relative to each other during later tests, i.e., the spirals were marked 'top' as shown in Fig. 3-3 such that the shielded and center conductor of the coaxial cables were respectively connected to the minus and plus terminals of the bifilar spiral.

The VSWR characteristics of the 16 spirals (with respect to 50 ohm) were measured at 0.6, 1.8 and 3.0 GHz and is shown in Table III-I. Five elements (16-7, 16-8, 16-11, 16-14 and 16-15) were selected from which a comprehensive set of data was collected. Pattern data was collected in accordance with the coordinate system of Fig. 3-4. The following transmitter polarization conditions were employed: (1) horizontal polarization (E_ϕ) with respect to ground, (2) vertically polarized (E_θ) with respect to ground, and (3) the transmitter polarization variable (to obtain the ellipticity of the patterns). Figures 3-5 through 3-7 are typical pattern data that were collected for spiral 16-7 at 0.6, 1.8 and 3.0 GHz. Figure 3-5 shows the horizontal, vertical and ellipticity patterns at 0.6 GHz and similar patterns are shown for 1.8 and 3.0 GHz in Figs. 3-6 and 3-7, respectively. The deterioration of the E_ϕ pattern at 1.8 GHz (Fig. 3-6a) is attributed to the unbalance excitation caused by the balun. The circularity of polarization of the radiated field may be considered to be very good

TABLE III-I

Spiral VSWR (No Ground Plane)

Ant. No.	0.6 GHz	1.8 GHz	3.0 GHz
16-1	1.47	1.85	2.10
16-2	1.45	1.90	2.10
16-3	1.85	1.95	2.40
16-4	1.39	2.00	2.20
16-5	1.77	2.10	2.80
16-6	1.22	1.80	2.00
16-7	1.50	1.90	2.70
16-8	1.19	2.00	2.30
16-9	1.38	1.95	1.70
16-10	1.25	2.00	2.90
16-11	1.11	1.75	1.75
16-12	1.35	1.75	1.87
16-13	1.47	1.85	2.30
16-14	1.35	1.85	1.95
16-15	1.34	1.75	1.95
16-16	1.55	1.55	2.10

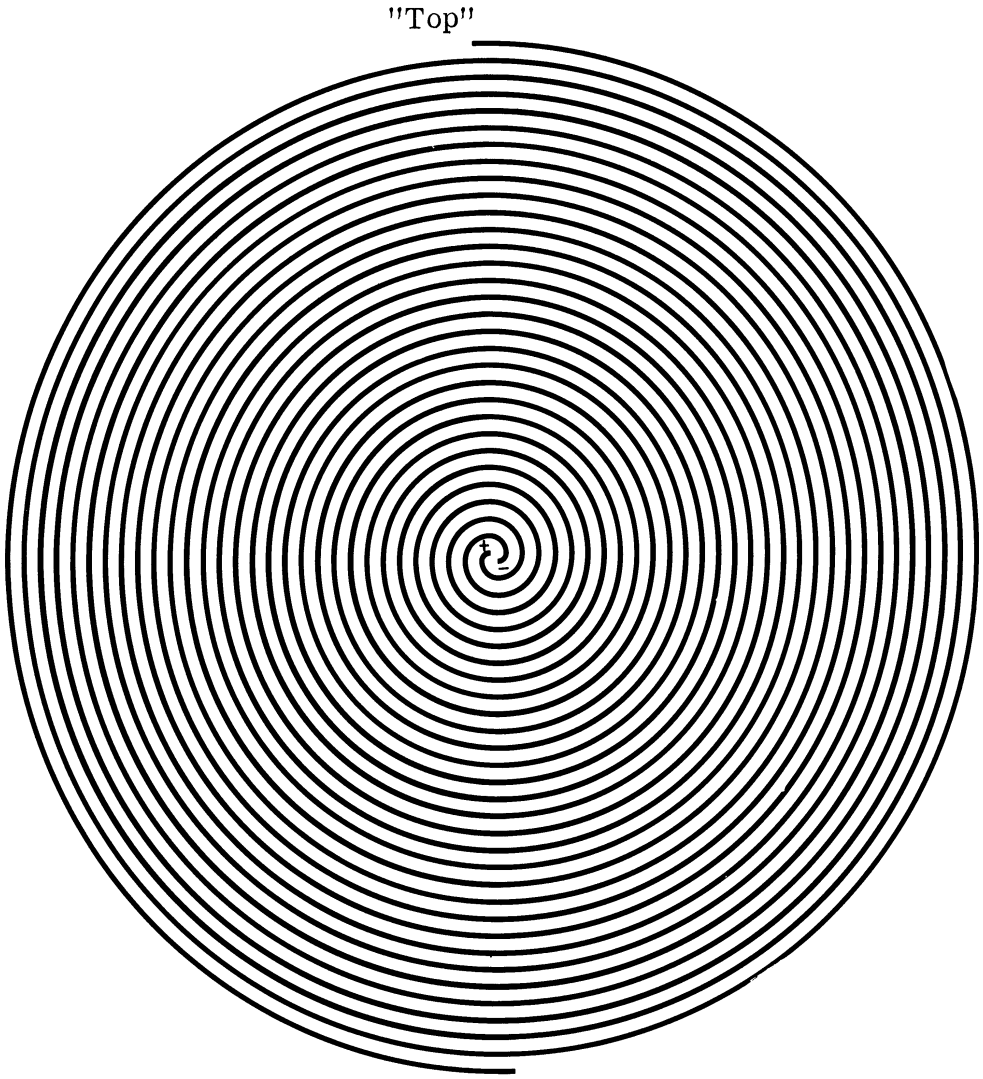

FIG. 3-3: 15 TURN BIFILAR SPIRAL

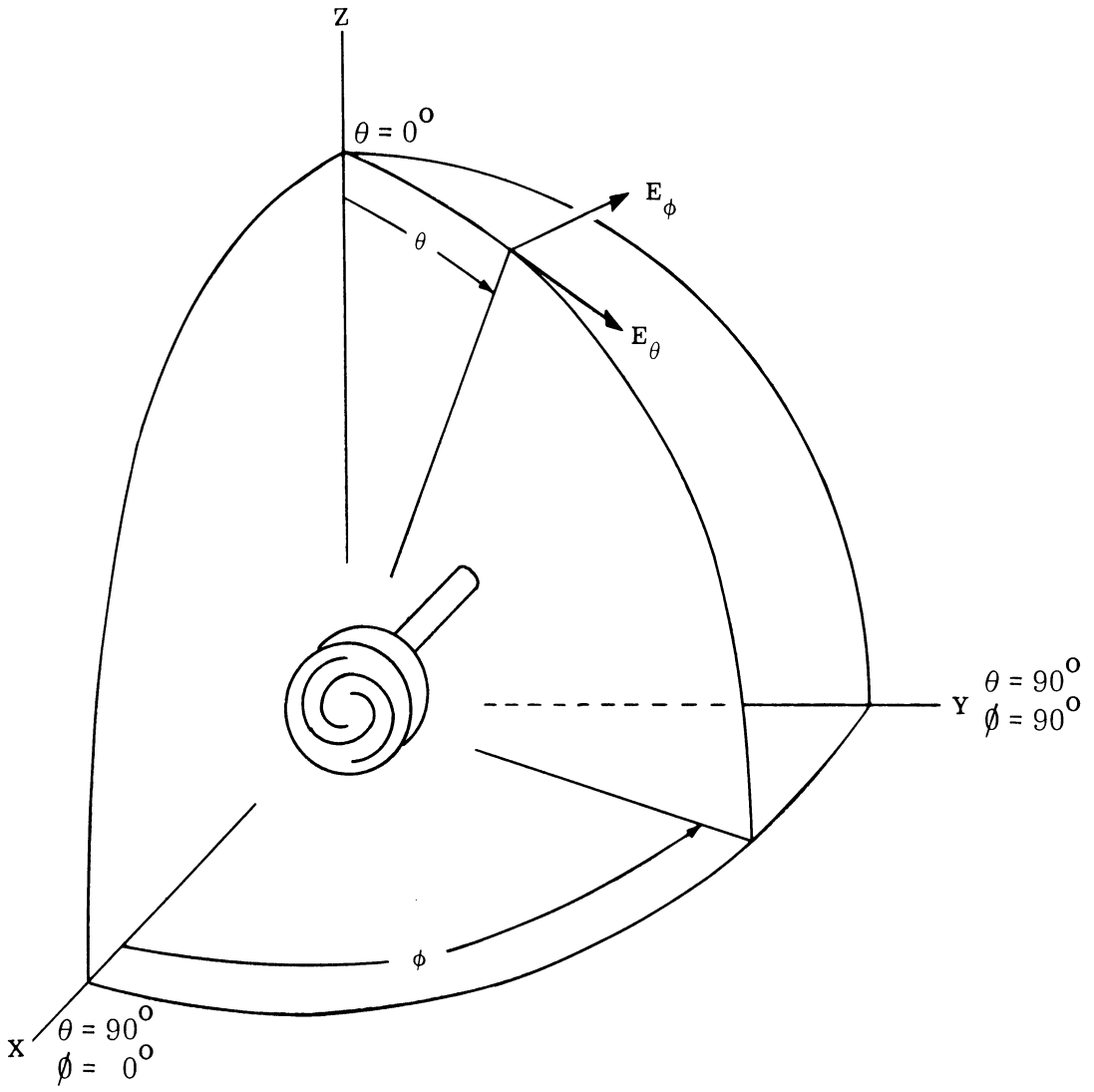

FIG. 3-4: SPIRAL ANTENNA COORDINATE SYSTEM

Pol. = E_ϕ
θ = 90°
ϕ = variable

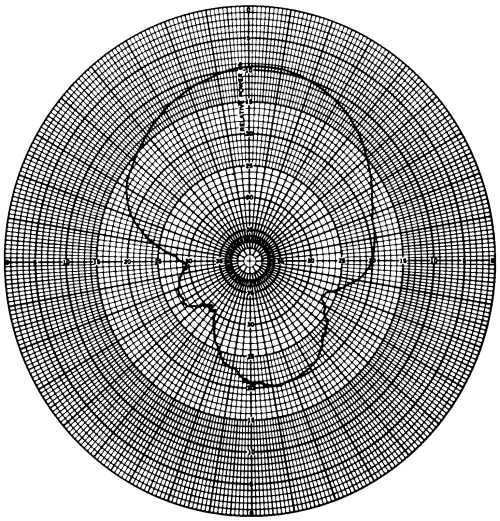

(a)

Pol. = E_θ
θ = 90°
ϕ = variable

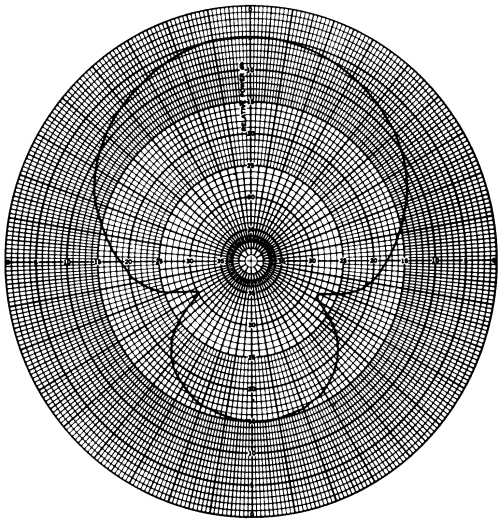

(b)

Ellipticity

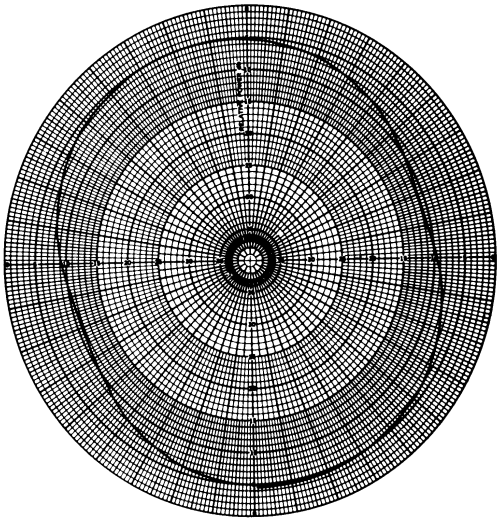

(c)

FIG. 3-5a, b, c: SPIRAL 16-7 PATTERN DATA AT 0.6 GHz

Pol. = E_{ϕ}
$\theta = 90^{o}$
ϕ = variable

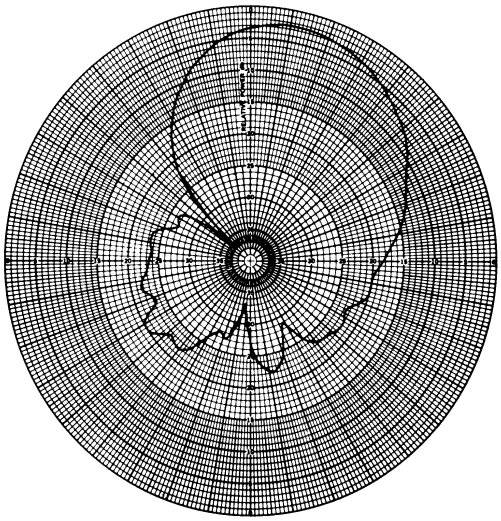

(a)

Pol. = E_{θ}
$\theta = 90^{o}$
ϕ = variable

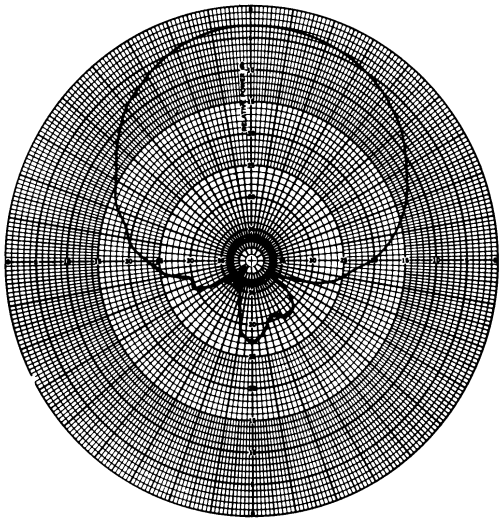

(b)

Ellipticity

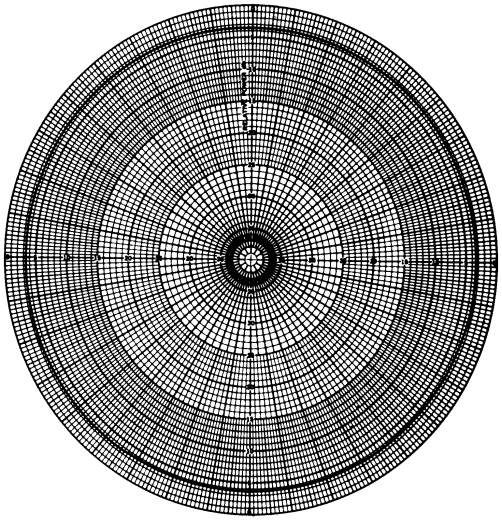

(c)

FIG. 3-6a, b, c: SPIRAL 16-7 PATTERN DATA AT 1.8 GHz

Pol. = E_ϕ
θ = 90°
ϕ = variable

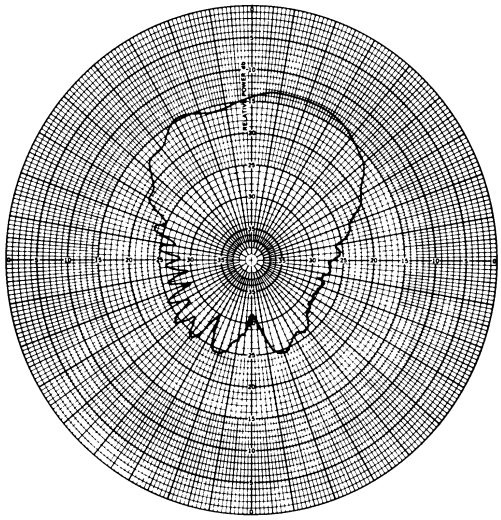

(a)

Pol. = E_θ
θ = 90°
ϕ = variable

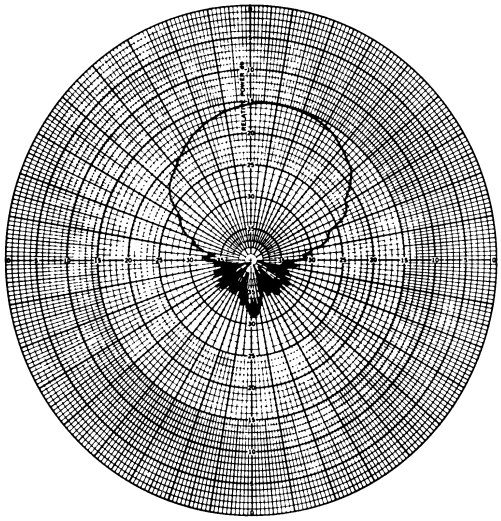

(b)

Ellipticity

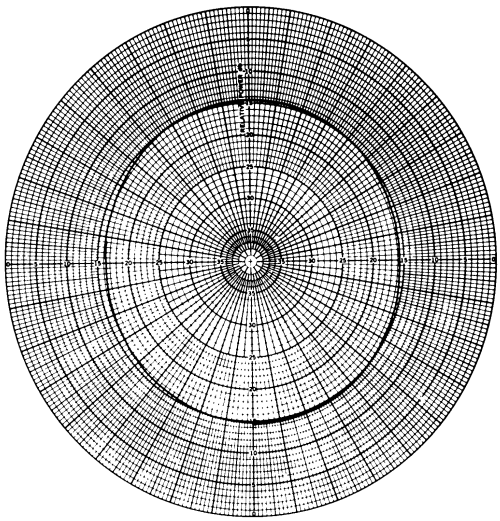

(c)

FIG. 3-7a, b, c: SPIRAL 16-7 PATTERN DATA AT 3.0 GHz

over most of the frequency range of interest except near the lowest end. With good agreement between the results of the five antennas mentioned above it was felt that the design configuration would be satisfactory and consideration was next given to typical data that would be obtained with a flat ground plane since the fabrication of the hemispherical ground plane had not been completed.

3.2.4 Spiral Experimental Data with Flat Ground Plane

A 4 x 6 foot flat ground plane was assembled and provisions made such that one to five spiral elemtns could be tested at a time. However, because of the limitation of time and funds data was collected only for a single and one pair of elements.

The impedance of four spirals (16-1, 16-2, 16-3 and 16-16) was measured and is referenced to the connector of Fig. 3-2, and is shown in Fig. 3-8 for a frequency of 1.8 GHz. This data was obtained by placing the spirals one at a time in the ground plane. It is found that the ground plane has slightly increased the VSWR in comparison to the Table III-I results.

Pattern characteristics of the 16 spirals were measured with the elements mounted individually into flat ground plane and data collected in accordance with the coordinate system of Fig. 3-9. Typical horizontal polarized (E_ϕ) patterns in $\theta = 90^\circ$, ϕ-variable plane for several elements (16-4, 16-7, 16-9, 16-8, 16-10 and 16-11) are shown in Fig. 3-10. It is evident from Fig. 3-10 that all the spiral antennas have approximately the same electrical performance. It is interesting to note that as compared to the case with no ground plane, the beam tends to be squinted from the axis of the spiral. The squinting is casued by unbalance currents in the balun which may excite higher modes in the antenna. However, because of the limited time, efforts were not made to correct this. This squinting tended to be prevalent only at the frequency of 1.8 GHz. In Fig. 3-10 the back lobe data was not recorded because of the inability to provide a reliable reading. It is felt that the individual pattern of a spiral antenna in the presence

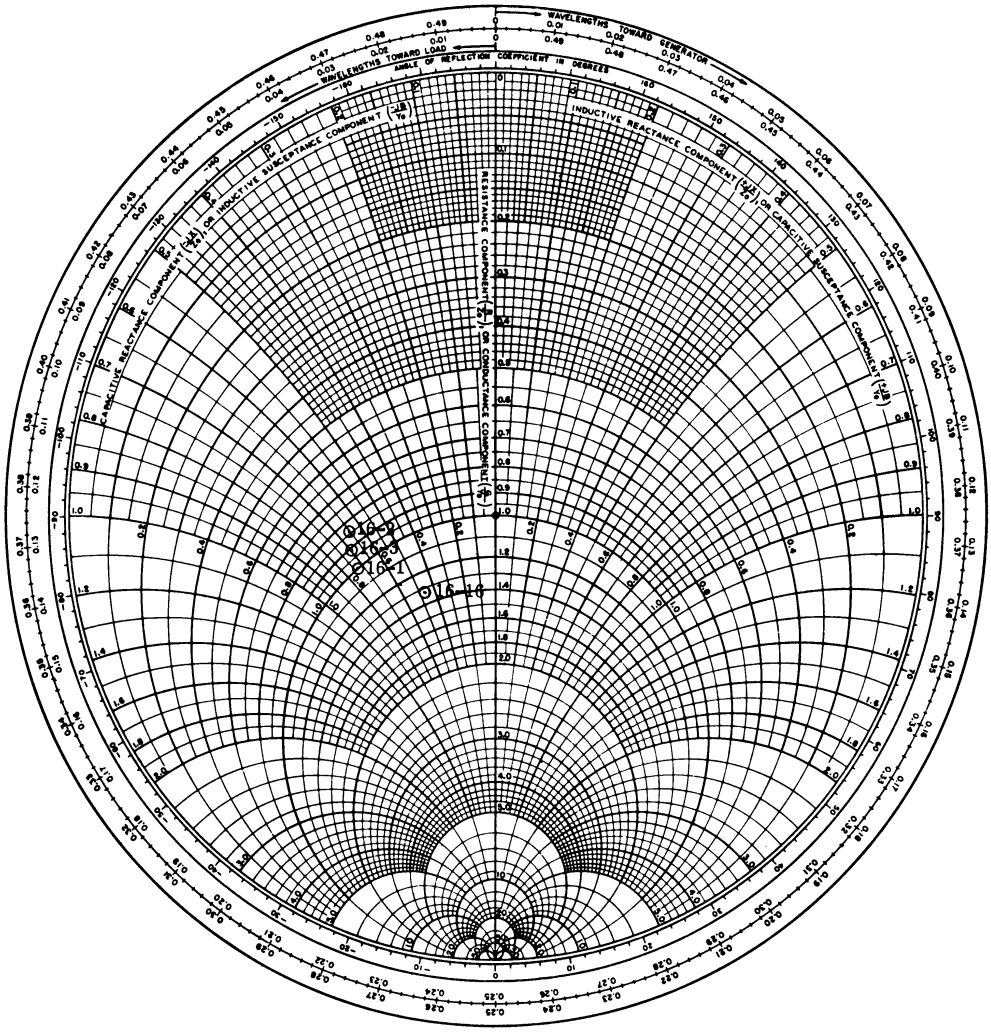

FIG. 3-8: SPIRAL IMPEDANCE AT 1.8 GHz

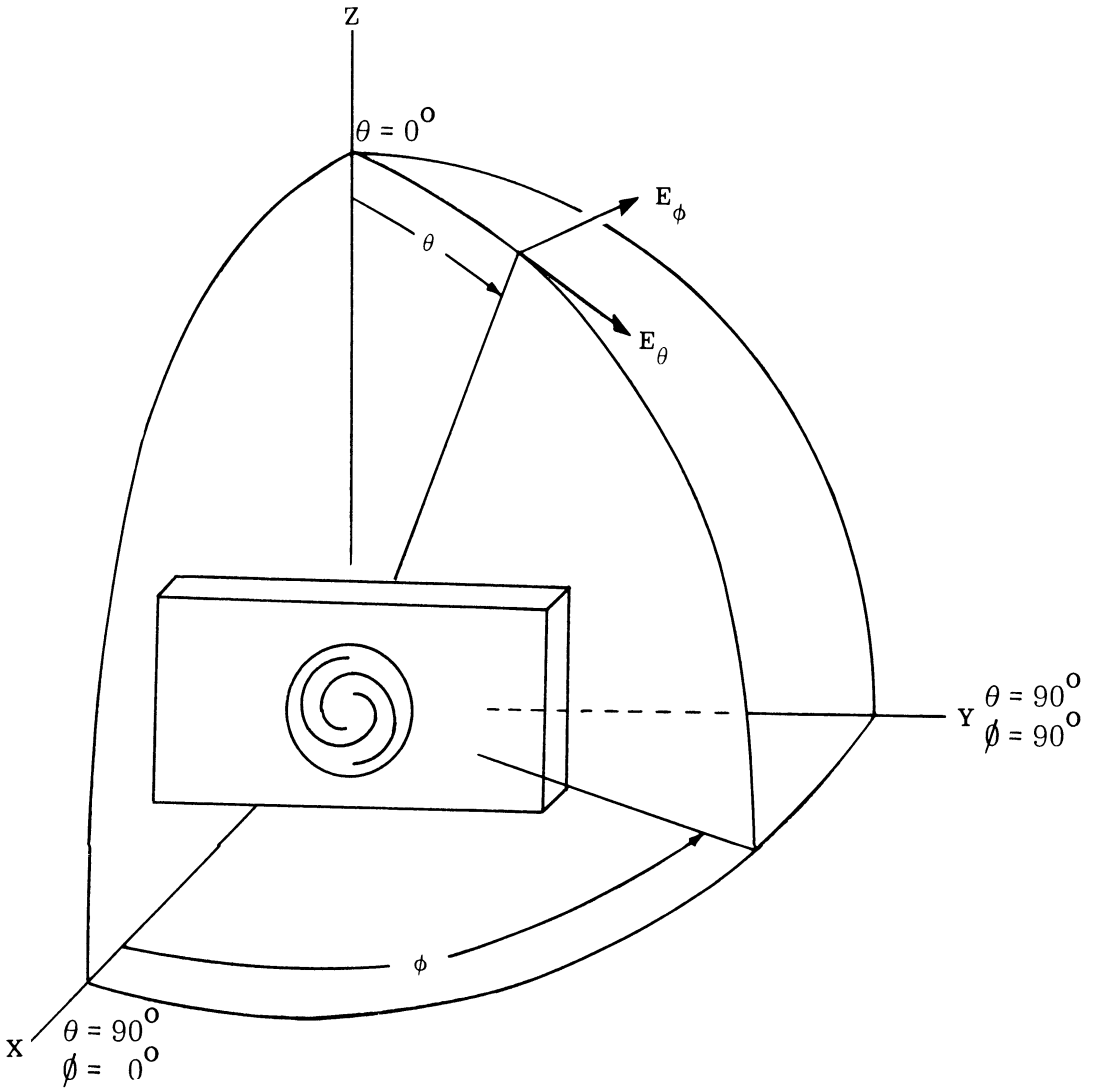

FIG. 3-9: FLAT GROUND PLANE COORDINATE SYSTEM

Spiral 16-4
Pol. = E_ϕ
$\theta = 90^o$
ϕ = variable

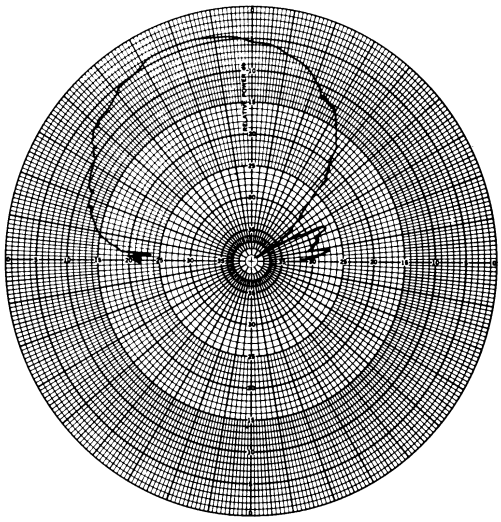

(a)

Spiral 16-7
Pol. = E_ϕ
$\theta = 90^o$
$\phi\delta$= variable

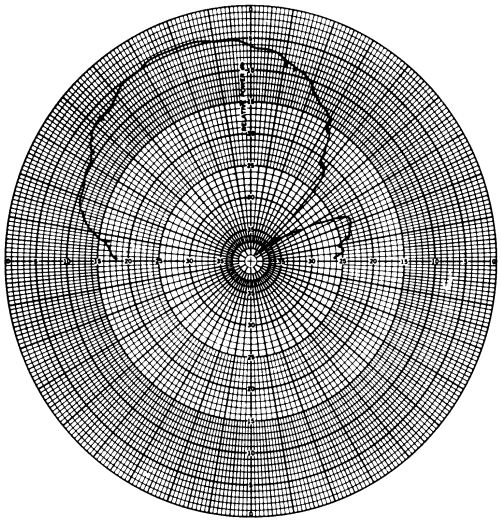

(b)

Spiral 16-8
Pol. = E_ϕ
$\theta = 90^o$
ϕ = variable

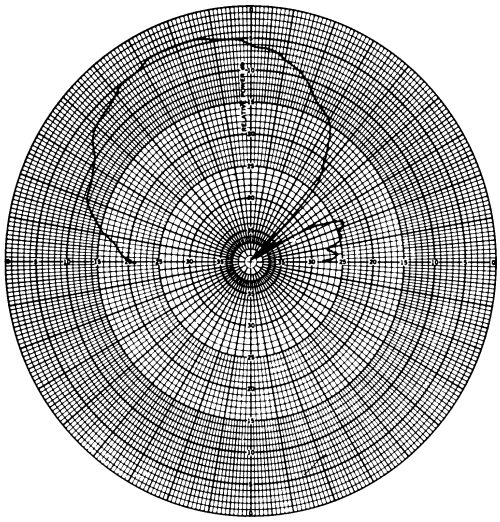

(c)

FIG. 3-10a, b, c: PATTERN OF SPIRAL WITH FLAT GROUND PLANE AT 1.8 GHz

Spiral 16-9
Pol. = E_ϕ
$\theta = 90^o$
ϕ = variable

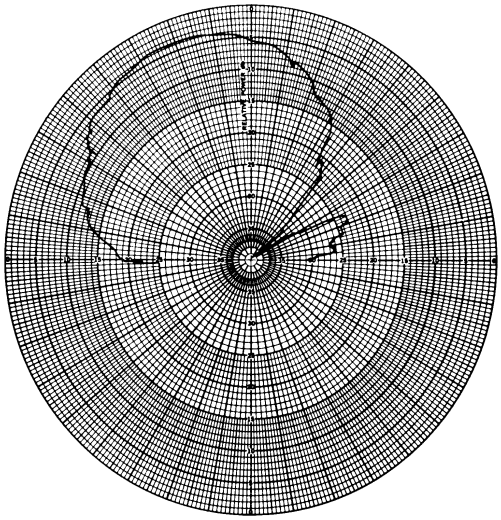

(d)

Spiral 16-10
Pol. = E_ϕ
$\theta = 90^o$
ϕ = variable

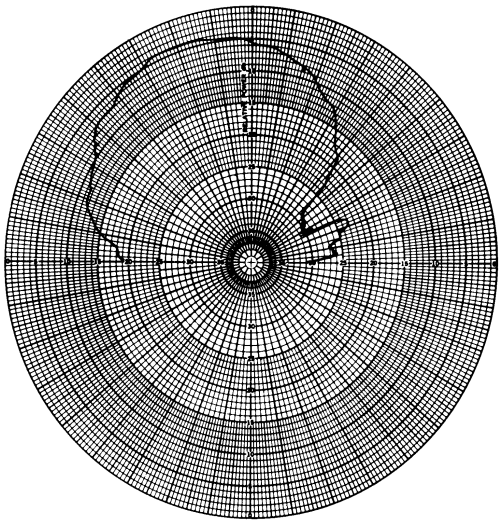

(e)

Spiral 16-11
Pol. = E_ϕ
$\theta = 90^o$
ϕ = variable

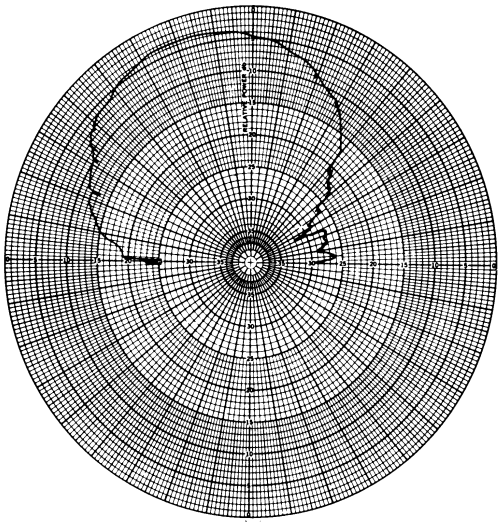

(f)

FIG. 3-10d,e,f: PATTERN OF SPIRAL WITH FLAT GROUND PLANE AT 1.8 GHz

of a spherical ground plane should be studied and compared with its corresponding pattern without ground plane. Because of time limitation it was not studied here.

3.3 Array Results

This section describes the results obtained from the study of three array configurations, namely a two element, a five element circular and a sixteen element spherical cap array. The two element array was studied in order to determine the phase variations in the radiated field caused by the rotation of the spiral about its axis. The five element circular array was studied to ensure that a uniform phase distribution could be obtained from the 8-way power divider. The array of sixteen spirals placed on a spherical cap was studied in order to verify our theorectical results.

3.3.1 Two Element Array Data

The two element array patterns were studied for the two configurations as shown in Fig. 3-11. The phase difference patterns were taken by physically orienting the reference mark ('top' of Fig. 3-2) of the reference antenna (16-1) to the upper half of the ground plane and that of the test antenna (16-N) to the lower half of the ground plane as shown in Fig. 3-11. The spiral 16-1 was employed as the reference antenna and the remaining 15 elements were referenced to determine the relative phase. Care was taken to ensure that the spirals were fed by equal phasing lines such that the impedance referred to the input of the feed cables was identical for each of the 16 spirals. All pattern data was collected at 1.8 GHz for E_ϕ polarization in the $\theta = 90^\circ$, ϕ variable plane (see Fig. 3-9). Phase difference and phase addition patterns are shown in Fig. 3-12. The data shown in Fig. 3-12 is typical of that obtained for the 16 spirals. The occurrence of a null at $\phi = 0^\circ$ for the phase difference patterns and a maximum at $\phi = 0^\circ$ for the phase addition pattern confirmed the theoretical prediction, discussed before,

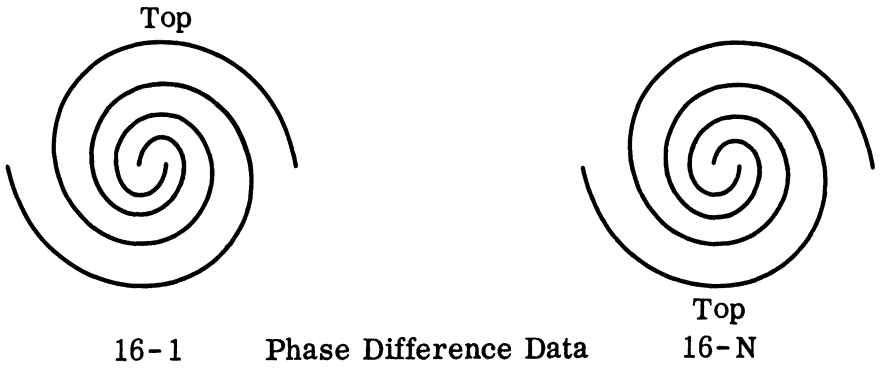

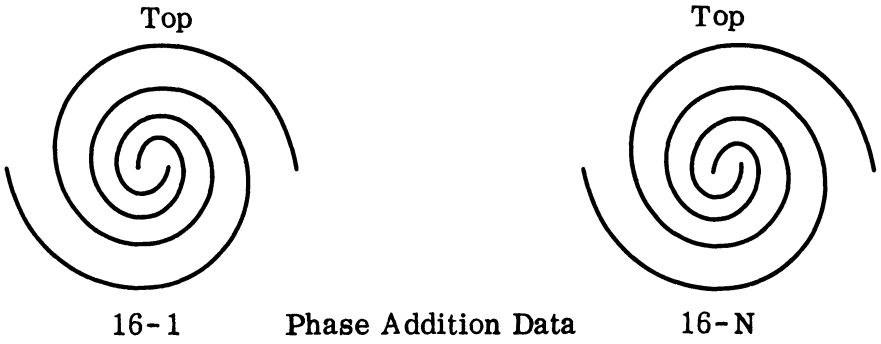

FIG. 3-11: ORIENTATION OF SPIRALS FOR PHASE DATA

Phase Difference
Pol. = E_ϕ
$\theta = 90^o$
ϕ = variable

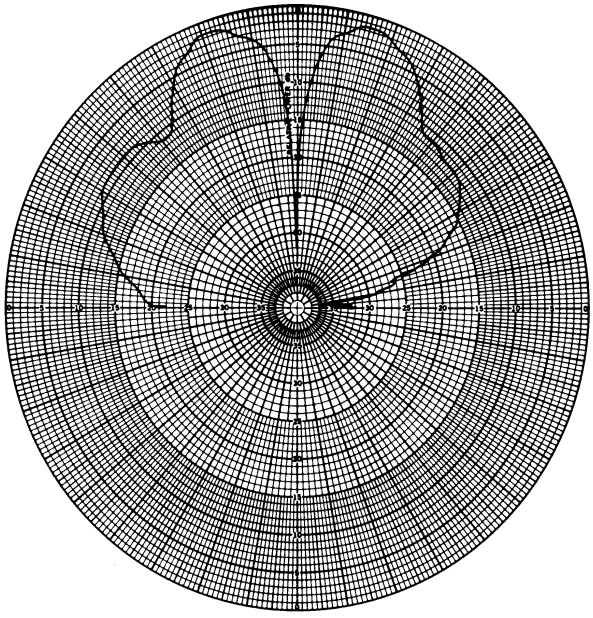

(a)

Phase Addition
Pol. = E_ϕ
$\theta = 90^o$
ϕ = variable

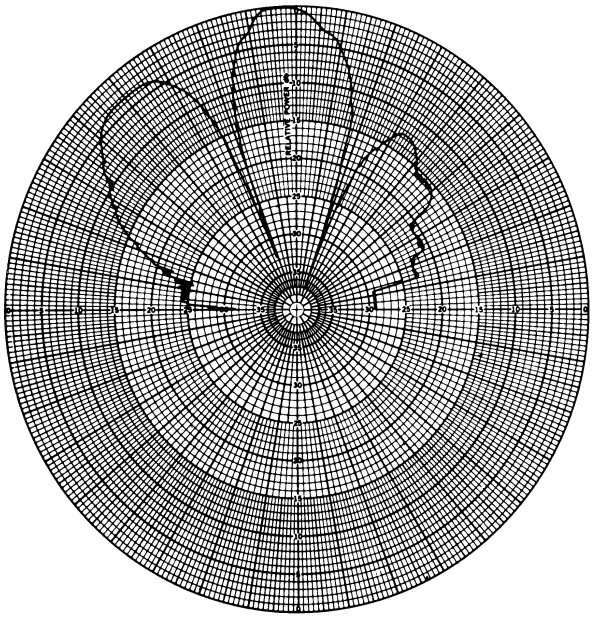

(b)

FIG. 3-12a, b: PATTERN PHASING DATA

that there is a one to one correspondence between the mechanical rotation of the spiral about its axis and the phase of the radiated field in the lowest mode of operation. After comparing the results obtained from all the 16 elements it was concluded that the phase characteristics of the 16 elements were essentially identical.

3.3.2 Five Element Circular Array (Hemispherical Ground Plane)

To obtain the necessary pattern data to evaluate the strip line power dividers, five spirals were installed in the 6' diameter hemispherical ground plane. The detailed design and construction of the strip line power divider and the hemispherical ground plane are described in Appendix A and Appendix B, respectively. Before discussing the results obtained from this aspect of the study it is appropriate to give a short description of the element arrangement on the hemispherical ground plane.

Sixteen holes were placed in the hemispherical ground plane as shown in Fig. 3-13 in accordance with the coordinate system of Fig. 3-14. One hole was located at the north pole ($\theta = 0^{o}$), a ring of five holes were equally spaced at $\theta = 15^{o}$; $\phi_n = n\,72^{o}$ (where n=0, 2, ... 5) and 10 holes were equally spaced at $\theta = 30^{o}$; $\phi_n = n\,36^{o}$ where n=1, 2, ... 10). To evaluate the electrical characteristics of the 8-way power dividers a five element array was assembled by placing five elements in the $\theta = 15^{o}$ ring of Fig. 3-13. Elements were not placed in the remaining 11 holes and therefore the holes remained uncovered during the tests for the 5 element array.

Both phase difference and phase addition patterns were collected along two principal planes (θ variable: $\phi = \left[0^{o}; 180^{o}\right]$ and $\phi = \left[90^{o}; 270^{o}\right]$) of the hemispherical array and for two polarizations (E_θ and E_ϕ). Phase difference patterns were obtained by orienting each spiral on the inner ring such that their phase reference vector was parallel to the $\phi = 0^{o}$, 72^{o} ... 360^{o} radials, as shown in Fig. 3-15, extending from the apex of the hemisphere; the corresponding reference

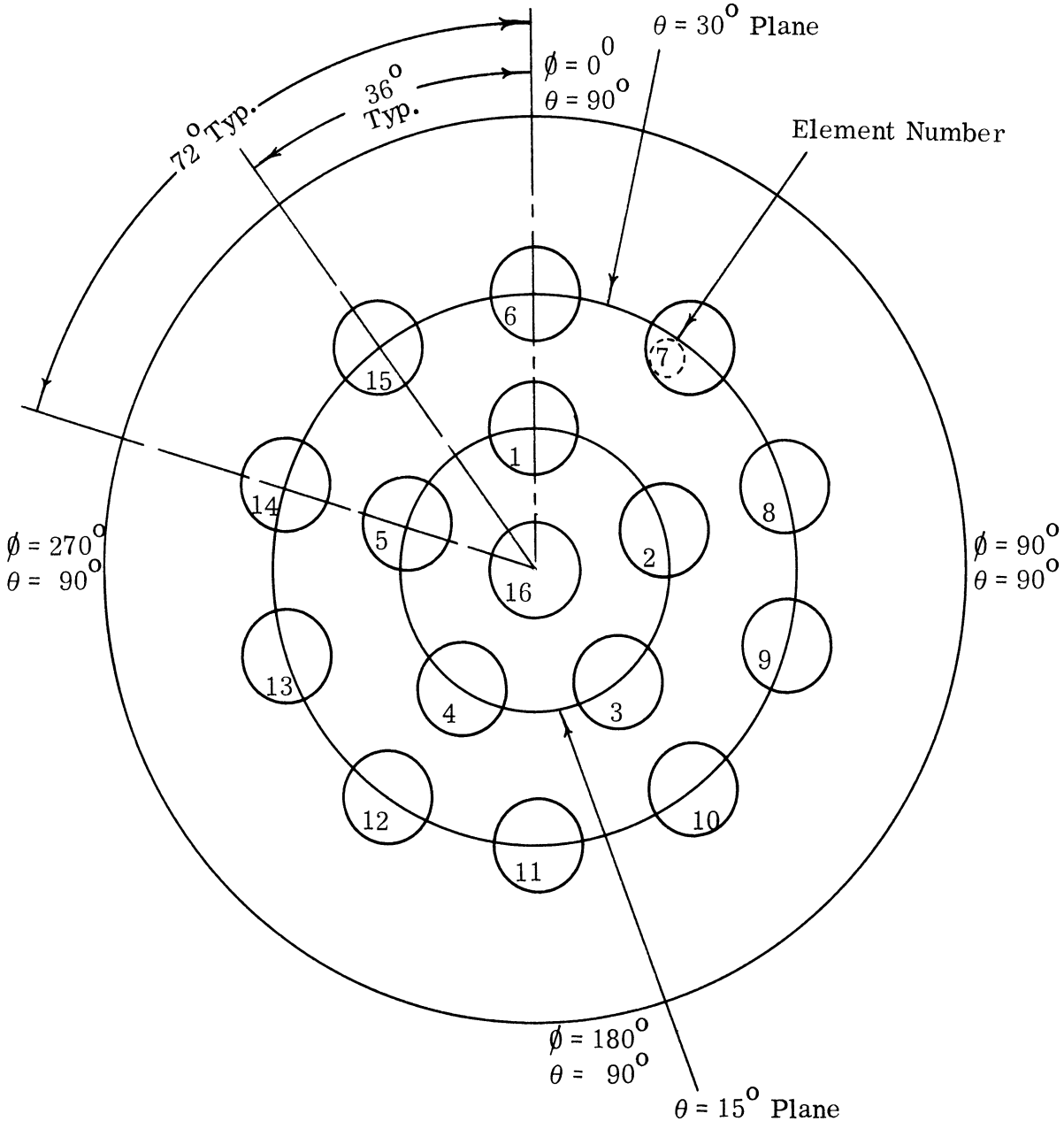

FIG. 3-13: PHYSICAL HOLE LAYOUT FOR HEMISPHERICAL ARRAY

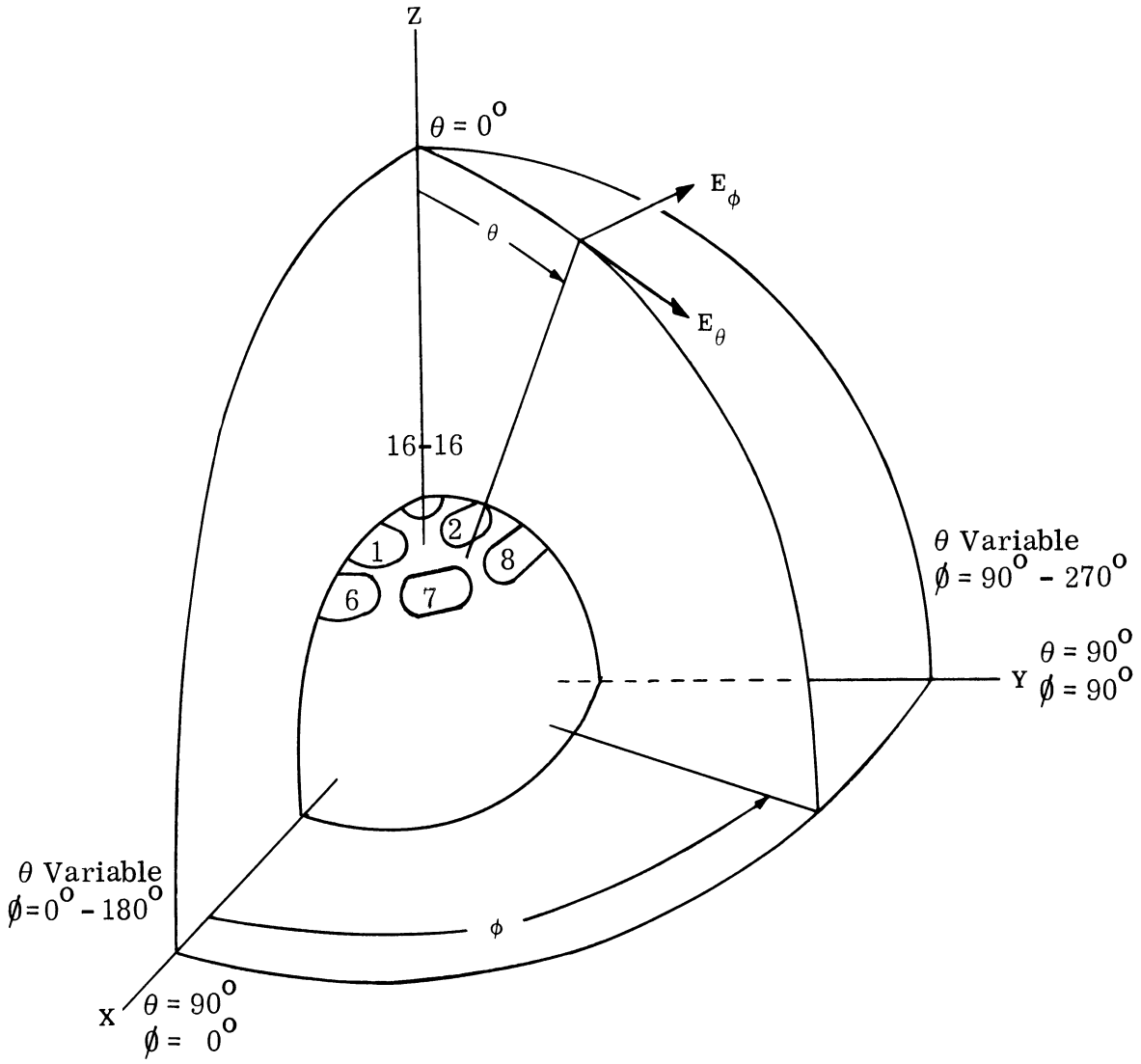

FIG. 3-14: COORDINATE SYSTEM FOR HEMISPHERICAL GROUND PLANE

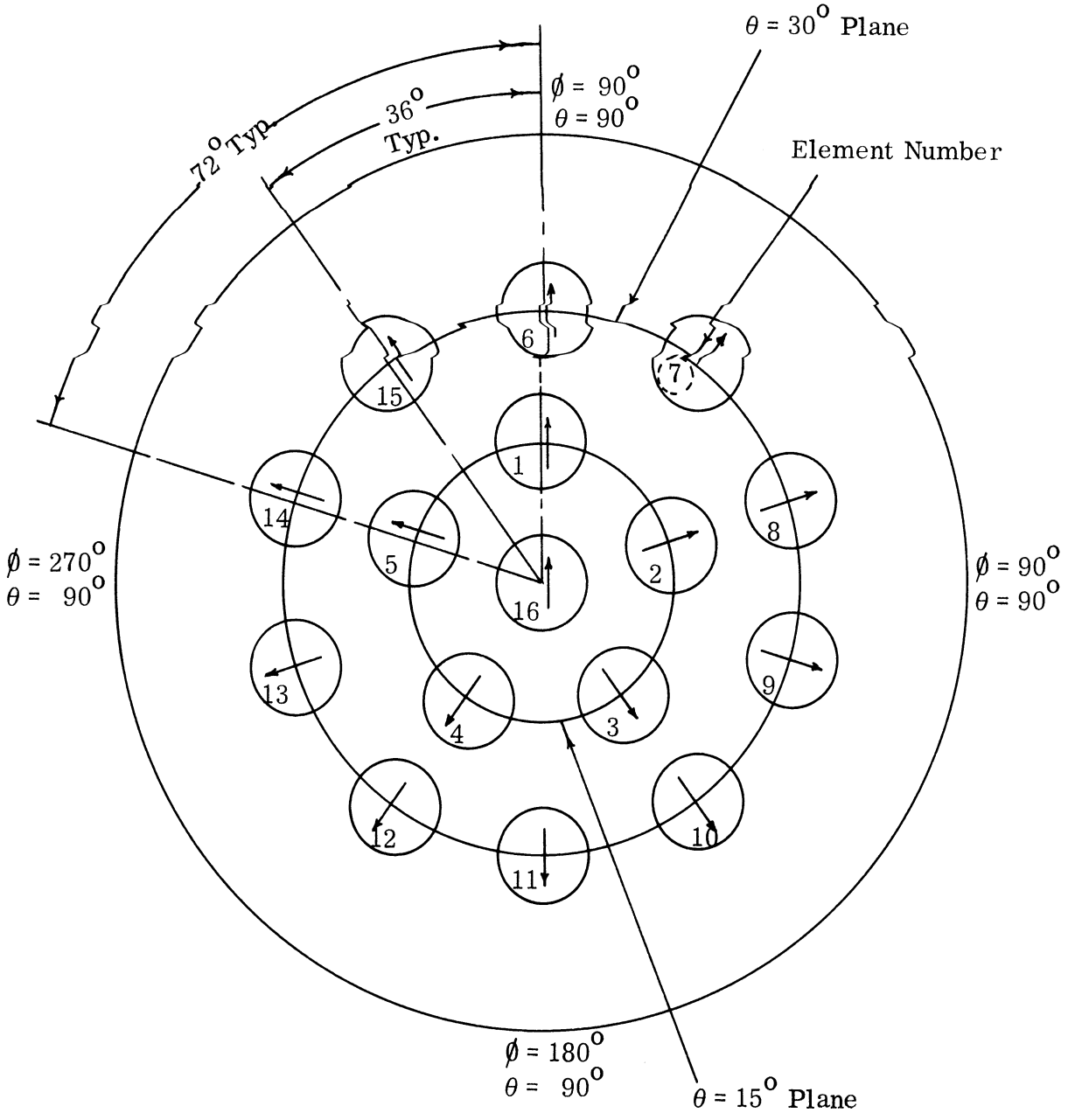

FIG. 3-15: PHASE DIFFERENCE ORIENTATION

vectors of the spirals on the outer ring were oriented parallel to 0^{o}, 36^{o}, 72^{o} ... , etc. Phase addition patterns were obtained by physically re-orienting the elements such that all reference vectors of the spirals were parallel as shown in Fig. 3-16. Both Figs. 3-15 and 31-6 show all 16 elements since they will be referenced later in the report.

Since an 8-way power divider was employed to excite the five element array, it was necessary to terminate the three unused terminals with 50Ω loads to minimize reflections from them. Typical phase difference and phase addition patterns are shown in Fig. 3-17 and Fig. 3-18, respectively. The multiple lobes in the patterns are the pseudo-grating lobes caused by the large spacing between the elements. Since the main purpose of this study was to study the performance of the power divider and the individual elements we do not discuss the patterns further at this time. The results given in this section indicated that the power divider and the individual spiral antennas were operating satisfactorily.

3.3.3 Sixteen Element Array (Hemispherical Ground Plane)

The element distribution of this array on the hemispherical ground plane is as shown in Fig. 3-13. This particular array was studied in order to verify some of the theoretical results and, moreover, this is very similar to the one proposed for the system implementation.

For the purpose of theoretical computation two assumptions were made that should be noted here. First, it was assumed that the far field radiation pattern of a spiral could be mathematically expressed as a cosine function over the hemisphere (Eq. 3.3). However, in practice this is not true but for the purpose of the present study, this was felt to be a good approximation for the pattern of the spiral. Second, it was assumed that E_{θ} and E_{ϕ} patterns for the spiral were essentially the same. Again, this assumption is not strictly true, but it was felt to be a reasonable assumption. The reader should, therefore, be aware that exact agreement between the theoretical and experimental results reported

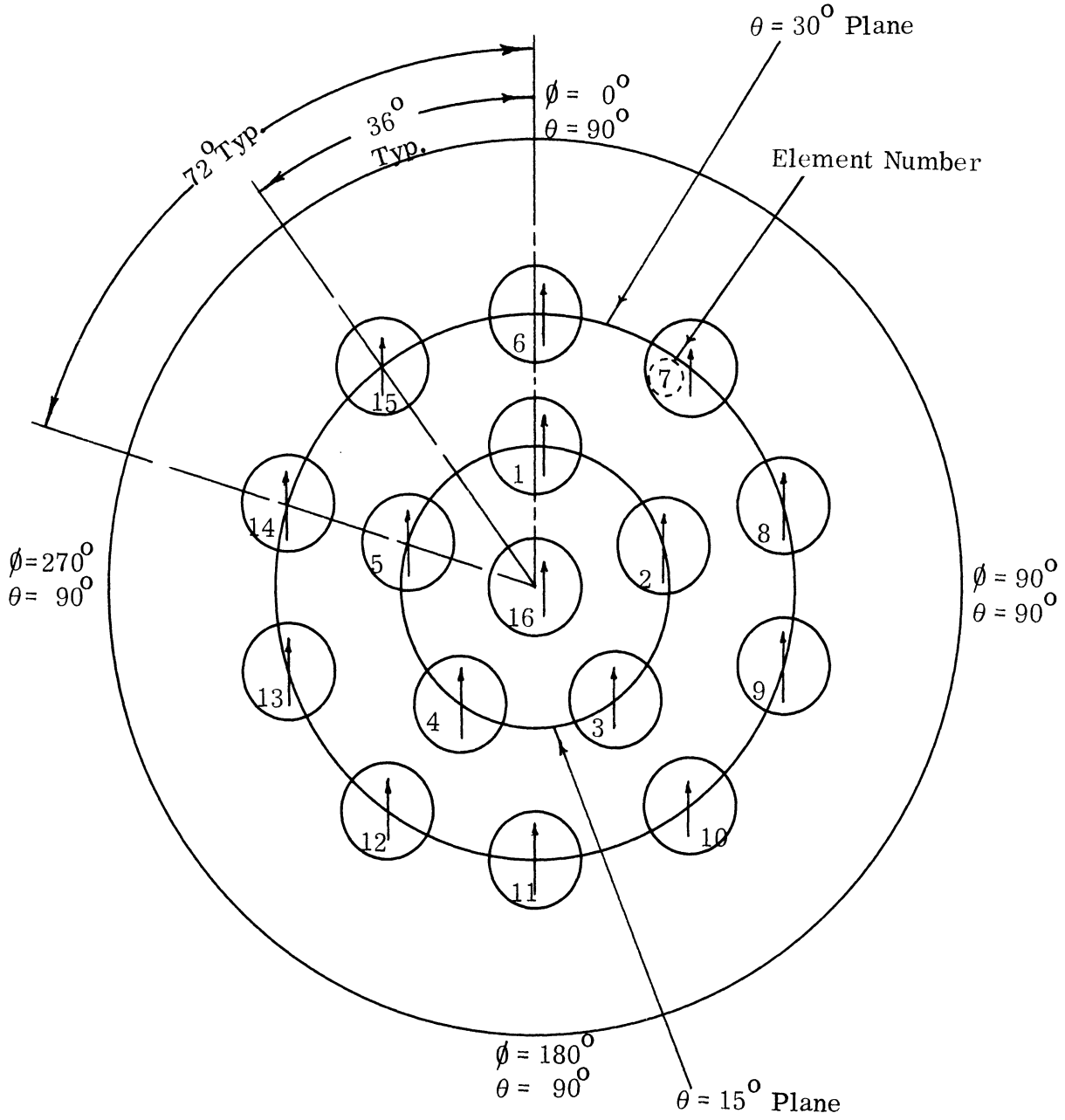

FIG. 3-16: PHASE ADDITION ORIENTATION

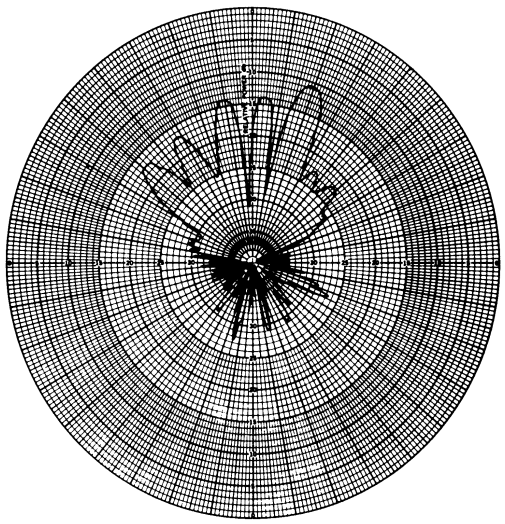

f = 3.0 GHz
Pol. = E_θ
θ = variable
ϕ = 90^o; 270^o

(a)

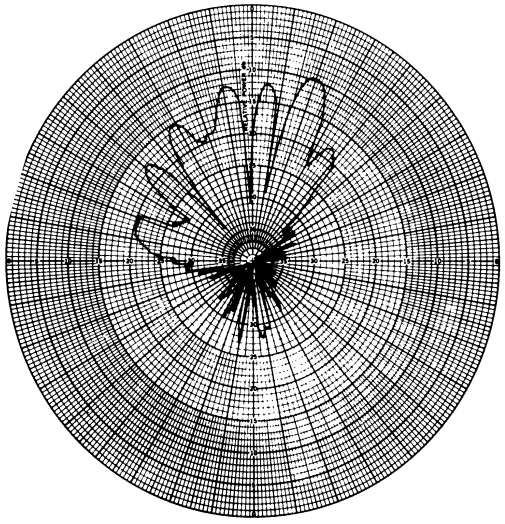

f = 3.0 GHz
Pol. = E_ϕ
θ = variable
ϕ = 90^o; 270^o

(b)

FIG. 3-17a, b: 5 ELEMENT ARRAY PHASE DIFFERENCE DATA

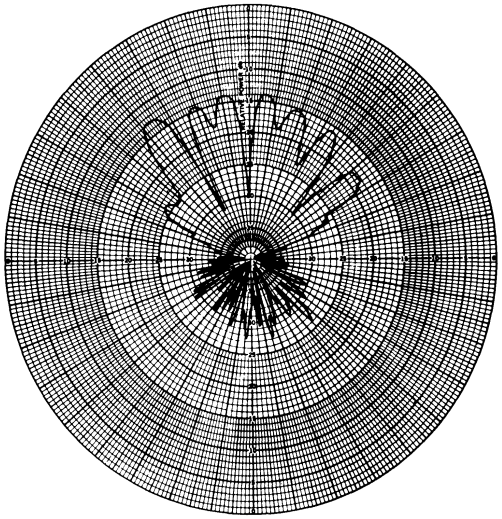

f = 3.0 GHz
Pol. = E_θ
θ = variable
ϕ = 0^o, 180^o

(c)

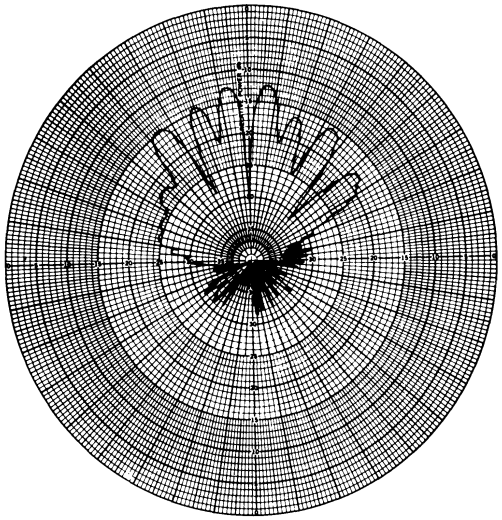

f = 3.0 GHz
Pol. = E_ϕ
θ = variable
ϕ = 0^o; 180^o

(d)

FIG. 3-17c,d: 5 ELEMENT ARRAY PHASE DIFFERENCE DATA

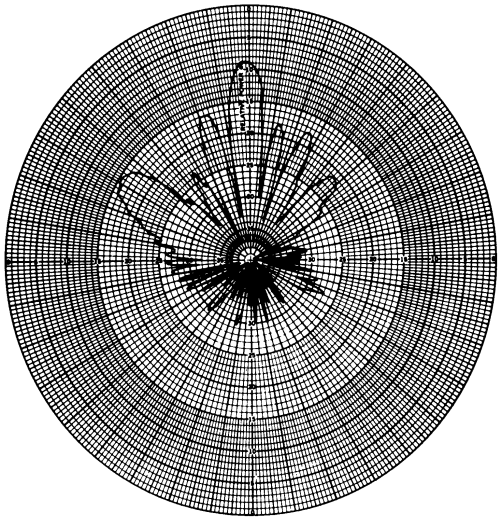

f = 3.0 GHz
Pol. = E_θ
θ = variable
ϕ = 90°; 270°

(a)

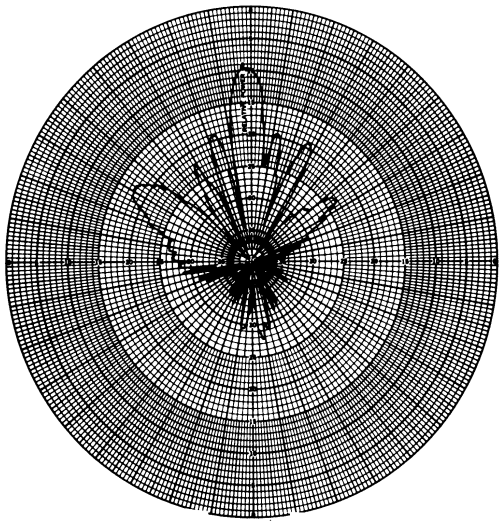

f = 3.0 GHz
Pol. = E_ϕ
θ = variable
ϕ = 90° ; 270°

(b)

FIG. 3-18a, b: 5 ELEMENT ARRAY PHASE ADDITION DATA

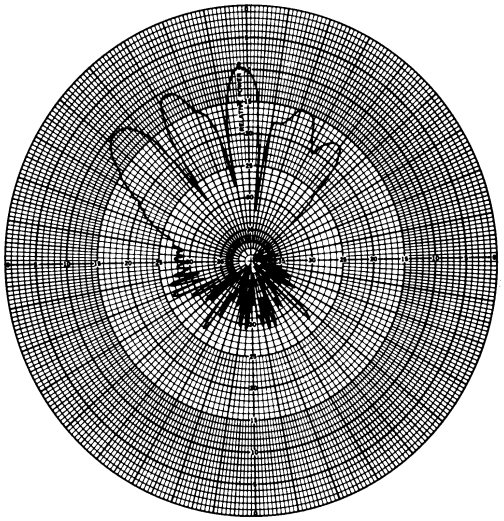

f = 3.0 GHz
Pol. = E_θ
θ = variable
ϕ = 0^o; 180^o

(c)

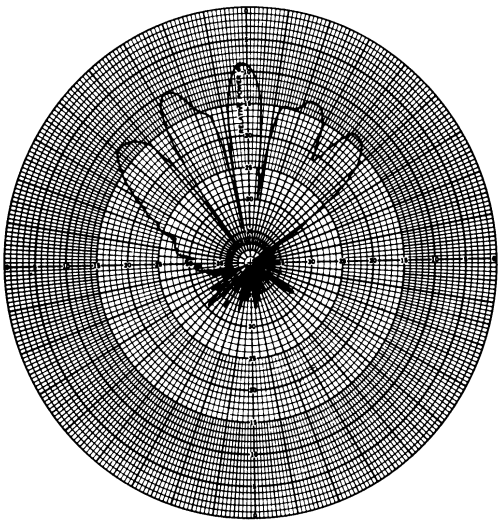

f = 3.0 GHz
Pol. = E_ϕ
θ = variable
ϕ = 0^o; 180^o

(d)

FIG. 3-18c, d: 5 ELEMENT ARRAY PHASE ADDITION DATA

here is not expected. It will be seen that inspite of these assumptions the two sets of results reported here demonstrate fair agreement and the dependability of the theory.

Theoretical data had been calculated previously for two frequencies (982 and 2620 MHz). This data was calculated for two conditions which were with and without time delay correction. A discussion of the time delay is now necessary. The time delay is to correct for the physical displacement of the spirals (located at $\theta = 15^{\circ}$ and 30°) from the north pole of the hemisphere. In practice this time delay is accomplished by installing transmission lines of the appropriate electrical length to correct for physical displacement of the spirals so that a uniform phase distribution will exist on a plane parallel to the surface that is normal to the Z axis and (tangent to the hemisphere at $\theta = 0^{\circ}$) of Fig. 3-14.

Perhaps it is appropriate to give a short discussion on the three types of patterns discussed in this section. The phase difference and phase addition patterns without time delay corrections refer to the cases when the spiral elements are oriented on the spherical surface as shown in Figs. 3-15 and 3-16, but they are fed with equal lengths of lines. The patterns with time delay corrections refer to those obtained from the array when the elements are oriented as in Fig. 3-16 but the lengths of the delay lines are chosen such as to produce a maximum along the desired direction.

A theoretical pattern is shown in Fig. 3-19 for the following conditions: 1) frequency of 982 MHz, 2) no time delay correction, 3) elements are oriented to produce a phase difference pattern (Fig. 3-15). Figure 3-20 shows experimental patterns for the 16 elements having the conditions noted above for the θ variable plane along $\phi = (0^{\circ}; 180^{\circ})$ for both E_{θ} and E_{ϕ} polarizations. Figures 3-21 and 3-22 are respectively theoretical and experimental patterns employing the same condition as noted above for 982 MHz.

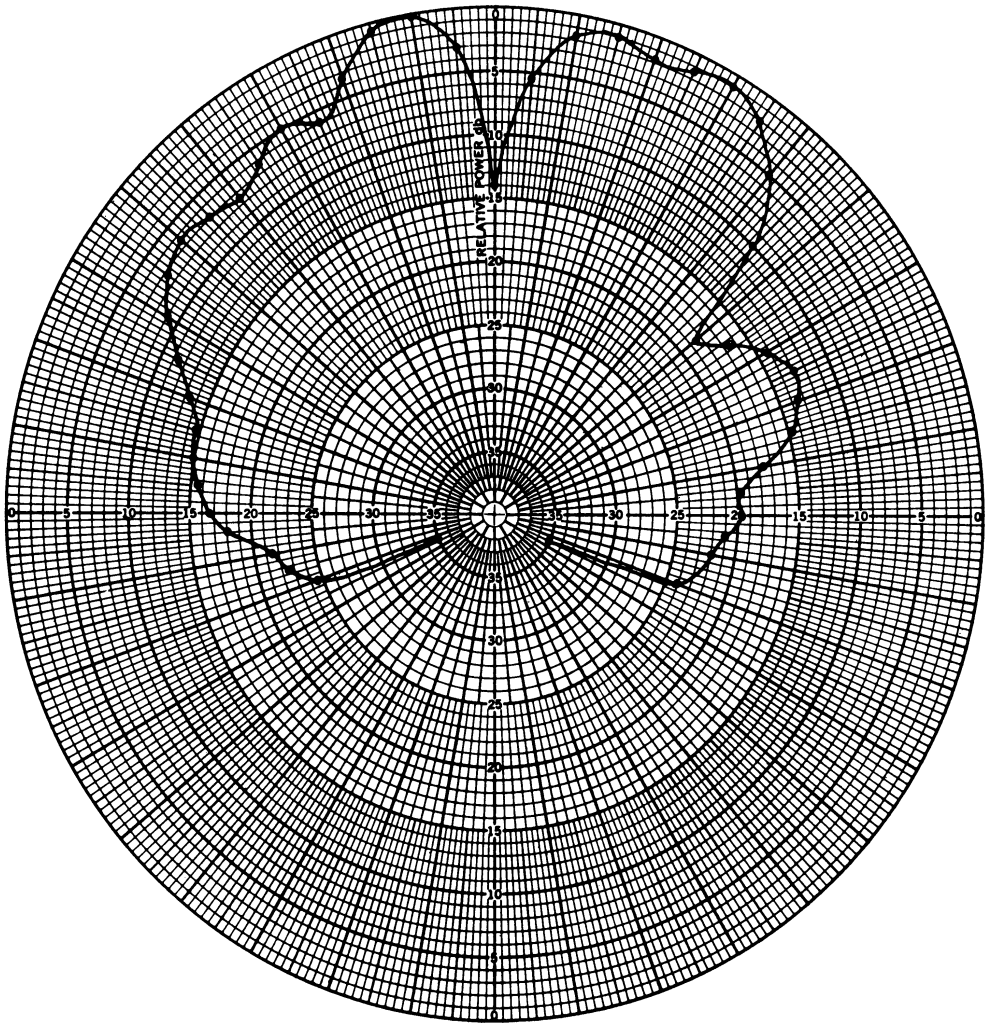

f = 982 MHz
θ = variable

FIG. 3-19: THEORETICAL PHASE DIFFERENCE PATTERN OF 16 ELEMENT ARRAY WITH NO TIME DELAY COORECTION

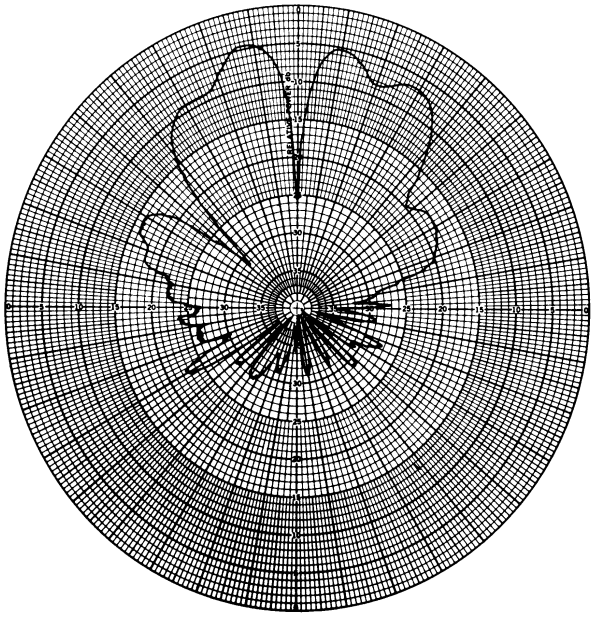

f = 982 MHz
Pol. = E_θ
θ = variable
$\phi = 0^o; 180^o$

(a)

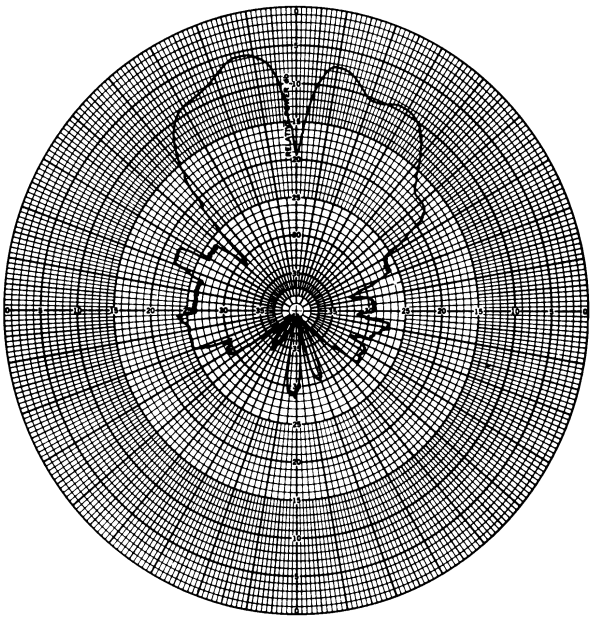

f = 982 MHz
Pol. = E_ϕ
θ = variable
$\phi = 0^o; 180^o$

(b)

FIG. 3-20a, b: EXPERIMENTAL PHASE DIFFERENCE PATTERN OF 16 ELEMENT ARRAY WITH NO TIME DELAY CORRECTION

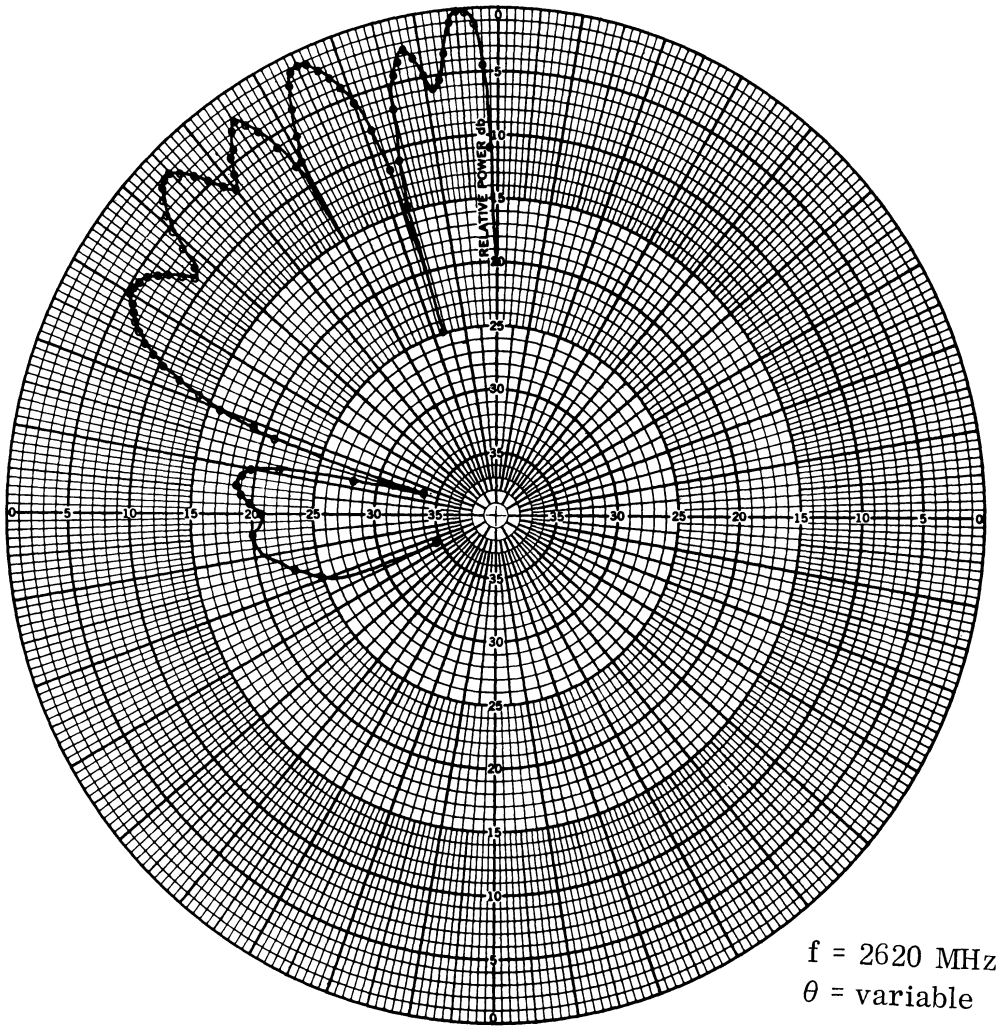

FIG. 3-21: THEORETICAL PHASE DIFFERENCE PATTERN FOR A 16 ELEMENT ARRAY WITH NO TIME DELAY CORRECTION

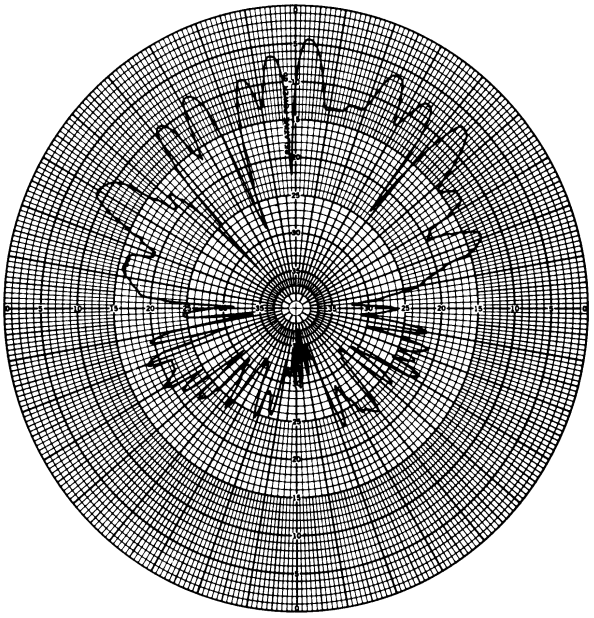

f = 2620 MHz
Pol. = E_θ
θ = variable
ϕ = 90°; 270°

(a)

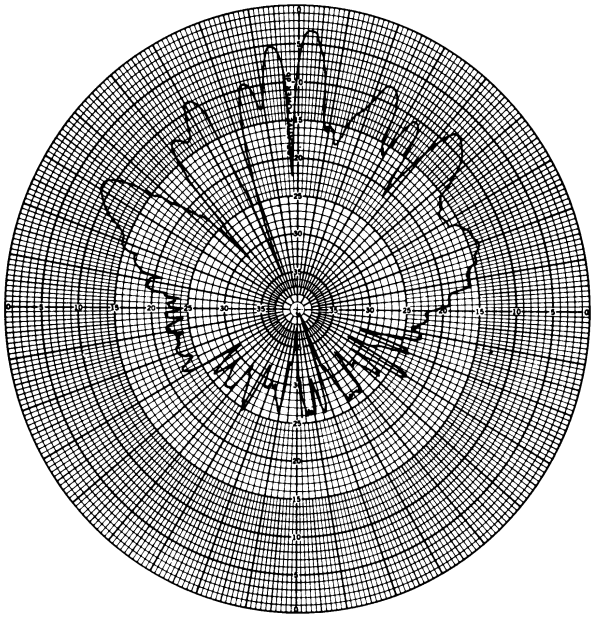

f = 2620 MHz
Pol. = E_ϕ
θ = variable
ϕ = 90°; 270°

(b)

FIG. 3-22a, b: EXPERIMENTAL PHASE DIFFERENCE PATTERN FOR A 16 ELEMENT ARRAY WITH NO TIME DELAY CORRECTION

Figure 3-23 is a theoretical phase addition pattern (Fig. 3-16) with no time delay correction for 982 MHz. Typical experimental patterns with θ variable, $\phi = (90^{\circ}; 270^{\circ})$ are shown for this case for 982 and 2620 MHz, respectively in Figs. 3-24 and 3-25. Each of these figures show the response of the 16 element array to both E_{θ} and E_{ϕ} polarized energy. From these figures it can be seen that no well defined major lobe is formed. The principal cause for the poor pattern response is due to the location of the in phase elements on the hemispherical surface rather than on a planar surface, as noted previously. To correct for this displacement the appropriate time delays for elements located at $\theta = 15^{\circ}$ and 30° were calculated and incorporated in the theoretical phase addition computer programs. Theoretical patterns for the 16 element array, with the above time delays included, were calculated for two principal planes ($\phi = [0^{\circ}; 180^{\circ}]$ and $[90^{\circ}; 270^{\circ}]$) at a frequency of 982 MHz and are shown in Fig. 3-26. Typical experimental data employing the appropriate time delays are shown in Fig. 3-27 for comparison. Again, data is shown for both E_{ϕ} and E_{θ} polarization. Figure 3-28 is a partial plot of a theoretical phase addition pattern that was calculated for a frequency of 2620 MHz with the appropriate time delays included in the computer program. This data was calculated for the θ variable, $\phi = (90^{\circ}; 270^{\circ})$ plane. Figure 3-29 illustrates typical experimental data that was recorded at 2620 MHz employing the appropriate time delays.

Considering the idealized pattern assumed for the individual spiral in the theoretical model, the agreement between the theoretical and experimental results with respect to the beamwidth, side-lobe levels and positions in the patterns is considered to be satisfactory. The strong lobes obtained in the patterns in the high frequency end (Fig. 3-29) are the pseudo-grating lobes caused by large effective spacing between the elements in this range. However, the grating lobe behavior is still much better than that obtained in the uniform planar antenna array. It is expected that the amplitudes of the pseudo-grating lobes will be

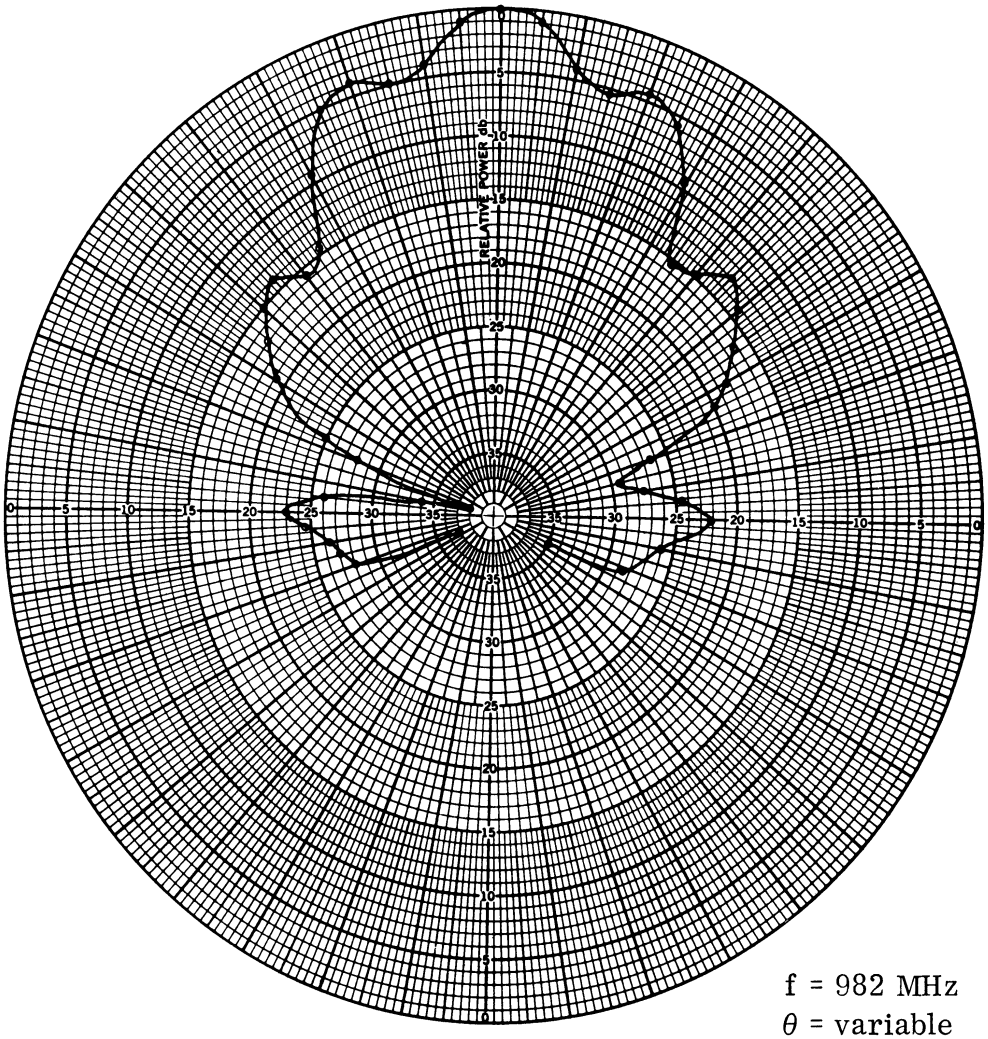

FIG. 3-23: THEORETICAL PHASE ADDITION PATTERN FOR A 16 ELEMENT ARRAY WITH NO TIME DELAY CORRECTION

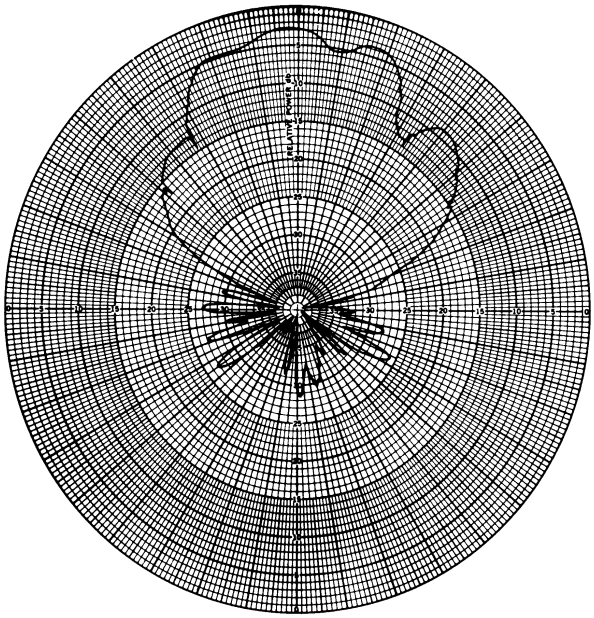

f = 982 MHz
Pol. = E_{ϕ}
θ = variable
ϕ = 90°; 270°

(a)

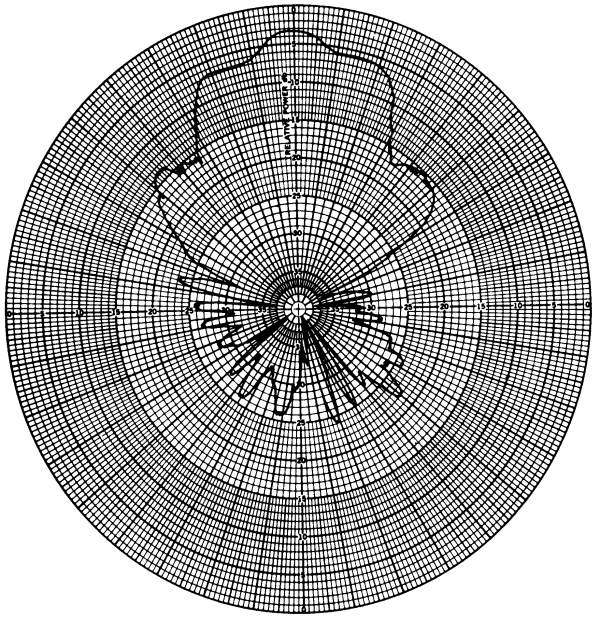

f = 2620 MHz
Pol. = E_{θ}
θ = variable
ϕ = 90°; 270°

(b)

FIG. 3-24a, b: EXPERIMENTAL PHASE ADDITION PATTERN FOR A 16 ELEMENT ARRAY WITH NO TIME DELAY CORRECTION

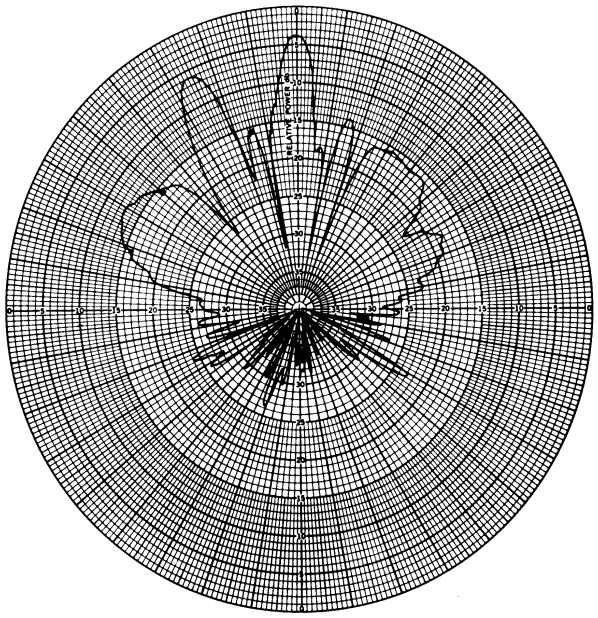

f = 2620 MHz
Pol. = E_{ϕ}
θ = variable
ϕ = 90^{o}; 270^{o}

(a)

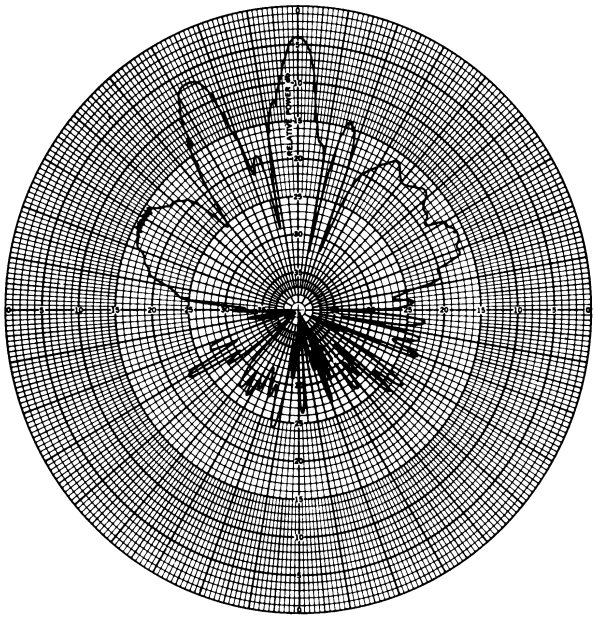

f = 2620 MHz
Pol. = E_{θ}
θ = variable
ϕ = 90^{o}; 270^{o}

(b)

FIG. 3-25a, b: EXPERIMENTAL PHASE ADDITION PATTERN FOR A 16 ELEMENT ARRAY WITH NO TIME DELAY CORRECTION

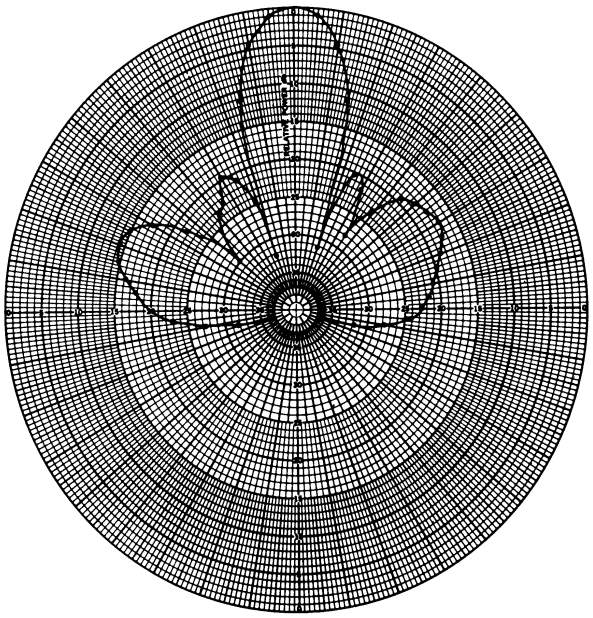

f = 982 MHz
θ = variable
ϕ = 0^o; 180^o

(a)

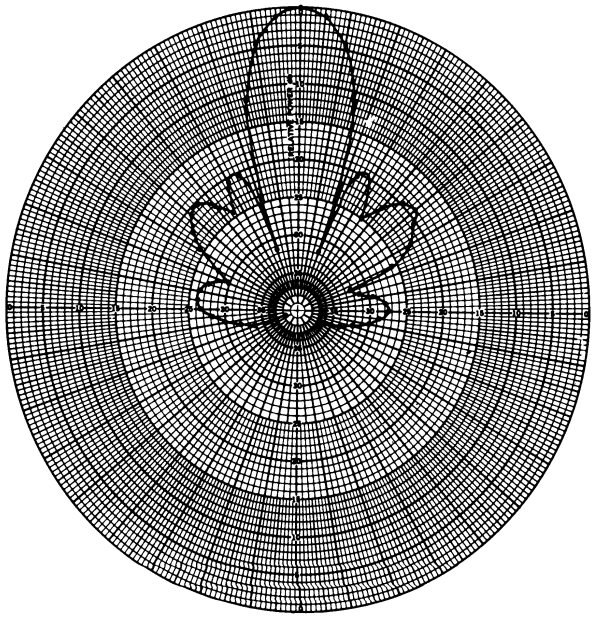

f = 982 MHz
θ = variable
ϕ = 90^o; 270^o

(b)

FIG. 3-26a, b: THEORETICAL PHASE ADDITION PATTERN FOR A 16 ELEMENT ARRAY WITH TIME DELAY CORRECTION

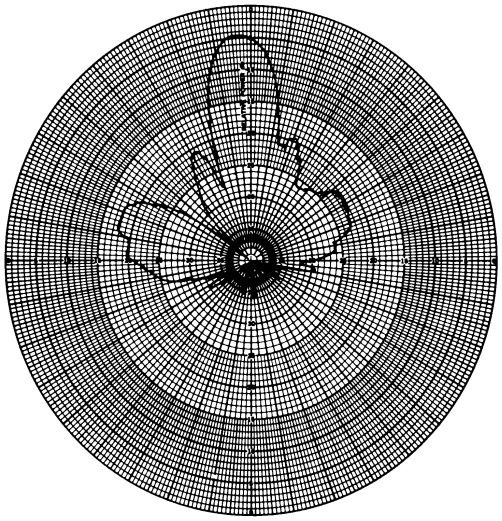

f = 982 MHz
Pol. = E_ϕ
θ = variable
ϕ = 0°; 180°

(a)

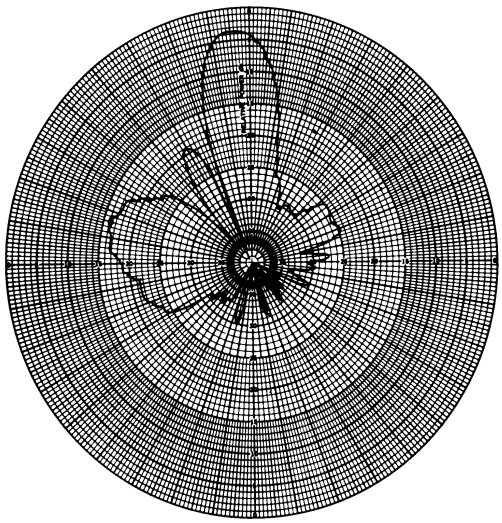

f = 982 MHz
Pol. = E_θ
θ = variable
ϕ = 0°; 180°

(b)

FIG. 3-27a,b: EXPERIMENTAL PHASE ADDITION PATTERN FOR A 16 ELEMENT ARRAY WITH TIME DELAY CORRECTION

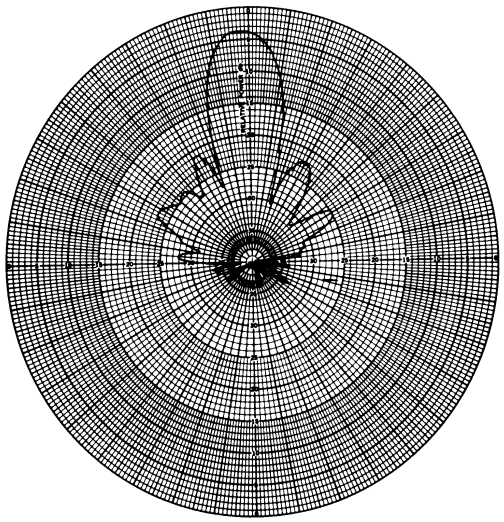

f = 982 MHz
Pol. = E_ϕ
θ = variable
ϕ = 90^o; 270^o

(c)

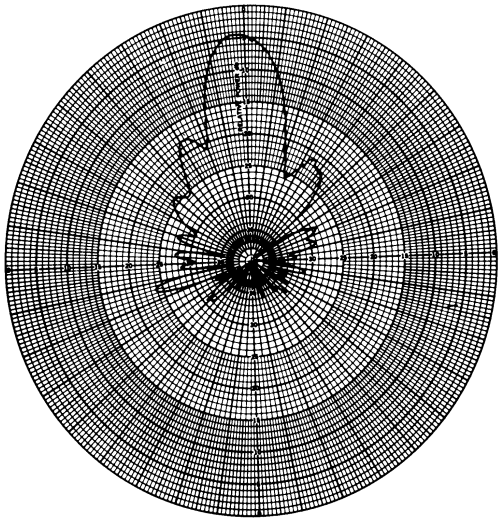

f = 982 MHz
Pol. = E_θ
θ = variable
ϕ = 90^o; 270^o

(d)

FIG. 3-27c, d: EXPERIMENTAL PHASE ADDITION PATTERN FOR A 16 ELEMENT ARRAY WITH TIME DELAY CORRECTION

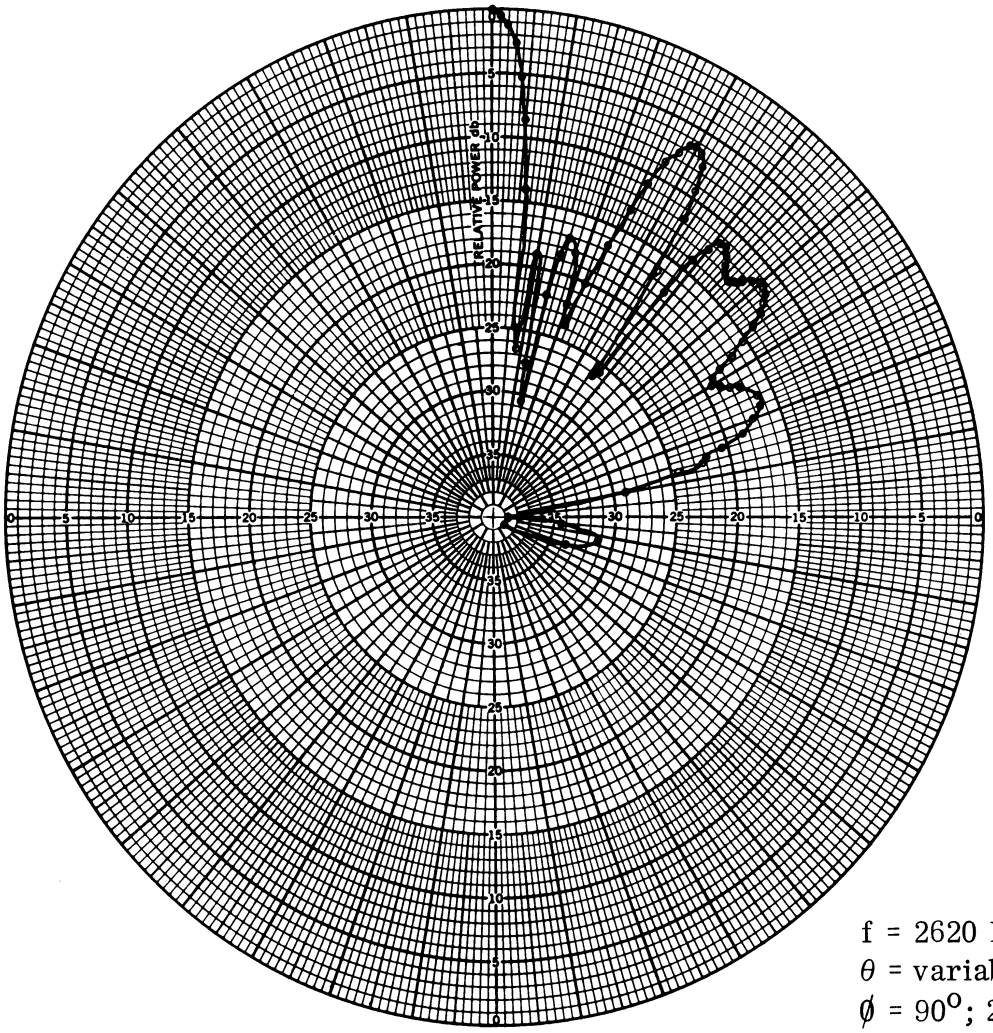

f = 2620 MHz
θ = variable
ϕ = 90^{o}; 270^{o}

FIG. 3-28: THEORETICAL PHASE ADDITION PATTERN FOR A 16 ELEMENT ARRAY WITH TIME DELCY CORRECTION

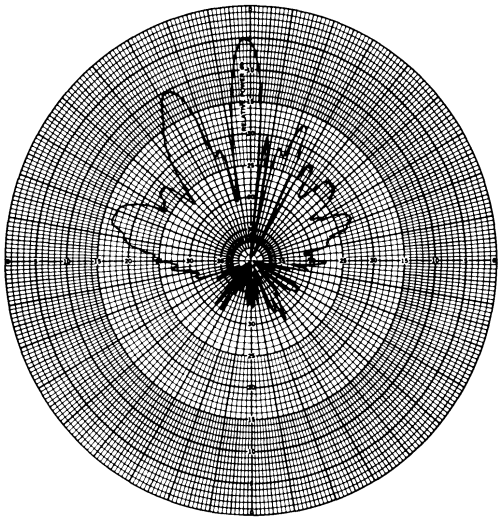

f = 2620 MHz
Pol. = E_ϕ
θ = variable
ϕ = 0^o; 180^o

(a)

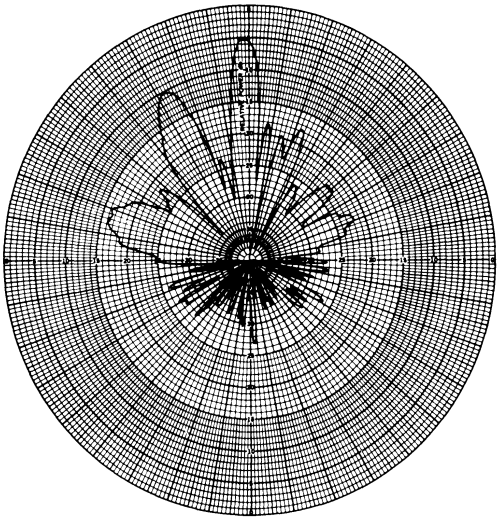

f = 2620 MHz
Pol. = E_θ
θ = variable
ϕ = 0^o; 180^o

(b)

FIG. 3-29a,b: EXPERIMENTAL PHASE ADDITION PATTERN FOR A 16 ELEMENT ARRAY WITH TIME DELAY CORRECTION

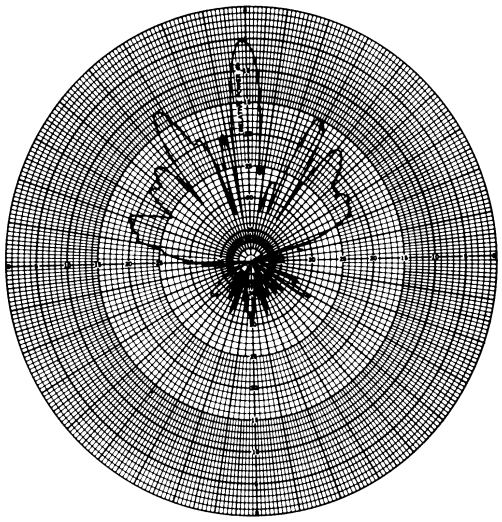

f = 2620 MHz
Pol. = E_ϕ
θ = variable
ϕ = 90°; 270°

(c)

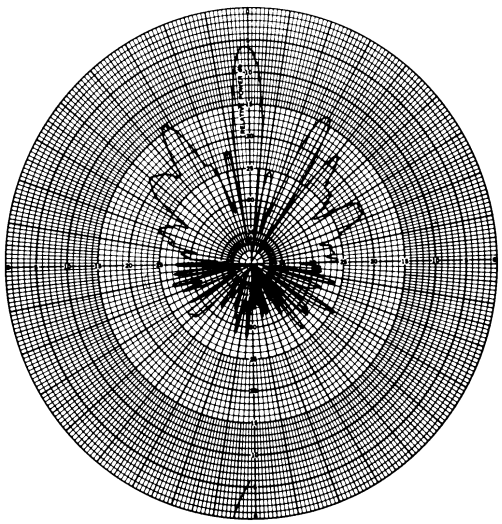

f = 2620 MHz
Pol. = E_θ
θ = variable
ϕ = 90°; 270°

(d)

FIG. 3-29c, d: EXPERIMENTAL PHASE ADDITION PATTERN FOR A 16 ELEMENT ARRAY WITH TIME DELAY CORRECTION

reduced if one uses a larger spherical cap antenna array containing more than 16 elements.

As noted previously, the purpose of this portion of the study was to verify the theoretical results. It is felt that results have demonstrated the general agreement between the two. The ellipticity of the field radiated by the 16-element array has not been studied here. However, after comparing the corresponding E_θ, E_ϕ patterns given, it may be concluded that the radiated field is very close to circularly polarized at the two frequencies considered. A photograph of the 16-element hemispherical array of spiral is shown in Fig. 3-30.

3.4 Coupling Investigation

A limited investigation on the coupling effects that may be associated with the hemispherical direction finder array has been conducted. During this study two spiral antennas were evaluated when located in close proximity (9 inches between center) to one another in a 4' flat ground plane. Impedance and pattern was obtained at 3 GHz. All pattern data was in accordance with the coordinate system of Fig. 3-9. Both data were obtained for the following conditions: 1) a single spiral, 2) a single spiral in the presence of a second spiral terminated in a 50Ω load, and 3) a single spiral in the presence of a second spiral terminated with a short. Impedance and pattern data for the above conditions are shown respectively in Figs. 3-31 and 3-32. This data is not felt to be complete but is shown to illustrate the effects that may result from coupling. It appears from this that the coupling may not be a serious problem. The coupling study should be expanded to consider additional frequencies, more antennas and electronic scanning techniques. Also, consideration must be given to the effects of coupling on the hemispherical surface.

3.5 Concluding Remarks

From the results reported in this section it can be concluded that the theory developed for the radiation characteristics of a spherical antenna array of

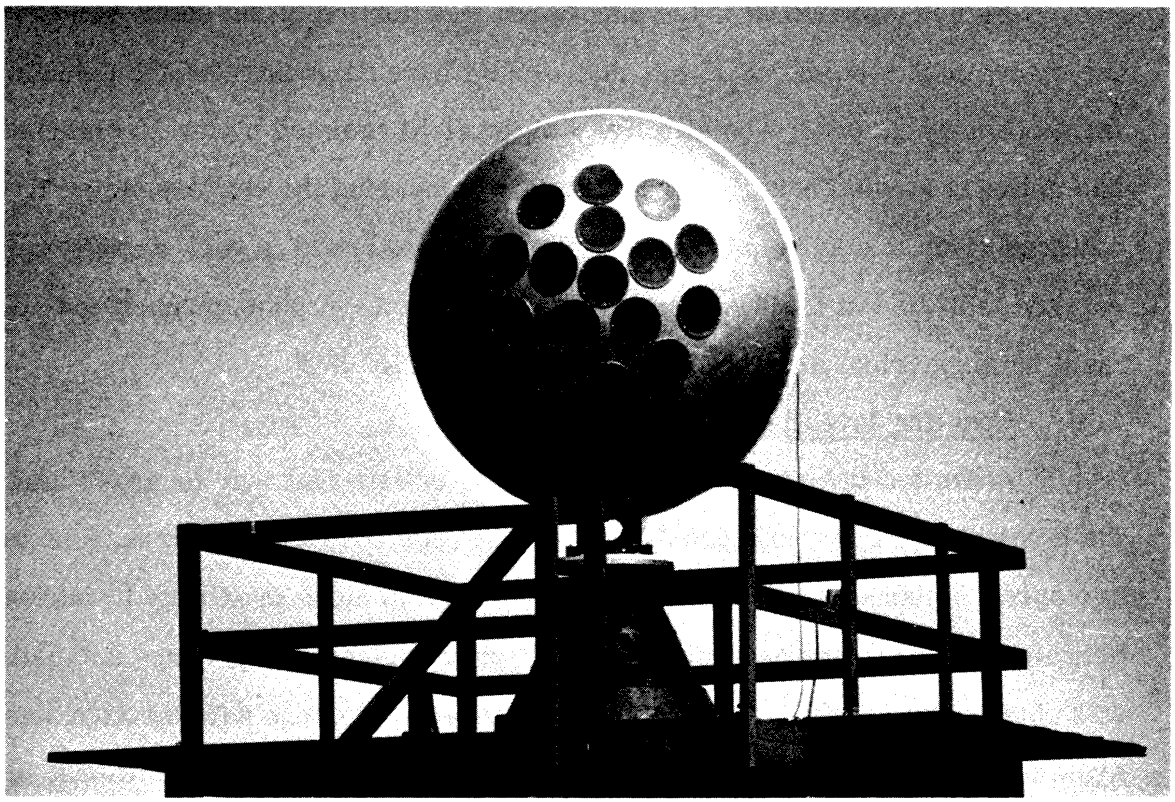

FIG. 3-30: 16 ELEMENT (SPIRAL) HEMISPHERICAL ARRAY

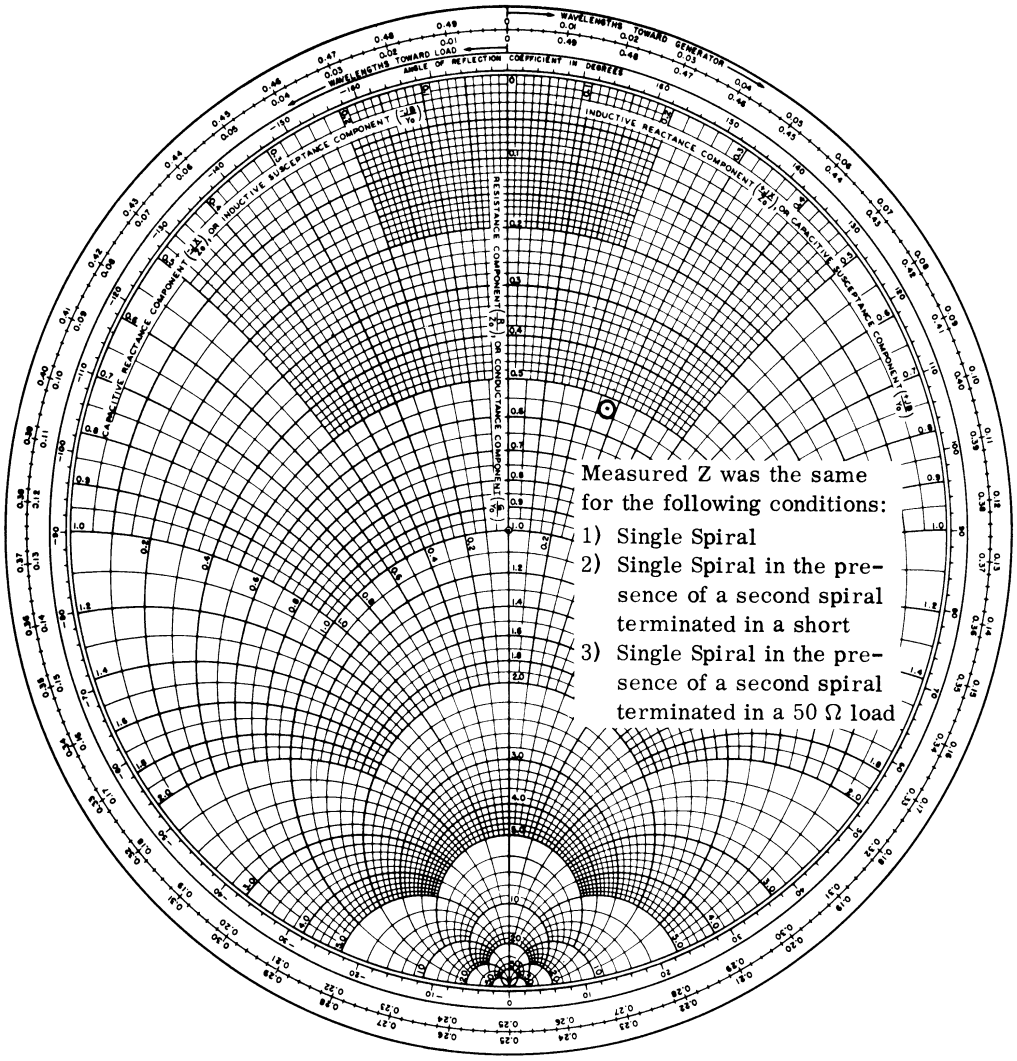

FIG. 3-31: IMPEDANCE DATA FOR COUPLING STUDY

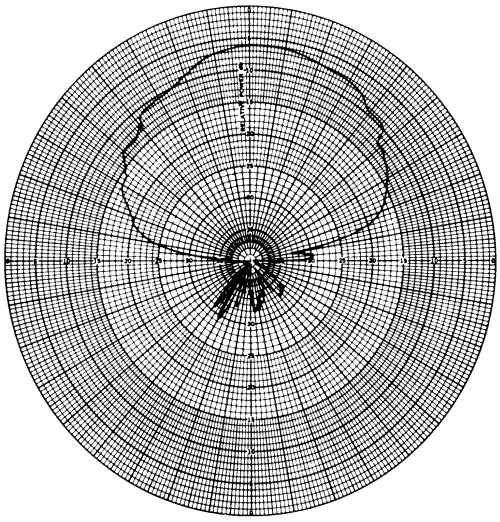

f = 3.0 GHz
Pol. = E_θ
$\theta = 90^o$
ϕ = variable

(a)

FIG. 3-32a: A SINGLE SPIRAL ANTENNA

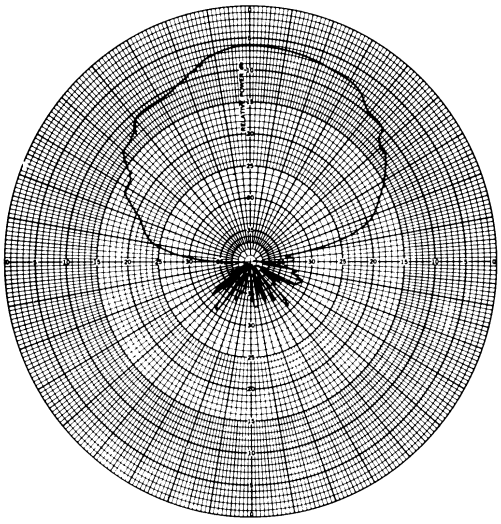

f = 3.0 GHz
Pol. = E_θ
$\theta = 90^o$
ϕ = variable

(b)

FIG. 3-32b: TWO SPIRAL ANTENNAS (One Antenna Active- One Antenna Terminated in 50 Ω)

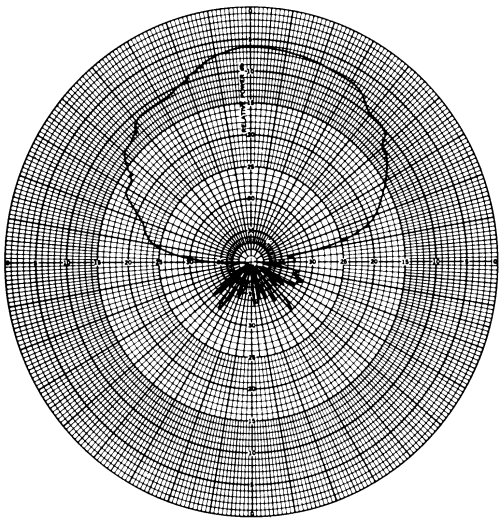

f = 3.0 GHz
Pol. = E_θ
θ = 90°
ϕ = variable

(c)

FIG. 3-32c: TWO SPIRAL ANTENNAS (One Antenna Active- One Antenna Terminated in a Short)

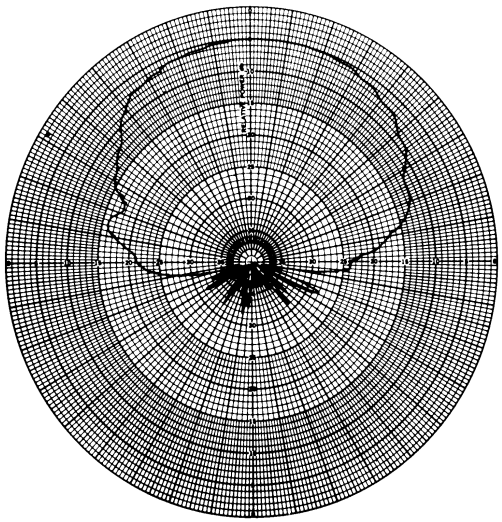

f = 3.0 GHz
Pol. = E_ϕ
θ = 90°
ϕ = variable

(d)

FIG. 3-32d: A SINGLE SPIRAL ANTENNA

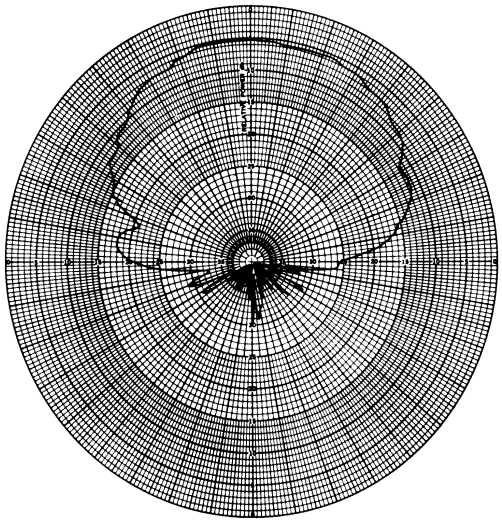

f = 3.0 GHz
Pol. = E_ϕ
$\theta = 90^o$
ϕ = variable

(e)

FIG. 3-32e: TWO SPIRAL ANTENNAS (One Antenna Active - One Antenna Terminated in 50 Ω)

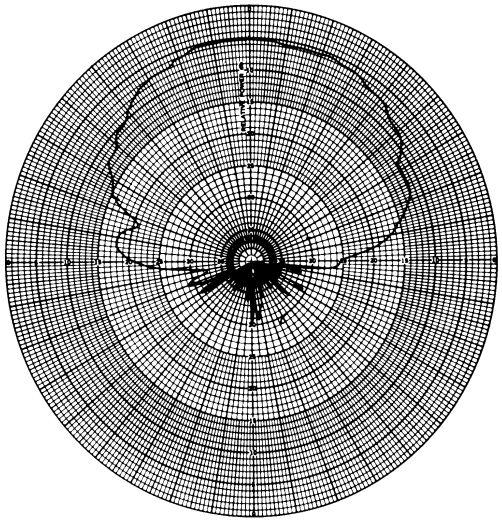

f = 3.0 GHz
Pol. = E_ϕ
$\theta = 90^o$
ϕ = variable

(f)

FIG. 3-32f: TWO SPIRAL ANTENNAS (One Antenna Active - One Antenna Terminated in a Short)

circularly polarized elements may be considered to be adequate for the design of such arrays. Shortage of time did not allow for sufficient study of a few other aspects of the problem. In particular, we feel more experimental work should be done to evaluate the pattern of a spiral on a spherical ground plane, the mutual impedance between spiral antennas and the directional characteristics of the 16-element array.

IV

A PROPOSED EXPLORATORY MODEL OF A SPHERICAL ARRAY DIRECTION FINDER SYSTEM

The purpose of this chapter is to illustrate the important design concepts of a possible exploratory model for spherical array direction finding system. With solid state diode switching of the received signals, the desired rapid spatial scan and broad frequency coverage can be achieved and only a single standard tunable receiver is required. The necessary phasing of the activated antenna elements for scanning a particular sector of the hemisphere is accomplished by introducing an appropriate nondispersive delay line to each element with diode switches. These switches and the programmed computer and interface equipment required to control them constitute a major part of the cost of the system. The phase adjusted signals are summed up and detected by means of a standard receiver, the output of which is displayed on a cathode ray scope or other suitable display device. The various components of the system are shown in the block diagram in Fig. 4-1; a more detailed breakdown of the operational components is given in Fig. 4-2. The PDP-8 digital computer is the heart of the control section. It is connected to the diode switches in the r.f. network by interfaces. These interfaces consist of logic circuits which direct, store and decode the computer commands. In the following sections the various components of the system are described in more detail.

4.1 Antenna Array

The spherical array consists of a number of flat spirals which are (almost) symmetrically located on a hemisphere. Different sectors (or caps) are used for the different regions to be scanned; each cap would be used for a number of different observation angles. The desired directivity dictates the number

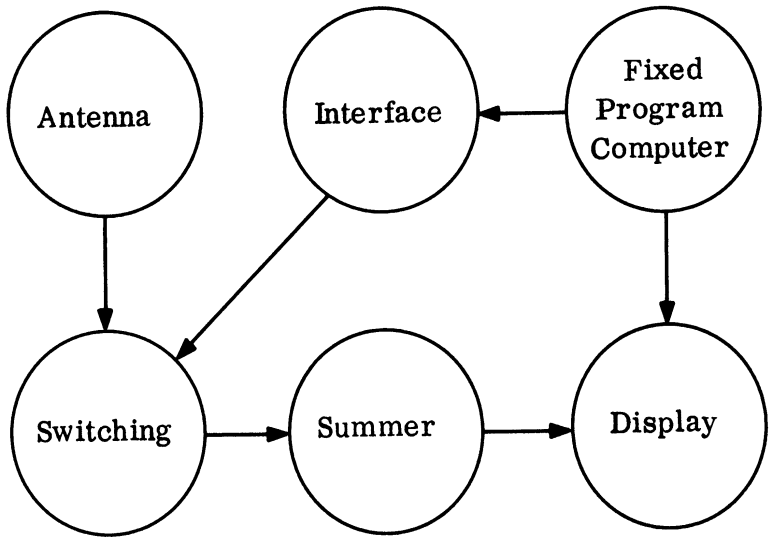

FIG. 4-1: BLOCK DIAGRAM OF VARIOUS COMPONENTS

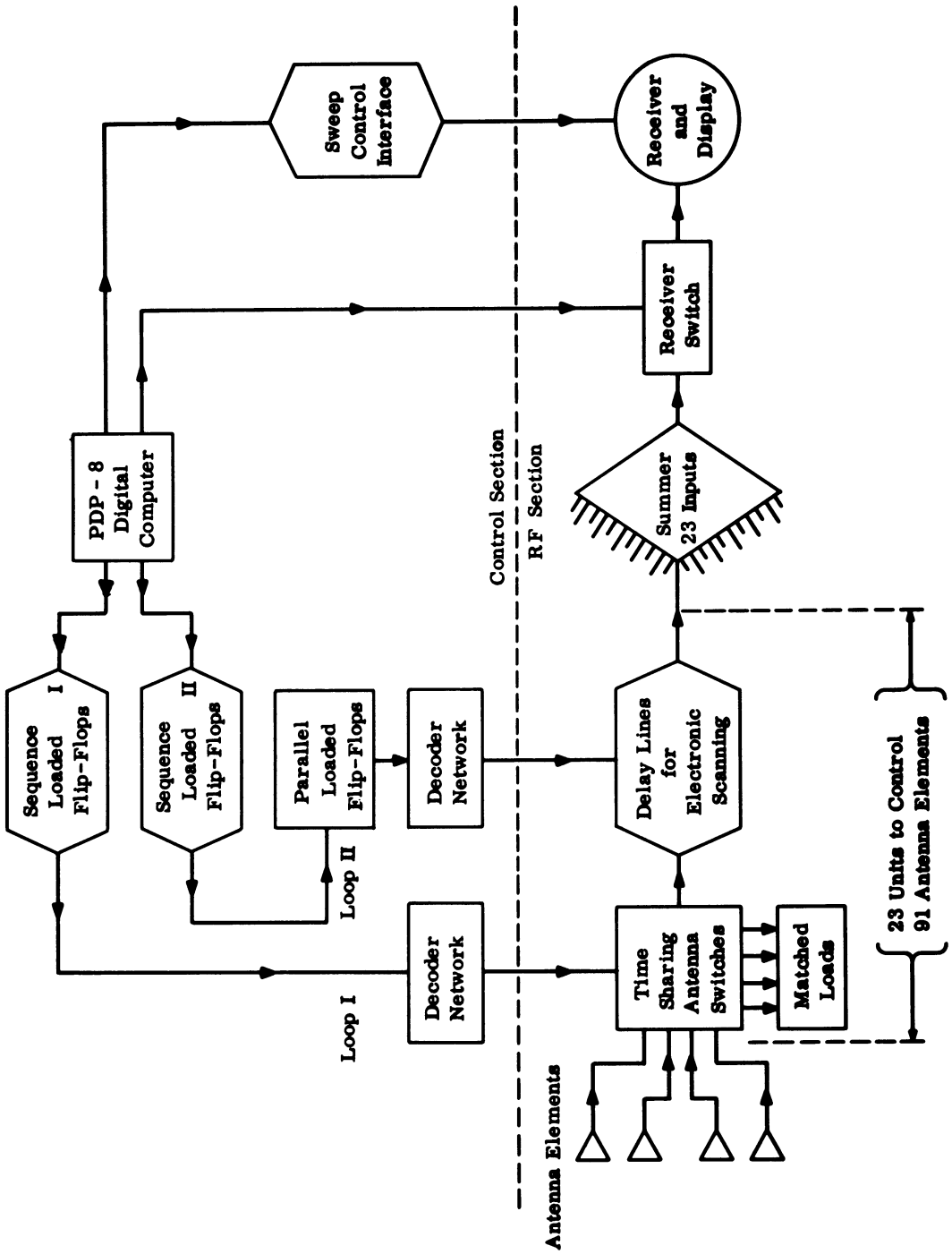

FIG. 4-2: BLOCK DIAGRAM OF RF AND CONTROL SYSTEMS FOR SPHERICAL ARRAY DIRECTION FINDER.

of active elements in the array and thereby the cost. As a reasonable compromise between cost and directivity, caps containing 16 to 19 elements (covering roughly 30^{o} half angle cone on the surface of the sphere) have been chosen for the design. Over the frequency band of operation the directivity of this activated cap varies approximately from 16 db to 21 db (Sengupta et al, June 1966, p. 12).

Since each active element must be properly phase controlled by an expensive switching network (while the majority of the elements are not in use), it is advantageous to employ one network for a number of elements (which therefore must never lie on the same cap.) An example of this subdivision is shown in Fig. 4-3 for a hemisphere containing 91 elements with caps containing 16-19 elements. Here, twenty-three identical switching circuits are used, all but one of which handles four elements. Other schemes are undoubtedly possible.

If more elements were specified in the cap size, then a larger number of switching networks would be required (with greater complexity and cost) and each network could handle fewer elements. Thus, a thirty-seven element cap would require at least thirty-seven switching networks each of which handles two or three elements.

For the element distribution given in Fig. 4-3, only four basic types of element distribution will occur in the cap if an element is always located at the center of a cap. These four cap types are shown in Fig. 4-4. A cross hatching code is used in Fig. 4-3 to locate the cap types. The table below summarizes the characteristics of these caps. The cap description is derived from the icosahedron geometry from which the element distribution was obtained. Standard positions for elements in the caps are depicted in Fig. 4-4 with an alphabetic coding. This symmetry must be utilized to make the problem manageable as far as the scanning requirements are concerned. If only types 1 and 2 are used for the centers of caps, the cap size must be large to prevent beam distortion when the beam is scanned away from the cap center. In addition, as the amount of steering

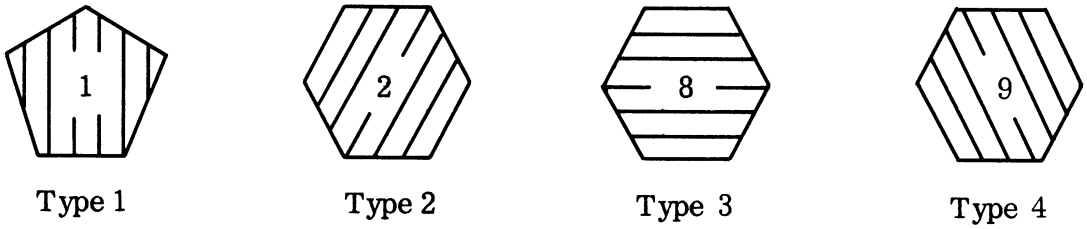

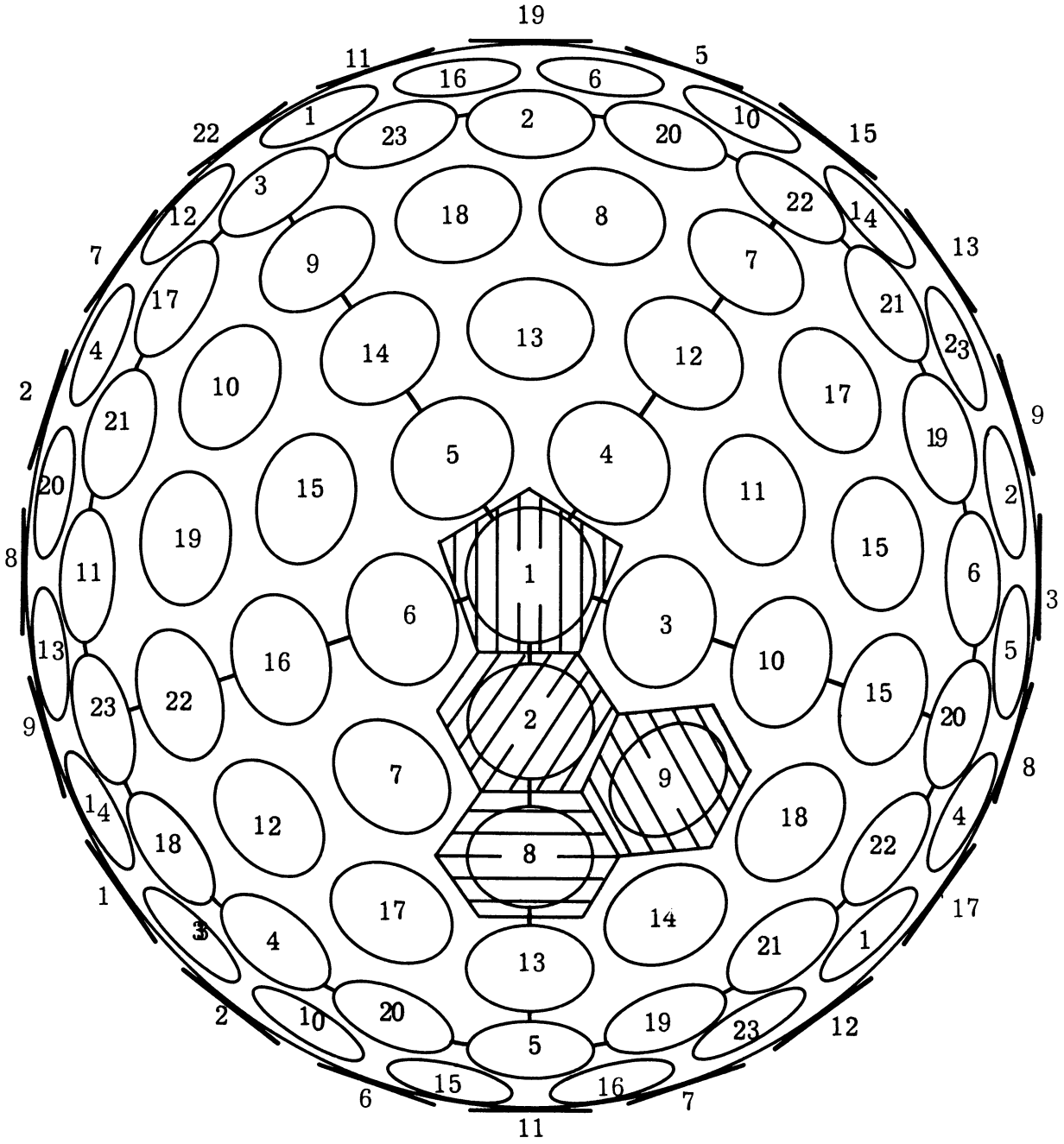

FIG. 4-3: POSSIBLE DISTRIBUTION OF ELEMENTS ON HEMISPHERE. The numbering indicates the 23 different switching networks.

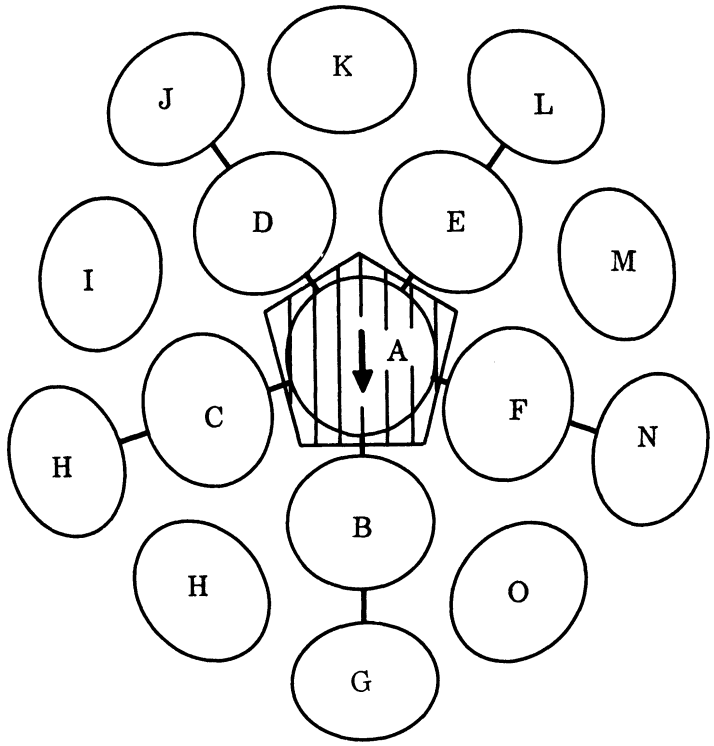

Type 1: Icosahedron Vertex

Number of elements in cap: 16
Number of occurrences on hemisphere : 6
Orientation:
towards $\theta = 0$ except the zenith element which is directed towards $\phi = 0$

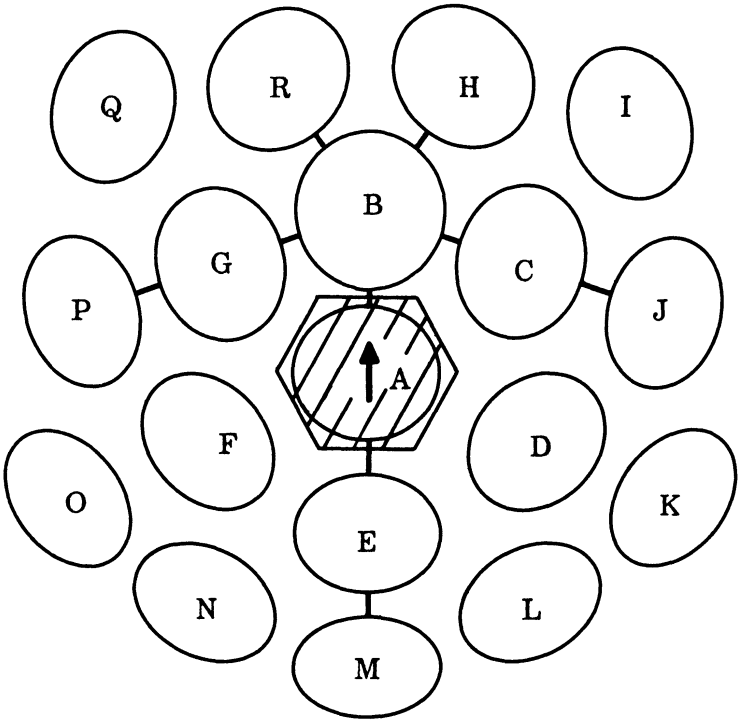

Type 2: Edge Intermediate

Number of elements in cap: 18
Number of occurrences on hemisphere : 30
Orientation:
towards nearest icosahedron vertex

FIG. 4-4: PORTIONS OF FOUR TYPES OF CAPS ILLUSTRATING ORIENTATION OF (AND ELEMENT SPECIFICATION WITHIN) CAP.

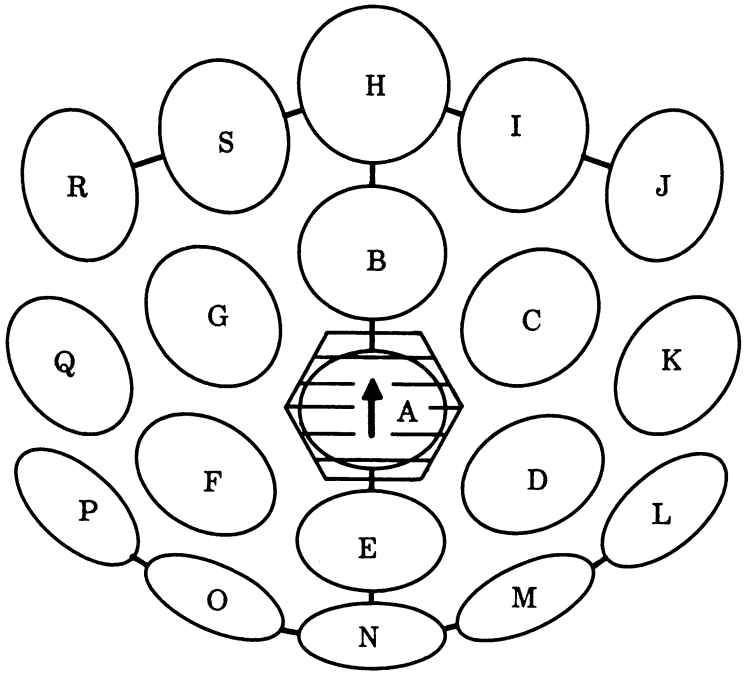

Type 3: Edge Center

Number of elements in cap: 19
Number of occurrences on hemisphere : 20
Orientation:
towrads = 0 or positive

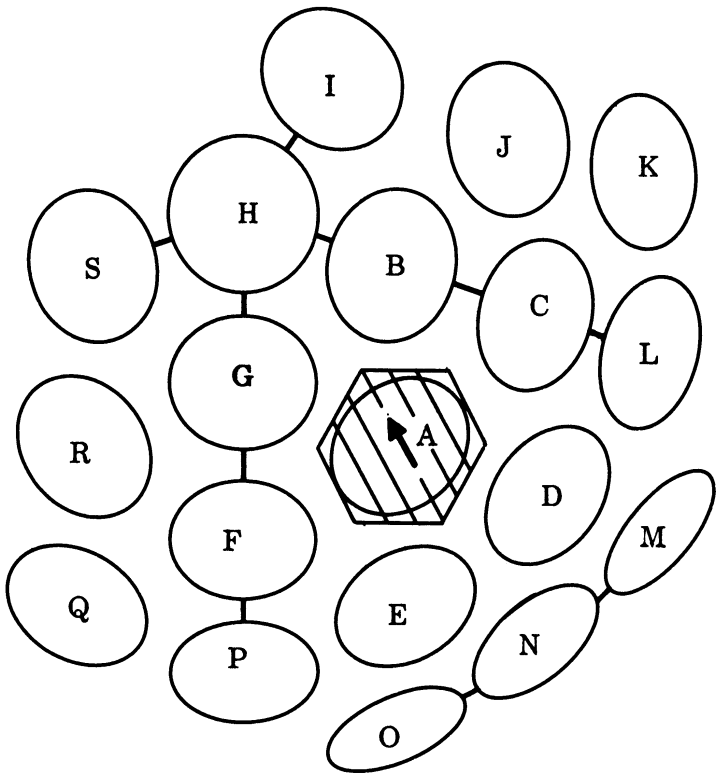

Type 4: Icosahedron Face

Number of elements in cap: 19
Number of occurrences on hemisphere : 35
Orientation:
towards nearest icosahedron vertex

FIG. 4-4: PORTIONS OF FOUR TYPES OF CAPS ILLUSTRATING ORIENTATION OF (AND ELEMENT SPECIFICATION WITHIN) CAP.

increases, so do the length of the necessary phase paths and thus both complexity and cost. Consequently, it now seems best to have as many caps as elements and to employ each element as a cap center.

TABLE IV-I

Cap Type	Cap Description	Number of Elements	Number of Occurrences
1	vertex	16	6
2	edge intermediate	18	30
3	edge center	19	20
4	face	19	35

The number of observations made over the hemisphere is determined by the minimum beamwidth. For the 30^{o} cap the minimum half power beamwidth is 6^{o}. In the present 91 cap system, when the half power beamwidth is less than 15^{o}, it is necessary to make more than one observation per cap. Seven observations per cap (637 per hemisphere) will supply total hemispherical coverage for a minimum beamwidth of 6^{o}. Fig. 4-5 shows seven adjacent elements or cap centers. Each cap is phased to look in seven directions, one directed along the normal to the element center and six equally spaced on a circle 6.1^{o} from the element center. The seven circles in Fig. 4-5 represent a segment of the geometry in Fig. 4-3. There may be several other possible sets of observation points providing various amounts of separation. We have described only one typical case. It should be noted that overlapping of observation points is not proposed.

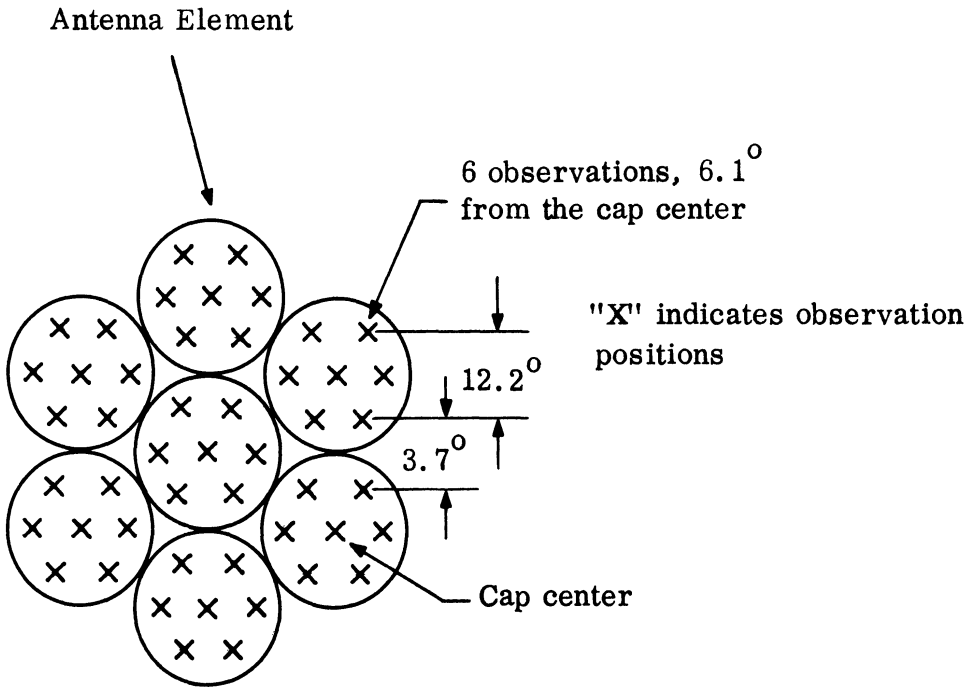

Seven adjacent cap centers showing
49 observation positions.

FIG. 4-5: CAP OBSERVATION POSITIONS

4.2 Antenna and Delay Line Switching

There are two basic parts to the switching networks: one which selects the proper element to be used with the phasing network and a second part which selects the proper time delay (see Fig. 4-2). A more detailed example is shown in Fig. 4-6 where the two parts are placed on one "card" for the case of four antenna elements feeding one card; twenty-three such cards would be needed in this example. In operation, those elements not contained in a cap must be switched to a matched load so that they may not produce undesirable effects. This first part of the switching network requires two diode switches per antenna element. One of the switches connects the antenna to the matched load and the other to the delay line when needed. At any given instant of time, at least three of the elements, in some cases, are connected to the matched loads and on some of the cards all the elements may be terminated in matched loads.

The second portion of the switching network in Fig. 4-6 consists of eight delay lines, four short and four long, so as to obtain sixteen possible delay combinations. Diode switches are placed at each end of these lines. When a line is not in use, both of its diodes are in the off mode so that no undesirable reflection may be introduced from either end of the line.

The four long delay lines are used to direct the antenna beam along a direction which passes through the center of the particular activated cap and is normal to the cap surface. The four short lines are used to steer the beam around this central direction in six steps. The incremental lenghts of the delay lines are determined by the upper unit of frequency (3 GHz) and the required accuracy at that frequency. Their actual lengths may be determined by using the theoretical expressions given in Chapter II. There may be other schemes of switching the delay lines. The one considered in Fig. 4-5 has been found to be best suited for the present purpose.

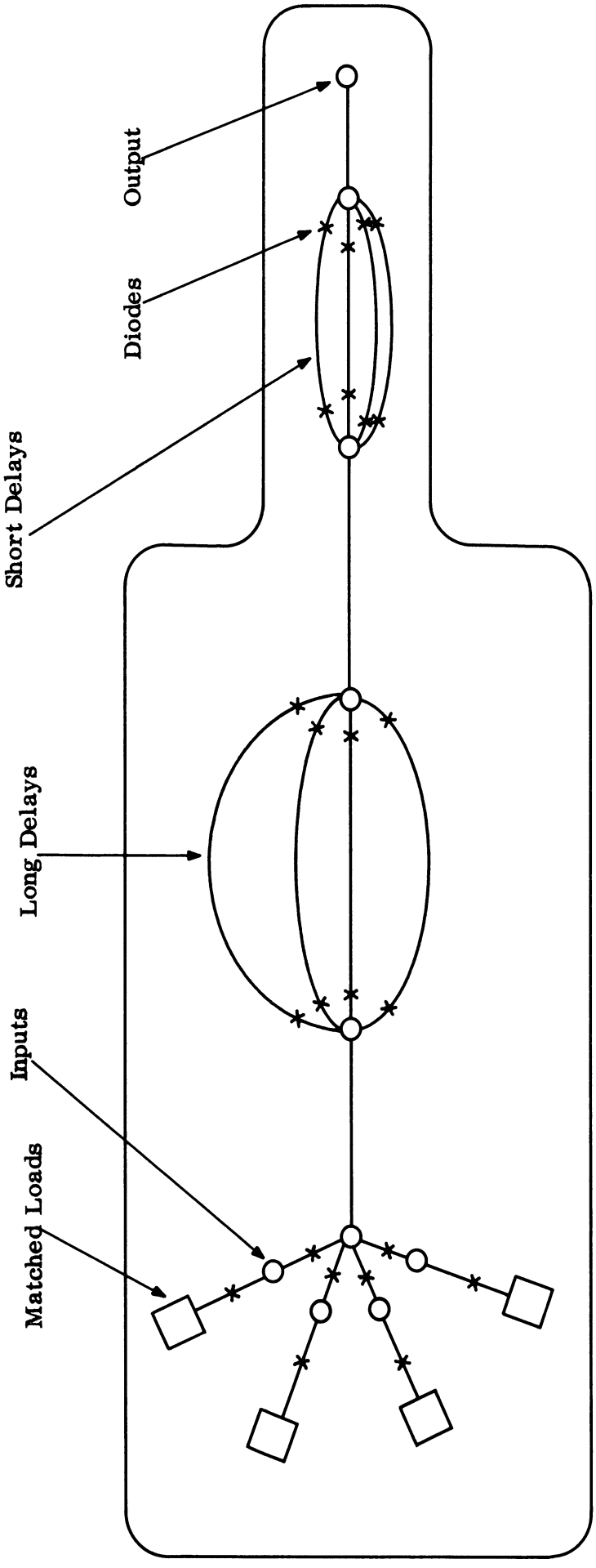

FIG. 4-6: POSSIBLE IMPLEMENTATION OF ONE OF TWENTY-THREE SWITCHING CARDS

4.3 Computer and Interface

In order to control the selection of proper antenna elements and associated delay lines for the proposed spherical array direction finder we have found The Programmed Data Processor-8 (PDP-8), a general purpose computer manufactured by the Digital Equipment Corporation, to be suitable for our purpose. The computer requirements are mostly dictated by the number of observation angles and the number of elements in an activated cap. It is less strongly influenced by the number of phase paths. In this section we discuss briefly how the computer performs the desired control operations required by the direction finder.

The Programmed Data Processor-8 (PDP-8) is a complete general-purpose digital computer with a high speed, random-access, magnetic-core memory which has a 4096 word storage capacity. Each word has 12 binary digits. Its 1.5 microsecond cycle time permits the PDP-8 to handle programmed input/output data transfers at rates up to 2 million bits per second.

In Fig. 4-2 the PDP-8 is shown in the control section where it directs the operation of the array. Digital instructions pass from it through the interface circuits to all the diode switches and display unit. The interface components for the time-sharing antenna switches and the delay line switches are described in more detail than the sweep control interface (Fig. 4-2). More work remains to be done on the sweep interface, but it should be routine. With the present program a direct instruction from the PDP-8 operates the receiver diode switch and no interface is needed in this branch.

Since the PDP-8 issues one instruction at a time (at a rate of a few microseconds per instruction) it is necessary to have buffer units which retain these instructions so that they can be applied to the switch as long as is required. Flip-flop circuits which have two operating states (on or off) act as buffers. The binary information in the flip-flop circuits is interpreted by the decoder networks which in turn supply the diode switches with on or off bias voltages.

Loop II in Fig. 4-2 has an additional unit (the parallel loaded flip-flop) compared to loop I. In loop I each of the time-sharing antenna switches is set sequentially, while in loop II the delay line switches are set simultaneously. Simultaneous switching is achieved in loop II by having the series flip-flop unit completely load the parallel flip-flop unit and then switching all the data in the parallel unit to the diodes in the delay lines. After the delay lines are activated the entire system is turned on and continues to observe at the same position until the parallel unit is loaded again. If it is found to be advantageous to introduce a parallel unit in loop I, this can be done; presently the cost involved does not justify this addition.

A flow diagram of the program for the PDP-8 is shown in Fig. 4-7. The actual program for the PDP-8 is given in Appendix C. Four loops are indicated in the flow diagram. Loops I and II are the same as those shown in Fig. 4-2 and are used to control cap changes and delay line changes respectively. The remaining two loops are the paths for controlling the scanning and tracking.

4.4 Summing Network

Referring to Fig. 4-2, the outputs of the switching network must be summed before being sent to the receiver and display device. In order to reduce the undesirable effects due to coupling each input to the summer must be isolated from each other. The summing process can be accomplished with an array of hybrid tees which may be of the coaxial type or the entire circuit may be designed as a strip line network. This area will require some more consideration.

4.5 Receiver and Data Display

It is assumed that a standard receiver will detect the output from the summer and apply the signal to the grid of a standard oscilloscope. Equipment for the sweep control interface exists which will convert digital signals from the computer to analog form for application to the x and y axes of the oscilloscope. During the time when changes are being made in the switching networks, the receiver switch

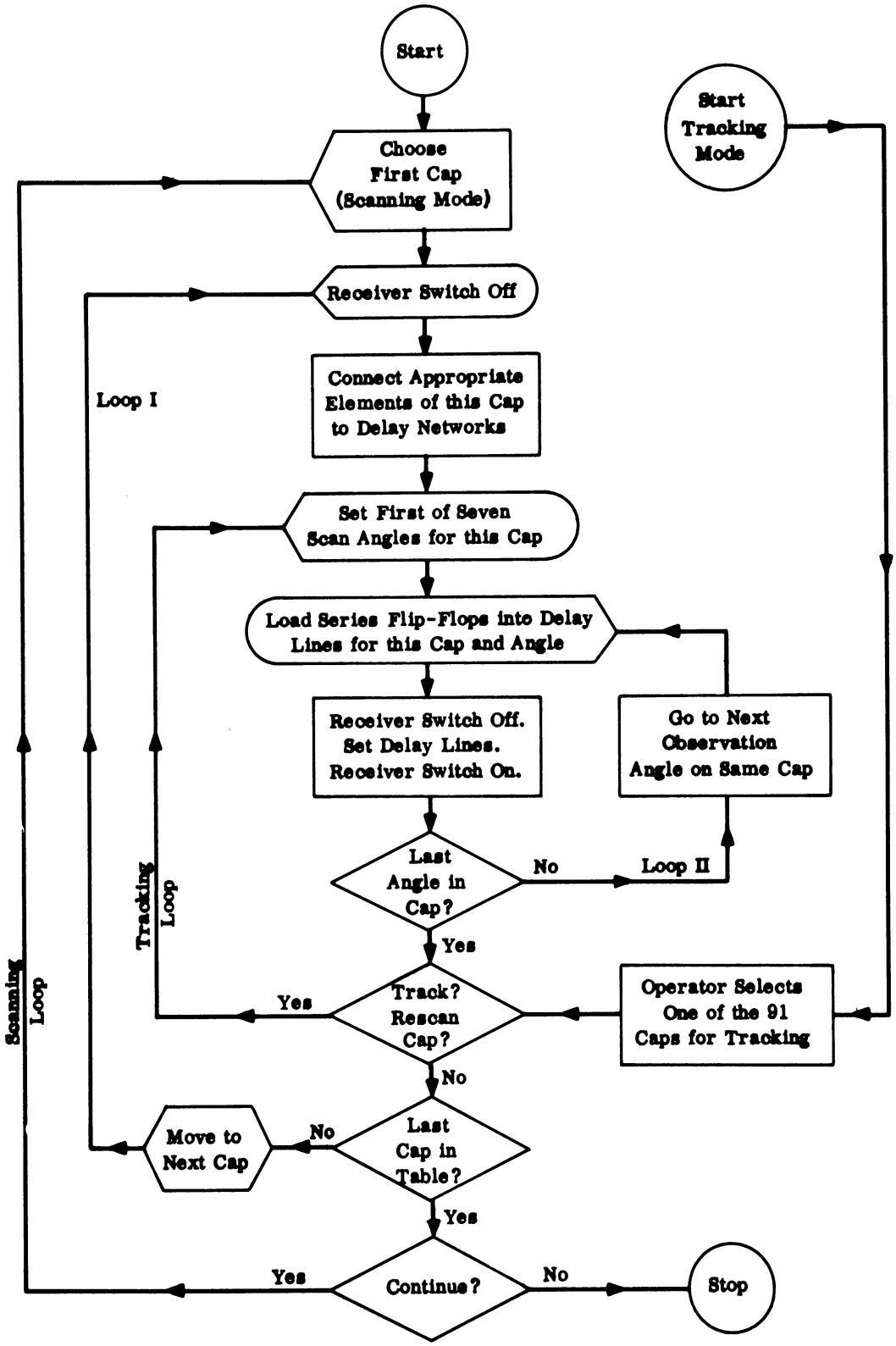

FIG. 4-7: FLOW DIAGRAM FOR PDP-8 DIGITAL COMPUTER.

will disconnect the summer output from the receiver so that switching transients will not be seen on the display system.

4.6 Concluding Remarks

The implementation of the exploratory spherical array direction finder proposed above seems to be feasible at a fairly moderate cost considering the complexities of the problem. No major state of the art advance is required although the cost of the rf diode switching circuits will be relatively high because of their complexity. The simple model (with 16-19 antenna elements in a cap) discussed above is estimated to have an overall gain that will vary 13 to 16 db over the frequency band. This gain is less than the 18 db desired by the user. Higher gain can be achieved by using more antenna elements per cap. However, this will considerably increase the cost of the entire system.

V

DATA PROCESSING ASPECTS OF THE DIRECTION FINDING SYSTEM

The data processing aspect of a direction finding system concerns the analysis of the signals induced in all the activated elements of the antenna array and the computation or display of the angle of incidence of each arriving wave or wave train within a given frequency band.

In this report one particular system for obtaining the angle of incidence has been adopted, which, considering the task statement for this project and the present state of the art, appears in our present judgement to offer the most satisfactory solution of the problem. In view of the continuously changing state of the art and other criteria, any subsequent research and development in DF-systems must necessarily probe for new and different data processing techniques. For this reason, the following section presents some of the ideas which have been considered and investigated during the work on this project and which may deserve some consideration for future applications.

Since the data are available continuously at all the antenna elements, the theoretical minimum time required for determining the angle of incidence is extremely short; one limitation is, of course, the spread in the time of arrival at the different points in the array; another one is the time required for recognition or identification of a signal, i.e., the observation of such characteristics as frequency, phase, amplitude, etc. In principle, it would be possible to process simultaneously within this minimum time all arriving radiations regardless of their frequency or angle of incidence. The requirement for anything approaching this ultimate speed has not so far been urgent enough to justify the extremely costly and complicated equipment that would be needed. The alternative is to

adopt some more or less sequential procedure whereby the specified ranges of frequency or solid angle or both are consecutively "searched" or "swept" by a single processing channel, or possibly a small number of such channels.

The sequential frequency search is accomplished by tuning the receiver or the processing channel in successive steps through the required frequency range, each step being equal to or smaller than the bandwidth of the channel. At each one of these frequency settings the angle of incidence may in principle be obtained either by direct computation from the data or by a sequential sweep of the whole required solid angle, let us say the hemisphere.

5.1 Simultaneous Equation Data Processing

If we disregard any reaction from the antenna array on the field, the electromagnetic field of any particular signal at the location of each antenna element $E(t + \tau_i)$ differs from the other only by a displacement τ_i in the time due to the difference in distance from the source. A set of τ_i-values referred to the same origin determines completely the direction of incidence of the signal. However, if the signal is relatively long and periodic, such a set may not be measured directly and unambiguously, since the field at any element location is invariant under the translation from t to t+nT, where n is any integer and T is the period. When the distance between elements is of the order of a wavelength or more, there is no obvious simple way of removing this ambiguity for a sine wave signal. For this reason, the (in principle) appealing scheme of computing the angle of incidence simply by solving a set of simultaneous equations does not appear feasible.

Other alternatives are a sequential search of the whole hemisphere or a simultaneous search of a number of sectors which jointly cover the whole hemisphere.

5.2 RF Phase-Shifting or Phase-Switching Methods

The traditional approach to the search process is the reciprocal of directional transmission; the antenna elements are connected to the common array terminals through delay lines which are adjusted so as to obtain the desired antenna pattern. The output of a receiver at the terminals reaches its maximum when the antenna pattern points in the direction of the signal source.

This is the scheme that has been adopted for the DF-system proposed in Chapter IV. It has a number of advantages: the antenna array has a single pair of r-f output terminals, to which any suitable standard receiver may be connected.

5.3 Correlation Methods for Data Processing

Another processing principle makes use of the correlations between the incident signal data and some reference signal data. The actual signals induced in the elements of the array are compared or correlated with the signals which would be induced if a source of the same frequency were located at a known elevation and azimuth (subsequently termed the "reference source", generating the "reference signals"). If the "bearing" of the reference source is programmed to scan the complete hemisphere, the correlation reaches a maximum, when the reference bearing coincides with the bearing of the unknown source. The output of the correlator versus the elevation and azimuth angles traces a pattern very similar to the radiation pattern of the array. The basic principle of correlation data processing and its application to direction finding was discussed in our earlier reports (Sengupta et al, March 1966; June 1966); it will not be repeated here.

Correlation processing has several attractive features and has been seriously considered for this project. For this reason a discussion is included in this report, and it is recommended that attention should be given to such methods of DF data reduction, since different objectives and a more advanced state of the art may tip the scales in favor of such a system.

One important problem in this data-handling system is the generation or storage of the reference data to be supplied to the correlator. However, for a given speed and angular resolution, no more information is required at each frequency than for the control of a phase-switching system, but the use of dispersionless delay lines in the latter case offers a considerable advantage, when a wide frequency range is to be covered.

The chief attraction of the correlation processing lies in the complete absence of microwave switches or phase shifters. Electronic scanning is performed by means of programmed variations of the pertinent parameters. Since a number of correlators may operate in parallel on the same data, more than one scanning spot may be controlled independently at the same time, permitting simultaneous searching and tracking, for instance.

The primary disadvantage of the correlation system is that each and every antenna element requires a certain amount of electronic equipment, such as converter, correlator and possibly amplifiers. This affects not only the cost and complexity of the system, but the signal-to-noise ratio may also be adversely affected. The latter will be the case if the electronic noise (receiver noise) is predominant, but not if the background noise radiation from the antenna environment is predominant.

VI

GENERAL DISCUSSION AND CONCLUSION

6.1 Discussion on the System Characteristics

As outlined in the Technical Guideline of the project, the direction finder system should satisfy the following design goals:

(1) the frequency bandwidth of the antenna array system shall not be less than 5:1;

(2) the VSWR of the combined antenna element group forming the search and direction finding beams shall not be greater than 3:1 over the band with respect to 50 ohms, measured at the combined output terminals;

(3) the coupling, scanning, data processing and computer technique employed in the system shall be such as to permit obtaining r.f. energy from a sufficient number of elements at any azimuth or elevation position to provide a gain of not less than 18 db with respect to half-wave dipole at all frequencies;

(4) the bearing accuracy shall be $\pm 1^{o}$ or better at any azimuth or elevation position;

(5) scanning rates employed in the system shall be compatible with existing receiver bandwidths;

(6) solid state components used for the coupling and scanning system shall not cause the introduction of cross-modulation in the presence of received signals up to 0.5 v/m of the antenna location; and,

(7) the system shall be capable of bearings on pulse, CW, AM and FM type signals.

On the basis of our investigation of the radiation characteristics of a spherical array of flat spiral antennas we feel that the frequency bandwidth, VSWR, and the gain requirements given above can be met in practice. Assuming an

average antenna beam of 10^{o} over the band of frequencies it should not be difficult to obtain a bearing accuracy of $\pm 1^{o}$, at any azimuth and elevation, with proper method of scanning. In our proposed system, the handling of the data and the scanning of the beam are done electronically in conjunction with a computer. Although we have not made detailed studies it seems probable that the scanning rate of the proposed system will be compatible with the existing receiver bandwidth. The azimuth and elevation direction finder system proposed here should be able to operate on CW, AM and FM signals. Cross-modulation properties of the solid state components used in the system and response of the direction finder to pulse signals have not been studied. From the results discussed in the present report we conclude that most of the design goals listed at the beginning of this section can be met in actual practice.

6.2 Future Work to be Done

As mentioned previously, the main purpose of this investigation has been to determine the feasibility of developing a broadband azimuth and elevation direction finder. The spherical array characteristics have been investigated both theoretically and experimentally with this end in view. Due to time limitations we have not been able to study all the relevant properties of the antenna array with the appropriate amount of thoroughness. The following topics need to be investigated more so as to facilitate the final system design:

(1) The effect of the spherical ground plane on the pattern and impedance of a flat spiral antenna should be studied over the range of frequency of interest. The VSWR characteristics of the spherical array should be measured.

(2) Although it has been shown from our 2-element array over a ground plane that the mutual coupling effects are not appreciable, the problem should be studied with more elements preferably on the spherical ground plane.

(3) The directional properties and the ellipticity of the polarization of the 16-element phased spherical array should be studied over the frequency band

and compared with theory.

(4) The scanning and switching techniques should be studied more intensively. The limited analysis already made was, however, sufficiently encouraging to justify the proposed scanning system for the direction finder.

The studies indicated above should facilitate the final system design of the broadband UHF azimuth and elevation direction finder.

6.3 Conclusion

As a result of this investigation we conclude that it is feasible to develop a broadband UHF azimuth and elevation direction finder with a complete hemispherical coverage. On the basis of our studies we have proposed an exploratory model of a spherical array direction finder which could be built at a moderate cost. It satisfies most of the requirements of the user except the gain. However, it is potentially capable of providing much higher gain at the expense of more complexity and cost.

During this investigation we have developed the theory of spherical antenna arrays of circularly polarized elements. From the investigation of the radiation characteristics of a spherical array we find that it has the following distinct advantages over the conventional planar arrays: (1) It is capable of operating with widely spaced elements because the grating lobe problem is much less severe. This makes the array broadband. (2) The special element distribution used makes it feasible to scan or steer the beam electronically over a complete hemisphere without an intolerable loss of gain.

Although in our proposed system we adopted the conventional technique of phase control for beam steering, we feel that the correlation processing of the output data from the antenna elements for direction finding purposes does have some advantages; this should receive more consideration.

VII

REFERENCES

Cohn, Seymour B. (1955), "Problems in Strip Transmission Lines," IRE Trans., MTT-3, No. 2, p. 119.

Du, Li-jen and C-T. Tai (1964), "Radiation Patterns of Four Symmetrically Located Sources on a Perfectly Conducting Sphere," The Ohio State University Research Foundation Report No. 1691-10.

Duncan, J.W. and V.P. Minerva (1960), "100:1 Bandwidth Balun Transformer," Proc. IRE, 48, pp. 156-164.

Harris, J.H. and H.E. Shanks (1962), "A Method for Synthesis of Optimum Directional Patterns from Nonplanar Apertures," IRE Trans., AP-10, No. 3, pp. 220-236.

Kaiser, Julius A. (1960), "The Archimedean Two-Wire Spiral Antenna," IRE Trans., AP-8, No. 3, pp. 312-323.

Microwave Engineers Handbook, (1966) (Horizon House, Microwave Inc., Mass.) p. 122.

Saunders Assoc., Inc., "Handbook of Tri-Plate Microwave Components," November 30, 1956, p. 68.

Sengupta, D.L., J.E. Ferris, R.W. Larson and T.M. Smith (1965), "Azimuth and Elevation Direction Finder Study," Quarterly Report No. 1, ECOM-01499-1, The University of Michigan Radiation Laboratory Report 7577-1-Q.

Sengupta, D.L., J.E. Ferris, G. Hok, R.W. Larson and T.M. Smith (1966), "Azimuth and Elevation Direction Finder Study," Quarterly Report No. 2, ECOM-01499-2, The University of Michigan Radiation Laboratory Report 7577-2-Q.

Sengupta, D.L., J.E. Ferris, G. Hok, R.W. Larson and T.M. Smith (1966), "Azimuth and Elevation Direction Finder Study," Quarterly Report No. 3, ECOM-01499-3, The University of Michigan Radiation Laboratory Report 7577-3-Q.

The Digital Logic Handbook, Digital Equipment Corporation, Maynard, Massachusetts, 1966-67 edition.

APPENDIX A

STRIP-TRANSMISSION LINE POWER DIVIDER

The commercial availability of copper-clad laminates and the simplicity of construction of strip-transmission line makes this an attractive technique to use for the power dividing networks for the hemispherical array study.

In strip-transmission line, the electromagnetic energy is guided by a flat-center conductor through a dielectric medium, bounded by flat ground planes (Fig. A-1). By varying the width of the center conductor strip one is able to obtain desired characteristic impedance, Z_o, of the transmission line. The characteristic impedance varies (Cohn, 1955) according to:

$$Z_o = \frac{94.15}{\sqrt{\epsilon_r}\left[\frac{w/b}{(1-t/b)} + \frac{C_f'}{.0885\,\epsilon_r}\right]}\ \Omega \qquad (A.1)$$

where

Z_o = characteristic impedance

ϵ_r = relative dielectric constant

C_f' = fringing capacitance ($\mu\mu$ f/centimeter) from one corner of the strip to the adjacent ground plane (Fig. A-2)

w = width of strip

b = ground plane spacing

t = thickness of strip

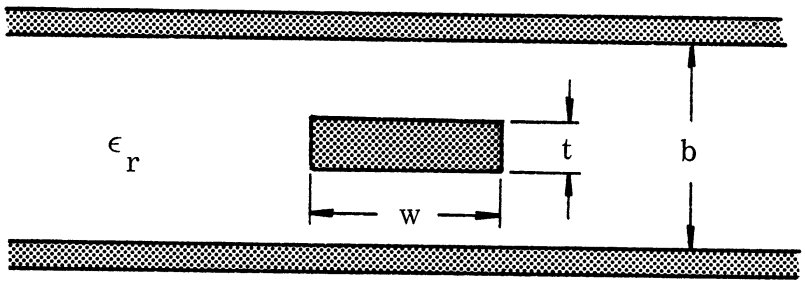

FIG. A-1: STRIP-LINE CONFIGURATION AND CRITICAL DIMENSIONS

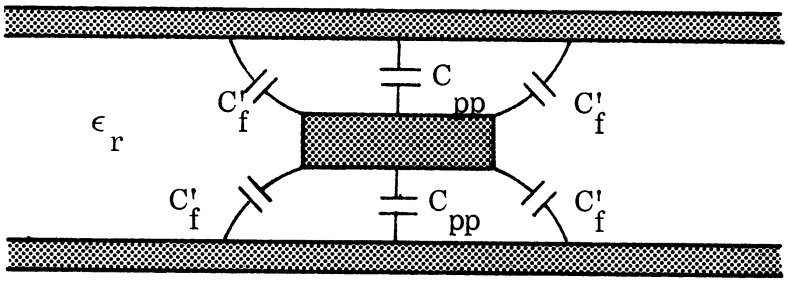

FIG. A-2: PARALLEL PLATE CAPACITANCE (C_{pp}) AND FRINGING CAPACITANCE IN STRIP TRANSMISSION LINE

An exact formula for C'_f (Cohn, 1955) is,

$$C'_f = \frac{.0885\,\epsilon_r}{\pi}\left\{\frac{2}{1-t/b}\,\mathrm{ln}\left[\frac{1}{1-t/b}+1\right] - \left[\frac{1}{1-t/b}-1\right]\mathrm{ln}\left[\frac{1}{1-t/b^2}-1\right]\right\}\mu\mu f/cm \qquad (A.2)$$

A graph of $\sqrt{\epsilon_r}\ Z_o$ versus w/b for values of t/b is shown in Fig. A-3. This graph is accuract to within 2 per cent.

There are two basic types of power dividers, (Fig. A-4) the "in-line" and "tee". Saunders Associates, Inc., has shown that the "in-line" power divider has inherently better matching characteristics than the "tee", (Fig. A-5) (Saunders Assoc. 1956). The branch arms of the junctions are effectively in parallel. Referring to Fig. A-4 for the matched condition and equal power division the characteristic impedance of each branch arm must be $2\,Z_o$, where Z_o is the characteristic impedance of the main arm. In other words, denoting the characteristic impedances of the branch arms, Z_1, Z_2, etc.,

$$\frac{1}{Z_o} = \frac{1}{Z_1} + \frac{1}{Z_2} + \frac{1}{Z_3} + \ldots\ldots\ldots, \qquad (A.3)$$

must hold. Unequal power divisions also may be obtained using the expression,

$$\frac{Z_1}{Z_2} = \frac{P_2}{P_1} \qquad (A.4)$$

where Z_1 and P denote respectively the characteristic impedance and power of an individual branch line.

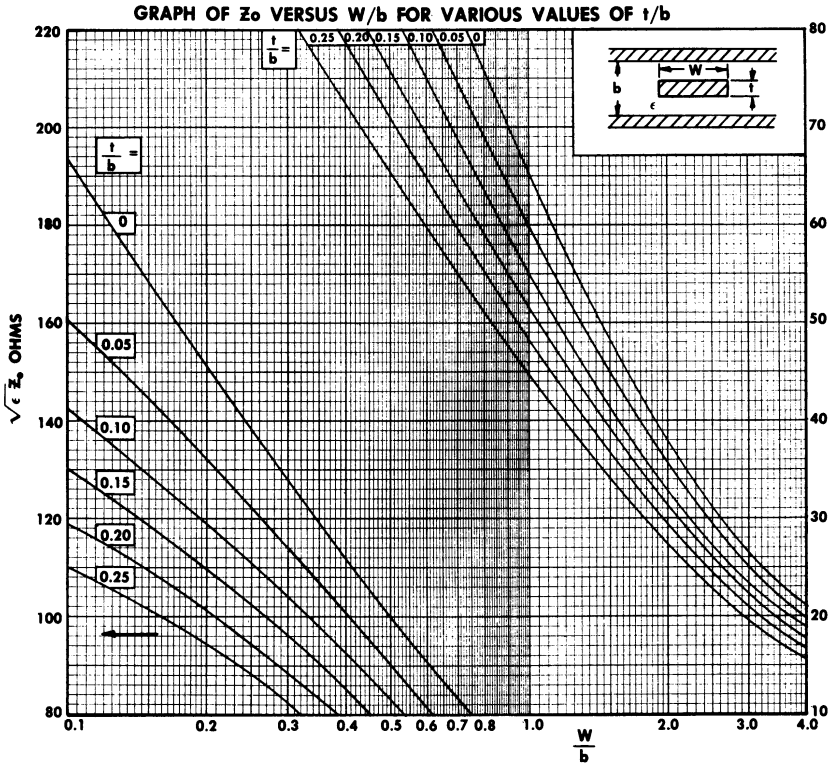

FIG. A-3: $Z_o \epsilon_r$ VERSUS w/b FOR VARIOUS VALUES OF t/b. (Microwave Engineer's Handbook)

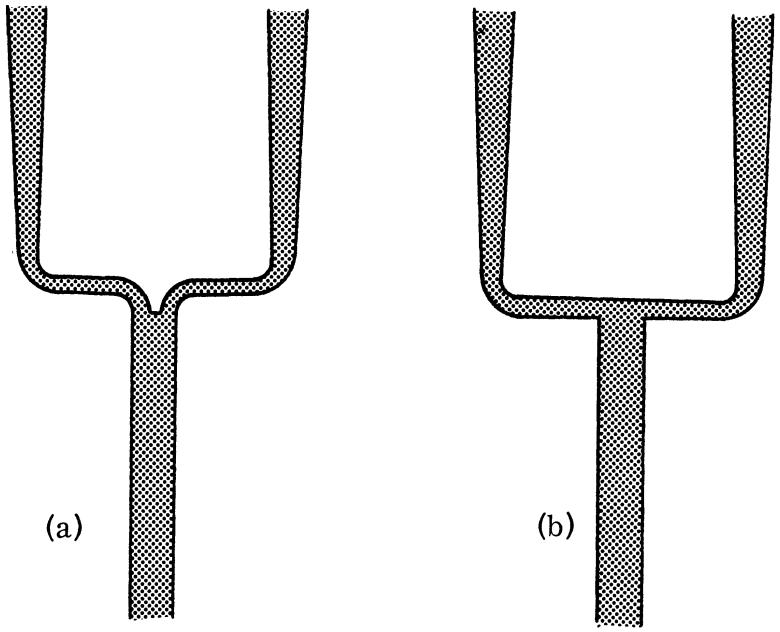

FIG. A-4: CENTER STRIP CONFIGURATION FOR POWER DIVIDERS - (a) "in-line", (b) "tee"

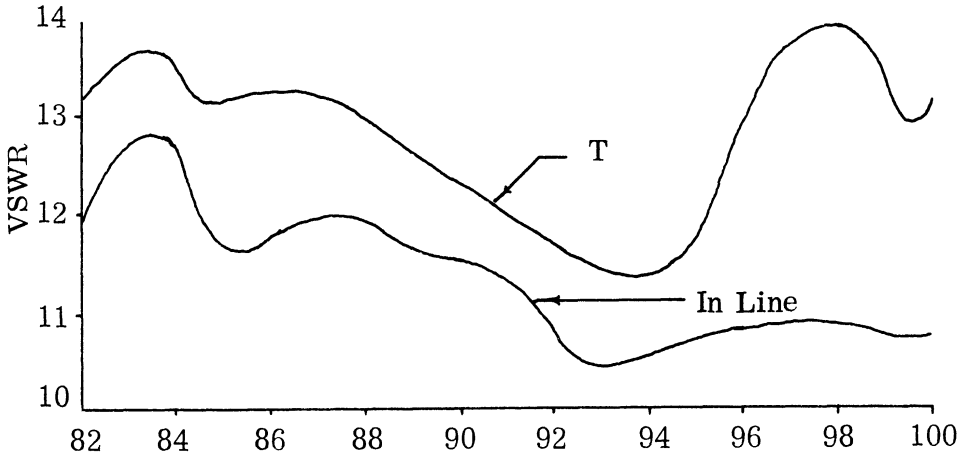

A-5: VSWR FOR "in-line" and "tee" POWER DIVIDERS (Saunders and Assoc. In., "Tri-plate Handbook")

The input and output connections of the power divider can be made by means of right angle coaxial-to-strip-line transitions. A regular coaxial panel receptacle (UG-58/U) with the base machined flush, and the center conductor shortened and soldered to the center strip, provides a good transition (Fig. A-6). The characteristic impedance of the strip line at the input of the coaxial connector should be the same as that of the connector.

To provide a match between the input of the directional coupler and the power dividing junction, a stepped or tapered transformer may be used. A $\lambda/2$ taper is sufficient for transformations of 2:1, (e.g., $50\Omega : 25\Omega$). For larger ratios of transformations, longer tapers are required for satisfactory matching.

Transmission in strip-line is in the TEM mode. To prevent higher order modes from propagating the width of the center strip should be smaller than $\lambda/2$ and the ground plane spacing should also be less than $\lambda/2$. Also, shorting pins between the ground planes, when spaced at $\lambda/2$ intervals help to maintain the ground planes at the same potential and also help to prevent the higher order modes from propagating.

A modified "tee" two-way power divider, using 1/8" thick Tellite 3B copper clad laminate, was built and tested (Fig. A-7). The input and output strips had a characteristic impedance of 50Ω. A $\lambda/2$ taper (at 300 MHz) was used from the 50Ω input to the 25Ω characteristic impedance junction. The VSWR versus frequency is shown in Fig. A-8, and the relative power division is shown in Table A-1.

Power dividers with a larger number of outputs and for higher frequency applications have been built using the principles outlined here. For higher frequencies (e.g., X-band), judicious selection of connectors and the dielectric medium in the copper clad laminate should be made to prevent excess loss.

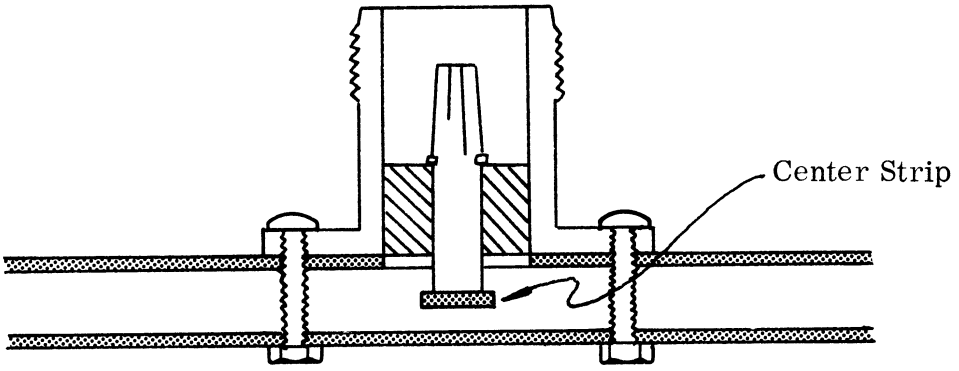

FIG. A-6: COAXIAL TO STRIP LINE TRANSITION USING FEMALE N-TYPE CONNECTOR (UG-58 A/U)

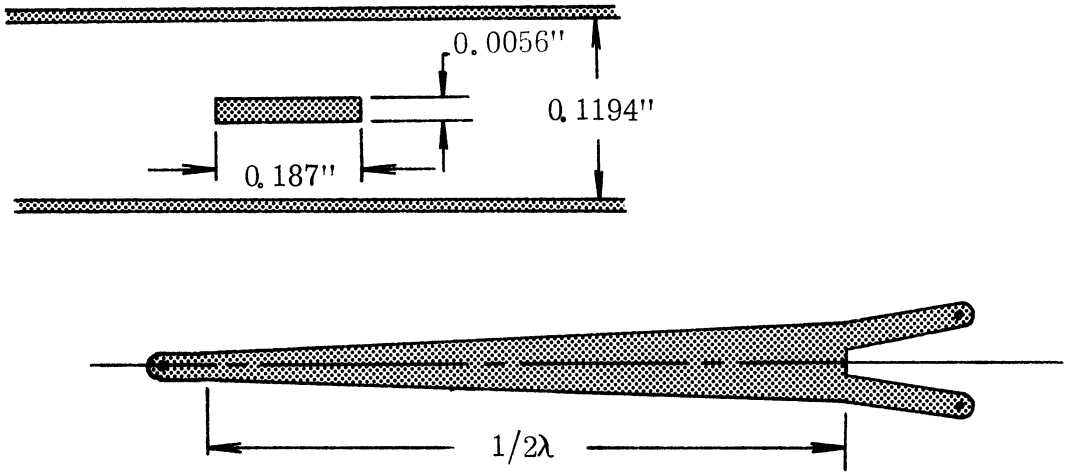

FIG. A-7: CENTER STRIP CONFIGURATION OF TWO-WAY POWER DIVIDER AND CENTER STRIP DIMENSIONS FOR 50 OHM CHARACTERISTIC IMPEDANCE

Frequency (MHz)	Power Output Relative to Power Input	
	1	2
600	-3 db	-3db
1800	-3 db	-3.2 db
3000	-3.5 db	-3.5 db

TABLE A-1: RELATIVE POWER DIVISION OF TWO-WAY POWER DIVIDER

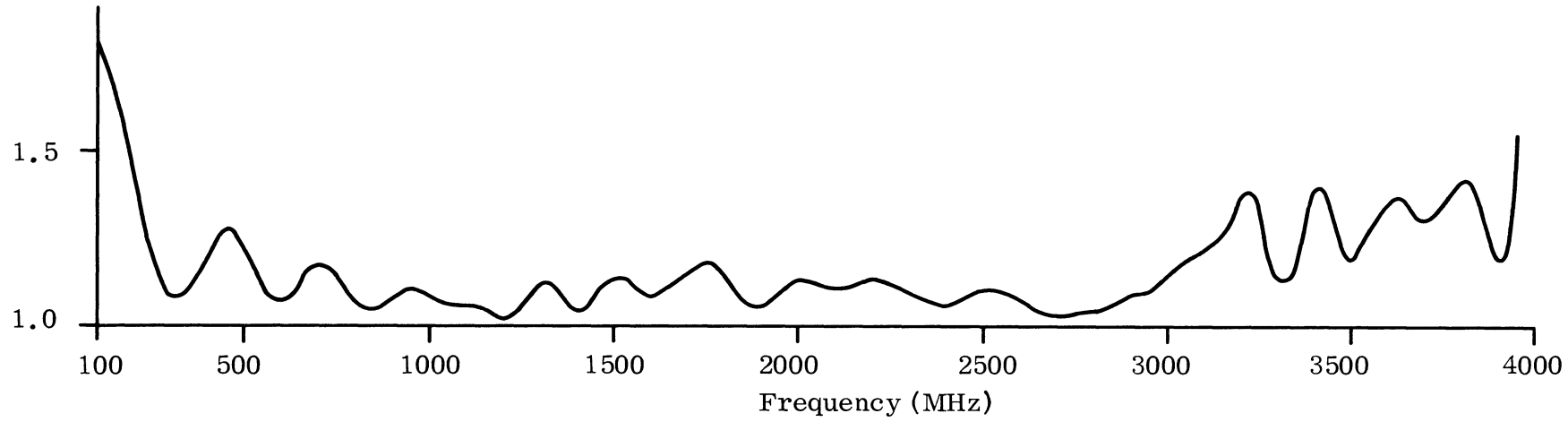

FIG. A-8: VSWR OF TWO-WAY STRIP LINE POWER DIVIDER

APPENDIX B

HEMISPHERICAL GROUND PLANE CONSTRUCTION

A six foot diameter hemispherical ground plane was needed for the final study of the circularly polarized antenna array. Because of cost considerations, a commercially manufactured hemisphere of this size was prohibitive. A silver painted fiberglass hemispherical shell has been fabricated to function as the spherical ground plane.

A mold was needed from which the fiberglass shell could be formed. Dental stone or dental plaster (Vel-Mix stone: Kerr Mfg. Co.) was used for the mold. A plywood frame was built to form the framework of the mold (see Fig. B-1). The interior of the framework was first lined with heavy paper then with ordinary window screen. The screen was used to provide reinforcement for the dental stone. The heavy paper served as a backing for the screen to keep excess amounts of the dental stone from flowing through the screen before it had hardened.

An aluminum "blade" (see Fig. B-2) cut in the form of an arc of a 6 foot diameter circle, was used in a wiper fashion to trowel the dental stone as it was applied to the mold framework. This blade was attached at the base to an axle located at the center of the hemisphere. At the top it was provided with rollers, which set in a track, to guide the blade around the hemisphere (see Fig. B-1).

Plaster was applied to the frame in small amounts and troweled with the blade. During the first plaster applications the mold was set on its edge (Fig. B-3a) and successively rotated 90^{o} as each section was filled in. For the final applications the mold was set on its base (Fig. B-3b). Due to the quick setting time of the plaster (3 to 5 minutes), it was difficult to trowel the plaster on the mold. A retarder solution, supplied by Kerr Mfg. Co., was mixed with the plaster to prolong the setting time (15-20 minutes) and allow more freedom when applying it to the

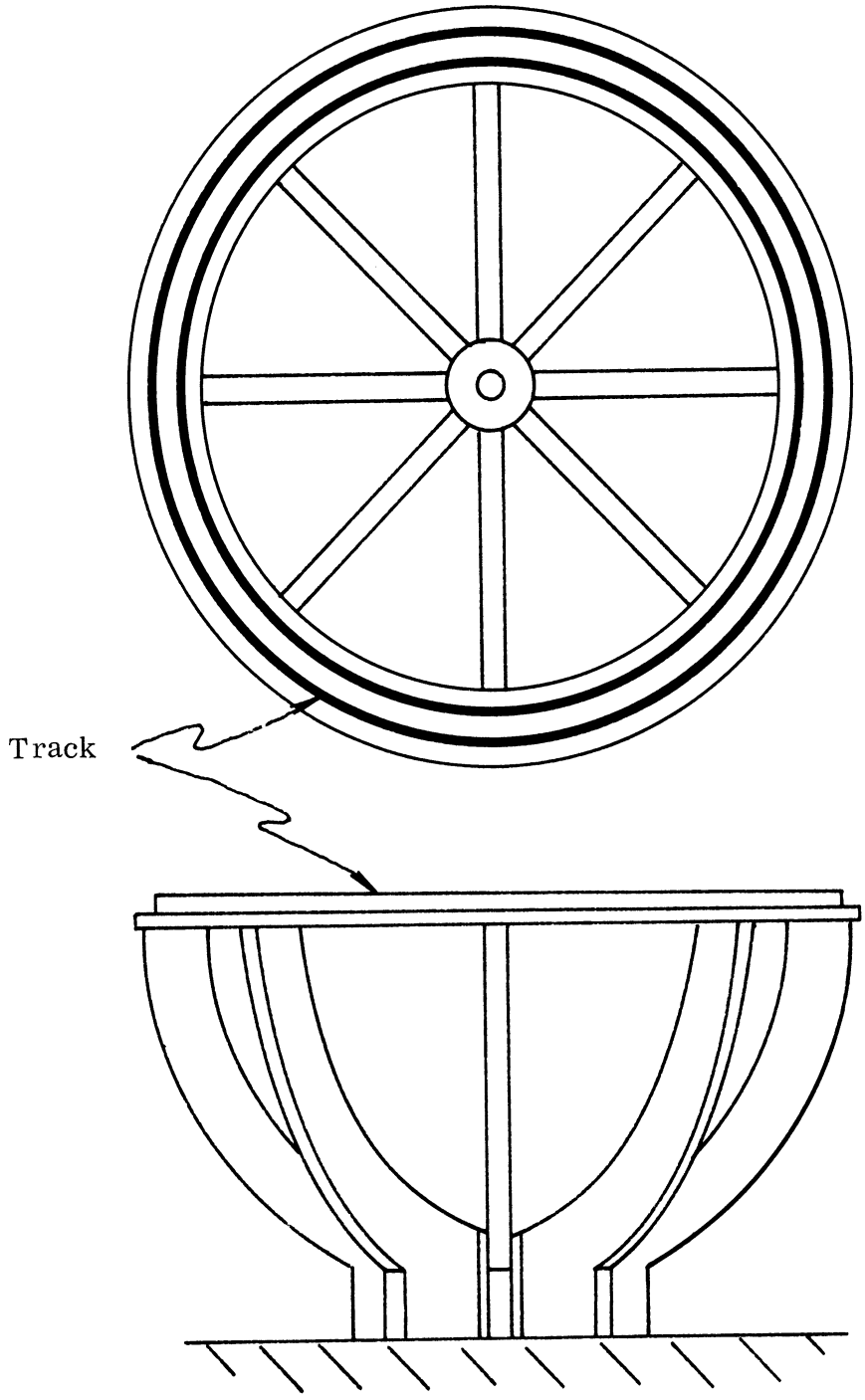

FIG. B-1: SHOWING WOODEN FRAMEWORK AND TRACK FOR A 6 FOOT DIAMETER MOLD

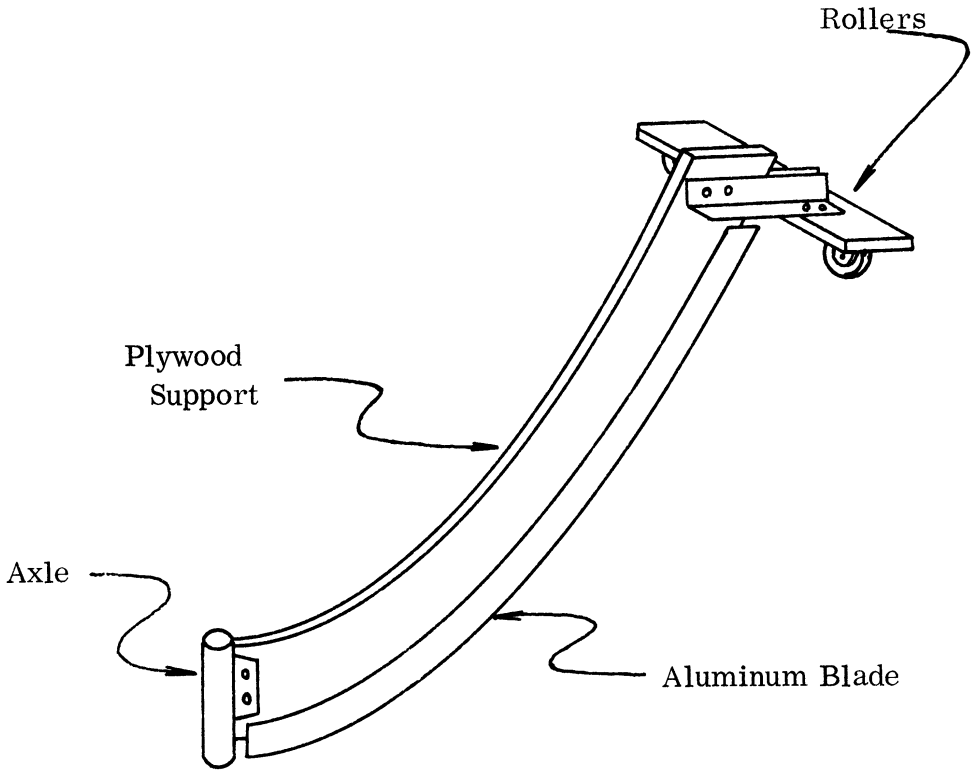

FIG. B-2: SHOWING SCRAPER BLADE ASSEMBLY.

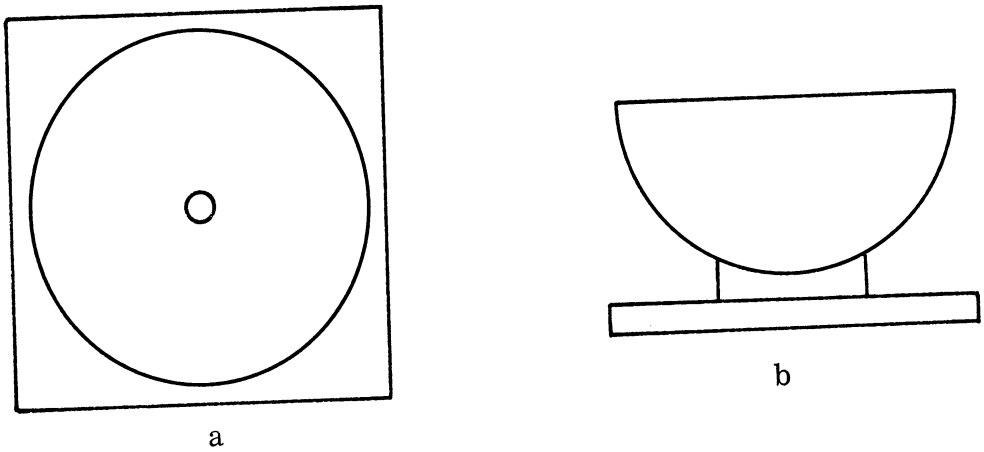

FIG. B-3: SHOWING THE ORIENTATIONS OF THE MOLD DURING PLASTER APPLICATIONS

mold. For the final applications of the plaster, it was desired to use a watery mixture and apply a thin coat to fill in the remaining small holes or gaps. When the blade was used to wipe the final coat, the excess ran to the bottom of the mold and formed a puddle of plaster. More success was achieved when the watery mixture, with retarder, was brushed on. This procedure left brush marks, but with the aid of an electric sander and very fine grit sandpaper, the surface was made smooth. A final step of wet sanding gave an extremely smooth surface. Although the surface had high and low spots, caused by insufficient wiper blade support, a final check showed that the maximum deviation was less than $\pm 1/8"$.

The mold was then sprayed with a mixture of glass fibers and epoxy to obtain the fiberglass shell. Before usage, the exterior of the hemispherical shell was metalized by applying silver paint.

For the fabrication of another concave mold, it is recommended only one-half section be made, and two fiberglass shells bonded together to form the hemisphere. A slight slanting of the scraper blade as well as a better means for supporting the blade, possibly with bearings in the axle and rollers, would aid in the fabrication of the mold. Finally, the use of retarder is highly recommended in making future molds.

APPENDIX C

PDP-8 PROGRAM FOR SPHERICAL ARRAY DIRECTION FINDER ANTENNA

The computer program described herein was written for the PDP-8 computer manufactured by the Digital Equipment Corporation. Its purpose is to control the selection of antenna elements and associated delay lines for the proposed spherical array direction finder. The program has not been tested on a computer and may still contain errors.

It is assumed that the reader is familiar with the operation of the PDP-8 (Digital Equipment Corporation, 1966) and with general programming conventions.

Since the program works entirely from tables contained in the core memory of the computer, the scan of the direction finder can be easily changed by changing entries in these tables. For purposes of this description, it is assumed that there are 91 caps, each being one of four types. The type of cap determines how many elements there are in it, and how many angles are to be scanned within the cap (by changing delay lines, but not elements).

NEW 'IOT' INSTRUCTIONS

In order for the computer to control the array, several 'IOT' (input-output transfer) instructions must be added to it. These instructions are described here as they relate to the program use of them, but their actual electrical implementation has been investigated and seems feasible.

'LE1', 'LE2', ... 'LE6'

These six new instructions are used to connect the appropriate antenna element (if any) to the proper card. When one of these is executed, the contents of the Accumulator (AC) are transferred to an external buffer. Since the AC contains 12 bits and only 3 bits are required for each card (allowing for a maximum

of 8 element selection conditions), then 4 cards may be set with each instruction. In this program, LE1 sets only 3 cards from the 9 high order bits in the AC, while the others set 4 cards each for a total of 23 cards.

'LDA'

This instruction is used to set the appropriate delay in each card. Execution of an 'LDA' does not actually change delay lines in a card but only sets up an external register to remember which delay is to be used next for each card. When an 'LDA' is executed the low order 4 bits of the AC are used to specify the delay and the high order 5 bits are used to determine to which card the delay is to be applied. The instruction 'RCN' is an 'LDA' with Card No. 31, which when executed, turns the receiver on. 'RCF' (LDA 30) turns the receiver off. 'DTR' (LDA 29) changes the delay in every card to correspond to the delay specified in the external register set up by the 'LDA's.

STRUCTURE OF TABLES

Table "A" - First location (lowest address) is called 'ATB'

This table contains one entry for each cap. Each entry has six words and each word is divided into four fields of 3 bits each. Each field contains the element selection number for the corresponding card. These words are designed to work with the 'LEx' instructions; the first word is put in the AC and 'LE1' is executed, the second is put in the AC and LE2 is executed, etc. The three low order bits of the first word, which are ignored by 'LE1', contain the type number of the cap.

Table "B" - First location is called 'BTB'

This table also contains one entry for each cap, but the length of the entries is variable and depends on the number of elements used in the particular cap. Each word is divided into two fields of six bits each. Each field contains the card number to be associated with each standard position. The first field in the first

word has the card number of the card for the element in standard position A. The second field in the first word has the card number for position B. The first field in the second word has the number for position C, etc.

Table "C" - First location for type n is called 'CnT'

There is one "C" table for each cap type. The first two words in each table contain, 1) the negative of the number of elements in the type, and 2) the negative of number of angles in that type. Following these two words are entries for each angle in the cap. Each entry contains one word for each element in the cap in order according to the standard position. Each word contains the delay for that position and angle. Actually only the four low order bits of each word are used.

CONSTANTS AND VARIABLES USED IN PROGRAM

LOCATION (OCTAL)	NAME	USE OR CONTENTS	
10	APR	"A" Table Pointer	auto-indexing locations
11	BPR	"B" table pointer	
12	SPP	Standard Position Pointer	
13	IT	Auto-indexing temporary	
20	CCR	Cap counter	
21	EQT	Start of card-std pos. equivalence table	
50 through 55	T1 through T6	Temporary storage	
60	AAT	ATB-1	
61	ABT	BTB-1	
62	AC1	C1T	
63		C2T	
64		C3T	
65		C4T	
66	AEQ	EQT-1	
67	NRC	-91 (negative of number of caps)	
70	C1	7700 (octal)	
71	C2	77 (octal)	
72	C3	3	
73	ACT	AC1	
74	NXP	200 (octal)	
75	ACP	SCP	
76	ACN	SCN	

The computer program itself starts in location 100 (octal) and ends in loc 225. Storage in core above this is used for the large tables. All addresses refer to page zero except jumps within one page. All indirect addressing is through page zero.

PROGRAM

```
SCN,    CLA             Start at first cap
        TAD     AAT
        DCA     APR     Set A table pointer
        TAD     ABT
        DCA     BPR     Set B Table pointer
        TAD     NRC
        DCA     CCR     Set cap counter

SCP,    TAD I   APR     Get first A entry
        DCA     T1      Save it
        TAD     T1
        AND     C3      Get type number
        TAD     ACT
        DCA     T2
        TAD I   T2      Get C address
        DCA     T2
        TAD I   T2      Get negative of number of elements
        DCA     T3
        TAD     T3
        DCA     T4
        TAD     AEQ
        DCA     SPP     Set EQT Pointer

STS,    TAD I   BPR     Get B entry
        DCA     T5
        TAD     T5
        AND     C1      First half
        DCA I   SPP     Save in EQT
        ISZ     T3      Count element
        JMP     MAN
        JMP     LDC     If done

MAN,    TAD     T5
        RTL             Rotate into other half
        RTL
        RTL
        AND     C1      Second half
        DCA I   SPP     Save in EQT
        ISZ     T3
        JMP     STS
```

(continued)

PROGRAM (continued)

```
LDC,  RCF                    Turn receiver off
      TAD      T1
      LE1
      CLA
      TAD I    APR
      LE2
      CLA
      TAD I    APR
      LE3
      CLA
      TAD I    APR
      LE4
      CLA
      TAD I    APR
      LE5
      CLA
      TAD I    APR
      LE6
      JMP I    NXT        Continue at start of next page

(200) CLA
      TAD      T2         Get C table address
      DCA      IT
      TAD I    IT         Get negative of number of angles
      DCA      T3

STP,  TAD      T4         Get negative of number of elements
      DCA      T1
      TAD      AEQ        Get EQT address
      DCA      SPP

NXE,  TAD I    IT         Get delay
      TAD I    SPP        Add card number
      LDA                 Set external register
      ISZ      T1         Count element
      JMP      NXE        Go back for next element

      RCF                 Turn receiver off
      DTR                 Transfer delays to cards
      RCN                 Turn receiver on
      ISZ      T3         Count Angle
      JMP      STP        Go back for next angle
      ISZ      CCR        Count cap
      JMP I    ACP        Go back for next cap
      JMP I    ACN        Restart at first cap.

      END                 End of program.
```

ACKNOWLEDGEMENTS

K. M. Jagdmann and W. E. Zimmerman prepared the material discussed in Appendices A and B. P. H. Wilcox was responsible for the Appendix C. A. J. Loudon helped in making the measurements. The authors wish to acknowledge their help.

THE UNIVERSITY OF MICHIGAN

DISTRIBUTION LIST FOR 07577 QUARTERLY REPORTS

Address	No. of Copies
Mr. E. M. Turner AVWE-3 Air Force Avionics Laboratory Wright-Patterson AFB, Ohio 45433	1
Mr. C. J. Sletten CRD Air Force Cambridge Research Laboratories L. G. Hanscom Field Bedford, Massachusetts 01731	1
Mr. C. L. Pankiewicz EMATA Rome Air Development Center Griffiss AFB, New York 13442	1
Mr. P. A. Lantz, Code 525 NASA Goddard Space Flight Center Greenbelt, Maryland 20771	1
USAEL Liaison Officer RAOL Rome Air Development Center Griffiss AFB, New York 13442	1
Mr. J. B. Norvell, R31 National Security Agency Ft. G. G. Meade, Maryland 20755	1
Mr. R. J Adams Code 5330 Naval Research Laboratory Washington, D. C. 20390	1
Mr. R. Fratila Code 362A Dept of the Navy, BuShips Main Navy Building Washington, D. C. 20360	1
U. S. Army Electronics Command AMSEL-HL-R Ft. Monmouth, N J. 07703	1
Mr. B. I Small, Code 3220C U. S. Navy Electronics Laboratory San Diego, California 92152	1
Harry Diamond Laboratories Technical Library Connecticut Ave., and Van Ness St., NW Washington, D. C. 20438	1

Mr. C. Craig IALOG/ESE U. S. Army Security Agency Arlington Hall Station Arlington, Virginia 22207	1
U. S. Army Electronics Command AMSEL-NL-R Ft. Monmouth, N. J. 07703	1
Defense Documentation Center DDC-IRE Cameron Station, Building 5 Alexandria, Virginia 22314	20 + card
Office, Assistant Secretary of Defense Research and Engineering Technical Library, Pentagon Room 3E1065 Washington, D. C. 20301	1
Defense Intelligence Agency DIARD Washington, D. C. 20301	1
Department of the Navy BuShips Technical Library Code 312, Room 1528 Main Navy Building Washington D C 20325	1
U. S. Naval Research Laboratory Code 2027 Washington, D. C. 20390	1
U. S. Navy Electronics Laboratory Technical Library San Diego, California 92101	1
AFSC Scientific and Technical Liaison Officer RTSND U S Naval Air Development Center Johnsville, Warminster, Pennsylvania 18974	1
Systems Engineering Group SEPIR Wright-Patterson AFB, Ohio 45433	1
ESD, AFSC, Scientific/Technical Information Div. (ESTI) L. G. Hanscom Field Bedford, Massachusetts 01731	2

Air Force Cambridge Research Laboratories
CRXL-R
L. G. Hanscom Field
Bedford, Mass 01731 2

NASA Repr. Scientific and Technical Information Facility
P O Box 5700
Bethesda, Md 20014 1

U. S. Army Electronics Command
AMSEL-WL-S
Ft. Monmouth, N. J. 07703 5

U. S. Army Electronics Command
EW-MET Commodity
AMSEL-EW, Management Office
Ft. Monmouth, N. J. 07703 1

U. S. Army Electronics Command
AMSEL-MR
225 S. 18th St.
Philadelphia Pa 19103 1

U. S. Army Electronics Command
AMSEL-IO-T 1

AMSEL-XL-D 1

AMSEL-RD-MAT 1

AMSEL-RD-MAF 1

AMSEL-RD-LNA 1

AMSEL-RD-LNR 1
Ft. Monmouth, N. J. 07703

U. S. Army Electronics Command
R and D Activity
White Sands Missile Range, New Mexico 88002 1

U. S. Army Electronics Command
Mountain View Office - Electronic Warfare Laboratory
Box 205
Mountain View, California 1

U. S. Army Engineer R and D Laboratories
STINFO Branch
Ft. Belvoir, Va. 22060 1

U. S. Army Electronics Command Intelligence Materiel Development Office Electronic Warfare Laboratory Fort Holabird, Md. 21219	1
U. S. Army Electronics Command ASDL-9 Liaison Officer Aeronautical Systems Division Wright-Patterson AFB, Ohio 45433	1
U. S. Army Electronics Command Liaison Officer EMPL Rome Air Development Center Griffiss AFB, New York 13442	1
US NBS Boulder Laboratories Technical Library Boulder, Colorado 80301	1
Department of the Army Chief, Research and Development Washington, D C 20315	2
Department of the Army Chief, Communications-Electronics CCEES-1A Washington, D C. 20315	1
U. S. Army Materiel Command R and D Directorate Washington, D. C 20315	2
U. S. Army S A S O C 52D Fort Huachuca, Ariz. 85613	1
U. S. Army Combat Developments Command Communications-Electronics Agency Fort Huachuca, Ariz. 85613	1
U. S Army Electronic Proving Ground Technical Library Fort Huachuca, Ariz. 85613	1
U. S. Army Security Agency AC of S, G4 (Technical Library) Arlington Hall Station Arlington, Va. 22207	2
Total List	75

UNCLASSIFIED

Security Classification

DOCUMENT CONTROL DATA - R&D

(Security classification of title, body of abstract and indexing annotation must be entered when the overall report is classified)

1. ORIGINATING ACTIVITY *(Corporate author)*
The University of Michigan Radiation Laboratory
Department of Electrical Engineering
Ann Arbor, Michigan 48108

2a. REPORT SECURITY CLASSIFICATION
UNCLASSIFIED

2b. GROUP

3. REPORT TITLE

Azimuth and Elevation Direction Finder Study

4. DESCRIPTIVE NOTES *(Type of report and inclusive dates)*
Final Report 1 September 1965- 1 September 1966

5. AUTHOR(S) *(Last name, first name, initial)*

Sengupta, Dipak L.; Ferris, Joseph E.; Larson, Ronal W.; Hok, Gunnar and Smith, Thomas M.

6. REPORT DATE	7a. TOTAL NO. OF PAGES	7b. NO. OF REFS
September 1966	103	11

8a. CONTRACT OR GRANT NO.	9a. ORIGINATOR'S REPORT NUMBER(S)
DA 28-043 AMC-01499(E)	7577-1-F
b. PROJECT NO. 5A6 79191 D902 01 04	
c.	9b. OTHER REPORT NO(S) *(Any other numbers that may be assigned this report)*
d.	ECOM-01499-4

10. AVAILABILITY/LIMITATION NOTICES

Each transmittal of this document outside the Department of Defense must have prior approval of USAECOM, AMSEL-WL-S, Ft. Monmouth, N.J. 07703

11. SUPPLEMENTARY NOTES	12. SPONSORING MILITARY ACTIVITY
	U.S. Army Electronics Command AMSEL-WL-S Fort Monmouth, New Jersey 07703

13. ABSTRACT

Radiation characteristics of a spherical antenna array of circularly polarized elements are studied both theoretically and experimentally. It is found that such an array is capable of providing broadband and complete hemispherical coverage suitable for direction finding purposes. The theory developed should be adequate for the design of such arrays.

On the basis of the above study an exploratory model of a UHF spherical array azimuth and elevation direction finder is proposed. The array uses flat spirals as individual elements. The necessary phasing of the antenna elements and the scanning of the beam for direction finding are accomplished by using delay lines and diode switches in conjunction with a general purpose computer.

An alternative method where a correlation processing technique is applied to the output data from the antenna elements for direction finding purposes is also discussed.

DD FORM 1 JAN 64 1473

UNCLASSIFIED

Security Classification

14. KEY WORDS	LINK A		LINK B		LINK C	
	ROLE	WT	ROLE	WT	ROLE	WT
Broadband Spherical Array Circular Polarization Direction Finder Flat Spiral Antenna Digital Control of Arrays Diode Switches						

INSTRUCTIONS

1. ORIGINATING ACTIVITY: Enter the name and address of the contractor, subcontractor, grantee, Department of Defense activity or other organization *(corporate author)* issuing the report.

2*a*. REPORT SECURITY CLASSIFICATION: Enter the overall security classification of the report. Indicate whether "Restricted Data" is included. Marking is to be in accordance with appropriate security regulations.

2*b*. GROUP: Automatic downgrading is specified in DoD Directive 5200.10 and Armed Forces Industrial Manual. Enter the group number. Also, when applicable, show that optional markings have been used for Group 3 and Group 4 as authorized.

3. REPORT TITLE: Enter the complete report title in all capital letters. Titles in all cases should be unclassified. If a meaningful title cannot be selected without classification, show title classification in all capitals in parenthesis immediately following the title.

4. DESCRIPTIVE NOTES: If appropriate, enter the type of report, e.g., interim, progress, summary, annual, or final. Give the inclusive dates when a specific reporting period is covered.

5. AUTHOR(S): Enter the name(s) of author(s) as shown on or in the report. Enter last name, first name, middle initial. If military, show rank and branch of service. The name of the principal author is an absolute minimum requirement.

6. REPORT DATE: Enter the date of the report as day, month, year; or month, year. If more than one date appears on the report, use date of publication.

7*a*. TOTAL NUMBER OF PAGES: The total page count should follow normal pagination procedures, i.e., enter the number of pages containing information.

7*b*. NUMBER OF REFERENCES: Enter the total number of references cited in the report.

8*a*. CONTRACT OR GRANT NUMBER: If appropriate, enter the applicable number of the contract or grant under which the report was written.

8*b*, 8*c*, & 8*d*. PROJECT NUMBER: Enter the appropriate military department identification, such as project number, subproject number, system numbers, task number, etc.

9*a*. ORIGINATOR'S REPORT NUMBER(S): Enter the official report number by which the document will be identified and controlled by the originating activity. This number must be unique to this report.

9*b*. OTHER REPORT NUMBER(S): If the report has been assigned any other report numbers *(either by the originator or by the sponsor)*, also enter this number(s).

10. AVAILABILITY/LIMITATION NOTICES: Enter any limitations on further dissemination of the report, other than those imposed by security classification, using standard statements such as:

(1) "Qualified requesters may obtain copies of this report from DDC."

(2) "Foreign announcement and dissemination of this report by DDC is not authorized."

(3) "U. S. Government agencies may obtain copies of this report directly from DDC. Other qualified DDC users shall request through _____."

(4) "U. S. military agencies may obtain copies of this report directly from DDC. Other qualified users shall request through _____."

(5) "All distribution of this report is controlled. Qualified DDC users shall request through _____."

If the report has been furnished to the Office of Technical Services, Department of Commerce, for sale to the public, indicate this fact and enter the price, if known.

11. SUPPLEMENTARY NOTES: Use for additional explanatory notes.

12. SPONSORING MILITARY ACTIVITY: Enter the name of the departmental project office or laboratory sponsoring *(paying for)* the research and development. Include address.

13. ABSTRACT: Enter an abstract giving a brief and factual summary of the document indicative of the report, even though it may also appear elsewhere in the body of the technical report. If additional space is required, a continuation sheet shall be attached.

It is highly desirable that the abstract of classified reports be unclassified. Each paragraph of the abstract shall end with an indication of the military security classification of the information in the paragraph, represented as *(TS), (S), (C), or (U)*.

There is no limitation on the length of the abstract. However, the suggested length is from 150 to 225 words.

14. KEY WORDS: Key words are technically meaningful terms or short phrases that characterize a report and may be used as index entries for cataloging the report. Key words must be selected so that no security classification is required. Identifiers, such as equipment model designation, trade name, military project code name, geographic location, may be used as key words but will be followed by an indication of technical context. The assignment of links, rules, and weights is optional.